A Dissertation Entitled

INTERNAL FRICTION DUE TO CRYSTAL LATTICE IMPERFECTIONS

Submitted to the University of London for the Degree of Master of Science by

Clive Reed Scorey, B.Sc.

December, 1965.

A B S T R A C T

This dissertation is concerned with internal friction due to crystal lattice defects. Particular attention is given to losses involving dislocation motion which are observed in metals. Five characteristic types of loss are distinguished experimentally. These are i) the Bordoni Peaks, ii) the Hasiguti Peaks, iii) a damping observed at high temperatures which increases exponentially with temperature, iv) a damping which is independent of the stress amplitude at which it is measured, providing this is small, and which is also dependent on the frequency of the stress wave, and v) a damping which is dependent on the measuring stress amplitude but independent of the measuring frequency. An attempt is made to relate each of these five losses to a specific dislocation damping mechanism. The individual damping mechanisms are based on one or other of three general processes by which energy may be lost from an oscillating length of dislocation. These are firstly a relaxation process, secondly a damped resonance process and thirdly a static hysteresis process.

Internal friction measurements are found to give information on, for example, the nature and distribution of point defects and dislocations, the interaction between point defects and dislocations, the magnitude of the Peierls stress and the dynamics of dislocation motion. In connection with the latter the string model of dislocation motion is compared with the kink model.

ACKNOWLEDGEMENTS

The author wishes to thank Dr. N.B. Cryer of the Physics Department, Chelsea College of Science and Technology, For his guidance and encouragement during the preparation of this dissertation.

I am also indebted to the Department of Scientific and Industrial Research for a maintenence allowance during the academic session 1964-65.

CONTENTS

CHAPTER 1.

Introduction

The dissipation of power in a specimen in some mode of mechanical vibration is known as internal friction. This phenomenon has been observed in solid specimens at stress wave frequencies from around 10^{-2} c/s up to many hundreds of megacycles. That motion of dislocations might be responsible at least in part for the internal friction observed in metals was first proposed by T.A. Read (40), in view of the sensitivity of the internal friction of metals to cold working and annealing. Much effort has since been spent investigating the internal friction of metals, providing information on, for example, the Peierls stress, the nature of point defects, dislocations and point defect - dislocation interactions. However, the data obtained from internal friction measurements show a wide variety in their dependence on a great many experimental parameters, making interpretations difficult.

The materials considered in this dissertation have been restricted almost entirely to metals in order to limit the amount of experimental data which would otherwise have to be included. This approach also avoids possible complications arising from the different nature of interatomic binding forces in non-metals (e.g. directional bonds) which may influence dislocation behaviour.

There are many mechanisms other than those involving dislocations which can contribute to the internal friction observed in a specimen. To evaluate the friction arising from a dislocation mechanism it is necessary first to know what other mechanisms are operative. A brief survey of some of these other causes of internal friction is therefore given in Chapter 3. In Chapter 2 the conditions under which internal friction, or damping, may occur in a crystal lattice are considered, as well as three processes by which energy may be removed from a stress wave. It is found that many dislocation damping phenomena may be interpreted in terms of these basic processes, which are (i) a relaxation process, (ii) a damped resonance process, (iii) a static hysteresis process.

In Chapter 4 experimental techniques are considered and some typical internal friction measurements are given. Five apparently distinct types of internal friction are identified, each one showing certain characteristic dependencies on experimental parameters. In later chapters specific dislocation mechanisms which have been proposed to account for these types of internal friction are discussed. In Chapter 5 the specific dislocation damping mechanisms leading to relaxation type losses are discussed and in chapters 6,7 and 8 those leading to a damped resonance or static hysteresis type of loss.

Finally, in Chapter 9 a critical survey of the current position in this field is given, together with some suggestions for further work.

CHAPTER 2.

Basic Concepts

2.1. When an oscillating stress is applied to a perfectly elastic material the resultant strain is in phase with the stress and there is no energy loss. The stress σ and strain ϵ may be related as

$$\sigma = G_1 \epsilon \qquad (2.1.)$$

where G_1 is a constant known as the elastic modulus. For there to be a dissipation of energy the material must possess non-linear or anelastic properties, when the strain will lag behind the stress in phase. The relation between stress and strain then assumes a more general form involving, perhaps, powers and time derivatives of stress and strain. To simplify the theory of the damping in this case it will be assumed in this chapter that the damping is small, so that the non-linear terms in the stress-strain relation will be much smaller than the elastic terms. Such an approximation is found to be justified in most experimental cases. If non-linear terms appear in the stress-strain relation an exact solution may be obtained as a Fourier series, and an approximate solution by neglecting all but the fundamental Fourier components. [Nowick (53)].

In general, whenever the stress-strain relation is non-linear in stress, strain or the first derivatives of these quantites the resultant damping is stress amplitude dependent. Thus the Standard Linear Solid, [Zener (48)] a model used with some success to account for the anelastic properties of solids, is unable to describe stress amplitude dependent damping since it assumes a linear stress-strain relation.

2.2. The Modulus Defect.

The phase lag between the stress and strain as a result of nonelastic behaviour will now be considered in terms applicable to all internal friction phenomena. For simplicity it is assumed throughout that the appropriate stress system can be defined by a single stress component, σ , and that only the principal strain, ϵ , corresponding to, σ need be considered. This is reasonable since only this strain appears in the expression for the work done by the stress [Nowick (53)].

The strain in a material under stress consists of an elastic component ϵ' and a nonelastic (plastic) component ϵ''. If the applied stress, or its fundamental Fourier component, is of the form

$$\sigma = \sigma_1 \exp(i\omega t), \tag{2.2.}$$

where ω is the angular frequency of the applied stress and t the time, then the elastic and plastic strains are respectively

$$\epsilon' = \epsilon_1' \exp(i\omega t), \tag{2.3.}$$

$$\epsilon'' = (\epsilon_1'' - i\epsilon_2'') \exp(i\omega t), \tag{2.4.}$$

where the subscripts 1 and 2 refer respectively to strains in phase with and 90° out of phase with the stress. These relationships are illustrated in Fig.2.1. The angle ϕ is the phase lag between the stress and strain, and is shown below to be a measure of the internal friction. We may write

$$\phi \doteqdot \frac{\epsilon_2''}{\epsilon_1'} . \tag{2.5.}$$

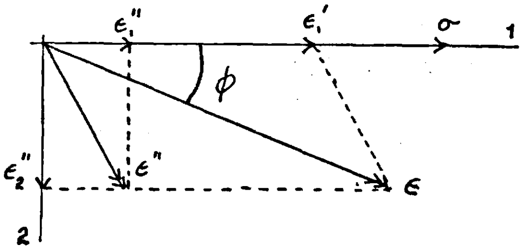

Fig. 2.1. PHASE RELATIONSHIPS BETWEEN THE STRESS AND THE COMPONENTS OF THE STRAIN.

Thus the friction is seen to depend to a first approximation on the component of nonelastic strain 90° out of phase with the applied stress.

A dynamic modulus G_2 and a complex modulus G_3 are defined by

$$G_2 = \frac{\sigma_1}{\epsilon_1' + \epsilon_1''}, \tag{2.6.}$$

$$G_3 = \frac{\sigma_1}{\epsilon_1' + \epsilon_1'' - i\,\epsilon_2''}. \tag{2.7.}$$

The elastic and dynamic moduli may be related as

$$G_1 = G_2\left(1 + \frac{\epsilon_1''}{\epsilon_1'}\right). \tag{2.8.}$$

Thus, as a result of the nonelastic behaviour, the dynamic modulus, which is the experimentally measured modulus, is smaller than the purely elastic modulus. This leads to the definition of a 'modulus defect' $\frac{\Delta G}{G}$ where

$$\frac{\Delta G}{G} = \frac{G_1 - G_2}{G_2} = \frac{\epsilon_1''}{\epsilon_1'}. \tag{2.9.}$$

The modulus defect is seen to be related to the component of plastic strain 90° out of phase with the stress. Further, ϕ and $\frac{\Delta G}{G}$ are related to the imaginary and real part of G_3 as

$$G_3 = G_1\frac{\Delta G}{G} + i\,G_1\phi. \tag{2.10.}$$

2.3. The Classification of Internal Friction Phenomena.

Internal friction may arise by several different basic loss processes, the friction in each case being distinguished by characteristic dependences on certain experimental parameters. Three common loss processes are introduced below.

(a) Relaxation loss processes.

The features of a relaxation loss may be obtained using the concept of the Standard Linear Solid [Zener (48)] which is described by

$$\sigma + \tau_1\frac{\partial\sigma}{\partial t} = G_+\left(\epsilon + \tau_2\frac{\partial\epsilon}{\partial t}\right), \tag{2.11}$$

where τ_1 and τ_2 are relaxation times defined in terms of the time the solid takes to relax under a constant strain and stress respectively. G_4 is a 'relaxed' modulus since it relates the stress and strain after complete relaxation. Equation (2.11.) may be solved by substituting the functions

$$\sigma = \sigma_0 \exp(i\omega t), \qquad (2.12.)$$

$$\epsilon = \epsilon_0 \exp i(\omega t - \phi), \qquad (2.13)$$

when

$$\tan\phi = \frac{\omega\Delta\tau}{1+\omega^2\tau^2}, \qquad (2.14.)$$

with $\Delta\tau = \tau_2 - \tau_1$ and $\tau = \sqrt{\tau_1\tau_2}$.

The energy lost per stress cycle, ΔW, is given by [van Bueren (61)]

$$\Delta W = Re \int_0^{\frac{2\pi}{\omega}} \sigma \frac{\partial\epsilon}{\partial t}\, dt = \pi\sigma_0\,\epsilon_0 \sin\phi . \qquad (2.15.)$$

The maximum stored energy during a cycle, W, is given by

$$W = \int_0^{\epsilon_0} \sigma\, d\epsilon \doteqdot \int_0^{\epsilon_0} \frac{\sigma_0\,\epsilon}{\epsilon_0}\, d\epsilon = \tfrac{1}{2}\,\sigma_0\,\epsilon_0 . \qquad (2.16.)$$

Thus the fractional energy loss per cycle is given by

$$\frac{\Delta W}{W} \doteqdot 2\pi\sin\phi \doteqdot 2\pi\phi . \qquad (2.17.)$$

The quantity, ϕ, and therefore $\tan\phi$ of equation (2.14.), is thus a measure of the damping. It is seen to be positive only when $\tau_2 > \tau_1$.

The modulus defect associated with the damping may be calculated from [van Bueren (61)]

$$\frac{\Delta G}{G} = Re\left(\frac{G_3 - G_3'}{G_3'}\right), \qquad (2.18.)$$

where G_3' is the value of G_3 at very high frequencies, $\omega\tau \gg 1$. Equation (2.18.) then yields

$$\frac{\Delta G}{G} = \frac{\Delta\tau}{\tau(1+\omega^2\tau^2)} . \qquad (2.19.)$$

This function and $\tan\phi$ of equation (2.14.) are plotted in Fig.2.2. as a function of ω .

The energy loss as a function of $\tan\phi$ is seen to approach zero at high and low frequencies and to have a maximum at a frequency $\frac{1}{\tau}$. The

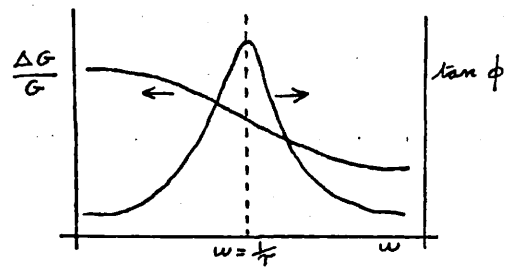

Fig. 2.2. THE FUNCTIONS $\tan\phi$ AND $\frac{\Delta G}{G}$ AS A FUNCTION OF FREQUENCY, ω.

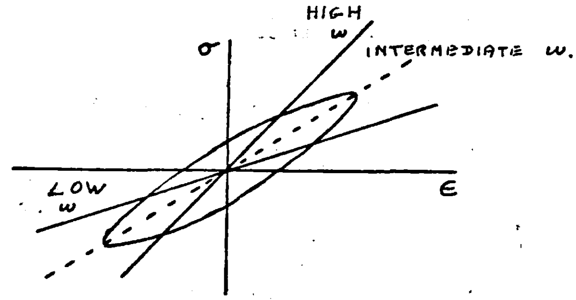

Fig. 2.3. THE STRESS–STRAIN RELATION AT DIFFERENT FREQUENCIES, ω.

modulus is seen to decrease over the relaxation region and to be constant outside this region. Fig.2.3. illustrates the stress-strain relation for a material showing a relaxation type loss. The curve is an ellipse in the region of energy loss, the slope of the major axis giving the complex modulus, [Nowick (53)] and the area of the ellipse the energy loss per cycle. At high and low frequencies the ellipse collapses to a straight line.

Relaxation processes involving, for example, dislocation motion can be expected to be strongly temperature dependent [Nowick (53)] according to the Arrhenius equation

$$\tau = \frac{1}{\omega_0} \exp\left(\frac{E}{kT}\right), \qquad (2.20.)$$

where ω_0 is an attempt frequency and E is an activation energy.

Although the treatment presented here for the Standard Linear Solid shows the characteristic features of a relaxation loss, more complicated treatments are usually required to describe particular experimental results.

(b) Damped resonance loss processes.

This is a type of frequency dependent damping which reaches a maximum when the frequency of the applied stress reaches the resonant frequency of, for example, a dislocation oscillating about its equilibrium position under the restraining influence of its line tension. [Koehler (52)].

The equation desribing damped oscillatory motion is of the form

$$A\frac{d^2x}{dt^2} + B\frac{dx}{dt} + Cx = F\exp(i\omega t), \qquad (2.21.)$$

where, applied to unit length of a dislocation, A represents the mass or inertia, B is the damping constant, C the line tension and the term on the right the applied stress. The fractional loss of energy per cycle is found to be given by [van Bueren (61)]

$$\frac{\Delta W}{W} = \frac{2\pi\,\omega/\tau_R}{\sqrt{(\omega_0^2-\omega^2)^2 + \omega^2/\tau_R^{\,2}}}, \qquad (2.22.)$$

where $\tau_R = \frac{A}{B}$, and ω_0 is the resonant frequency of the dislocation. Again the friction passes through a maximum at $\omega = \omega_0$ and is independent of the stress amplitude. There as several differences, however, between this type of loss and a relaxation loss. In the latter case a variation in τ results only in a shift of the peak frequency and the shape of the damping curve is influenced mostly by $\Delta\tau$. In the damped resonance case the frequency of the maximum damping depends little on τ_R, while the peak width is proportional to $\frac{1}{\tau_R}$. Hence to distinguish between relaxation and damped resonance internal friction, the behaviour of the corresponding relaxation times must be considered. For example, an increase in temperature results in a rapid increase in the frequency of the maximum relaxation damping, while the frequency of the maximum damped resonance loss is hardly affected (only through C).

In fact it may be shown [van Bueren (61)] that damped resonance and relaxation phenomena transform continuously into each other when A

and B tend to infinity and the ratio $\frac{A}{B}$, or τ_R, is held constant.

(c) Static hysteresis loss mechanism.

A static hysteresis loss is characterised by a marked stress amplitude dependence and little dependence on frequency. It is associated with irreversible changes of state. In the case of mechanical hysteresis for example, suppose that as the stress in a material is increased there is a corresponding value of strain, reached instantaneously, and that the same is true when the stress is decreased after reaching a maximum value. If, however, the strain for a given stress during unloading is not the same as the corresponding value during loading, a permanent residual deformation may remain after the removal of the stress, and there will be an energy loss per cycle given by the area enclosed in the stress-strain curve for the cycle. Fig.2.4. shows a typical such curve.

If for each stress during the cycle the corresponding strain is reached instantaneously, then the form of the hysteresis loop is independent of the rate of traversal, i.e. the applied stress frequency. However, the internal friction is dependent on the amplitude of the applied stress. This behaviour is to be contrasted with that illustrated in Fig. 2.3.

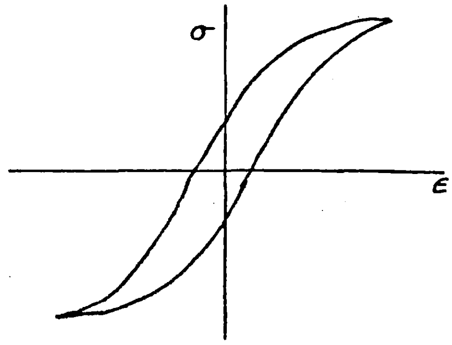

Fig. 2.4. AN ILLUSTRATION OF A TYPICAL STATIC HYSTERESIS LOOP.

CHAPTER 3.

Survey of Loss Mechanisms

A brief survey is given here of some of the ways in which energy may be dissipated from a stress wave, excluding mechanisms involving dislocations.

3.1. Direct Scattering by Crystal Defects.

Scattering of energy out of a beam will result in attenuation of the beam. Scattering of stress waves in a crystal is brought about by the presence of gradients in the elastic properties of the crystal such as will exist at surfaces and around defects. It is very difficult to separate scattering effects from the total absorption in a specimen. The problem of scattering in a medium containing scattering centres of many shapes, sizes, distributions and cross-sections as a function of frequency etc. is very complex and only simple cases have been studied in detail [Ying & Truell (56) , Einspruch, Wittenholt & Truell (60)].

Because of the anisotropy of the grains in a polycrystalline metal there is a discontinuity in the elastic constants at the grain boundaries and scattering results. [Mason & McSkimin (48) , Papadakis (65)].

3.2. Thermal Conductivity Losses.

When a material is subjected to a stress the resultant strain is accompanied by a change in temperature, the compressed parts becoming warmer than the extended parts, giving rise to temperature gradients, an irreversible heat flow, and so a dissipation of energy. For longitudinal waves the loss is inversely proportional to the wavelength until very high frequencies are reached, when the thermal path is too short for a temperature gradient to be maintained and no thermal attenuation occurs. [Mason (58), Mücke (56)]

Thermal losses do not occur for shear waves since the strain is homogeneous throughout the material and the temperature changes are the same everywhere.

For a flexural motion of a thin bar the thermal path is determined by the dimensions of the bar. At very low frequencies, the isothermal limit, the transfer of mechanical energy into heat and vice versa takes place reversibly, so there is no net heat generated per cycle. At very high frequencies, the adiabatic limit, there is not time for any heat to flow, and again there is no loss. The attenuation as a function of frequency therefore exhibits a relaxation behaviour. [Zener, Otis, Nuckolls (38)].

Another type of loss, called the Zener loss [Zener (48)] occurs in polycrystalline materials. It is a thermoelastic relaxation loss resulting from heat flow from grains that have received more compression in the course of the wave motion than adjacent grains. This loss arises from the elastic anisotropy of the grains, which may be fairly large in some metals, e.g. Pb.

3.3. Losses in Ferromagnetic Materials.

(a) The 'ΔE' effect.

This loss arises because of the magnetostrictive effect. [Bozorth (51)] In a positive magnetostrictive material, for example, a compressive stress tends to reduce the magnetostrictive expansion of a domain with polarisation directed along the stress, and to increase the magnetostrictive expansion of a domain directed perpendicular to the stress. The result is that domains at right angles to the stress grow at the expense of domains directed parallel to the stress. The net strain is therefore increased, so that Youngs Modulus, E , is decreased. This effect occurs also in ferroelastic materials. [Mason (58)].

(b) The Micro-eddy current effect.

This loss has its origin in the eddy currents generated by the stress induced motion of domain walls. [Bozorth, Mason, McSkimin (51), Kittel (58)].

(c) The microhysteresis effect.

This loss occurs because the stress-domain wall displacement curve is not a straight line but a hysteresis loop. The effect is also observed in ferroelectric materials. [Mason (58)].

3.4. Losses in Piezoelectric Materials.

In a piezoelectric crystal losses arise from the oscillating electric fields generated by a stress wave. The electric fields also lead to an increase in the effective values of the relevent elastic constants. [Kyame (49), Koga et al (58)]. Special effects are observed when the crystal is also semiconducting [Hutson & White (62)], or photoconducting [Cobsecht & Bortschat (59)].

3.5. The Interaction of Stress Waves with Conduction Electrons in Metals.

Losses arising from this interaction are significant only below about 10°K. [David (64)]. The interaction is analogous to the interaction of electrons with thermal lattice vibrations, although the latter have a somewhat different energy spectrum. This loss has been considered by Steinberg (58) and Morse (59). Special effects are observed when a magnetic field is present.

3.6. The Interaction of Stress Waves with Thermal Lattice Waves.

An interaction between a stress wave and thermal lattice waves in which the stress wave may lose energy, is possible because of the anharmonic nature of the lattice forces. Theoretical treatments have been given by Mömmel & Drensfeld (60) and Woodruff & Ehrenreich (61). In effect, one wave causes a displacement of atoms which may introduce gradients in the elastic properties of the lattice which may, in turn, scatter a second wave.

3.7. The Interaction of Stress Waves with Nuclear Spin Systems.

When a lattice is distorted by a stress wave the electric field gradient at the site of a nucleus varies periodically with the frequency of the stress wave. This field gradient produces the necessary time dependent perturbation of nuclear spin energy states to bring about transitions involving absorption of energy from the stress wave. [Truell & Elbaum (62)].

3.8. Induced Electronic Transitions.

An energy loss from an electromagnetic wave, at microwave frequencies, is possible as a result of electron transitions between energy levels produced by the splitting of one level by a magnetic field (paramagnetic resonance). The transition may be induced similarly by high frequencystress waves, which will then lose energy. [Truell & Elbaum (62)].

3.9. The Stress Induced Ordering of Defects.

This effect was first demonstrated by Snoek (41). In an unstrained lattice there may be several positions for a point defect where the elastic energy is the same. If the application of a stress separates these energy states, there will be an irreversible redistribution of defects amongst the new energy states. In this way energy may be extracted from a periodic stress wave. [Berry (62)].

A similar redistribution of point defects may occur in the stress field of a dislocation. [Shoeck & Seeger (59)]. Stress induced reorientation of defects also gives rise to a damping peak. [Dey & Quader (65)]. A large damping may also occur near the transition temperature of an order-disorder transition in ordering alloys, because of stress induced ordering. [Kê & Ma (57), Bradley (65)].

3.10. Grain Boundary Relaxation Losses.

Some low frequency (~1 c/s) relaxation peaks observed in aluminium, [Kê (49)], pure silver and gold, [Pearson & Rotherham (56)], and in pure iron, [Leak (61)] have been interpreted in terms of a stress induced grain boundary diffusion, or a stress induced grain boundary slip.

CHAPTER 4.

Experimental Methods and Typical Results

In this chapter the methods by which internal friction is usually measured will be described, and some typical results will be given. Five characteristic types of damping are identified and in later chapters distinct dislocation processes will be associated with each. Other dislocation damping phenomena may exist which have not been sufficiently investigated for any theoretical interpretation to be attempted. We begin by defining some of the quantities commonly used as a measure of the damping, and relating them to the phase lag ϕ .

4.1. Experimental Measures of the Damping.

(a) The attenuation factor, α .

Consider a plane stress wave

$$\sigma = \sigma_0 \exp(-\alpha x) \sin(\omega t - kx), \qquad (4.1.)$$

where k is the propagation constant and α the attenuation per unit distance. The term $\sigma_0 \exp(-\alpha x)$ gives an exponential envelope to the sine function and, since it is this envelope which determines the attenuation, we write

$$\sigma(x) = \sigma_0 \exp(-\alpha x). \qquad (4.2.)$$

It is assumed that α is not a function of x. Equation (4.2.) leads to

$$\alpha = -\frac{d}{dx}\left[\ln_e \sigma(x)\right], \qquad (4.3.)$$

or, considering the attenuation between two points x_1 and x_2, where $x_1 < x_2$,

$$\alpha = \frac{1}{x_2 - x_1} \ln_e \frac{\sigma(x_1)}{\sigma(x_2)} \quad \text{NEPERS / UNIT LENGTH}, \qquad (4.4.)$$

or

$$\alpha = \frac{20}{x_2 - x_1} \ln_{10} \frac{\sigma(x_1)}{\sigma(x_2)} \quad \text{db / UNIT LENGTH}. \qquad (4.5.)$$

(b) The logarithmic decrement.

If x_1 and x_2 are separated by one wave-length λ, then using the equation (4.4.)

$$\alpha \lambda = \Delta , \qquad (4.6.)$$

where Δ is the logarithmic decrement.

(c) The width of resonance.

The friction is sometimes measured in terms of the width of a resonance peak. If ω_0 is the peak resonant frequency and ω_1 and ω_2 are the frequencies at which the stress wave amplitude has fallen to $\frac{1}{\sqrt{2}}$ its peak value, then in analogy with electrical circuit resonance we define [Zener (40)]

$$Q^{-1} = \frac{\omega_2 - \omega_1}{\omega_0} . \qquad (4.7.)$$

The four quantities ϕ, α, Δ, Q^{-1} are all measures of the fractional energy loss $\frac{\Delta W}{W}$ from a stress wave per cycle, and for small damping are related as [Nowick (53)]

$$\frac{\Delta W}{W} \cdot \frac{1}{2\pi} = Q^{-1} = \frac{\Delta}{\pi} = \phi . \qquad (4.8.)$$

(d) The modulus defect.

When the friction is measured by the resonant frequency technique described below, the modulus defect is related to ϕ and to the fractional change in resonant frequency $\frac{\Delta f}{f}$ as [van Dueren (61)]

$$\frac{\Delta G}{G} = \phi = 2 \frac{\Delta f}{f} . \qquad (4.9.)$$

The fractional velocity change of the stress wave, $\frac{\Delta v}{v}$, in the presence of damping is related similarly to the modulus defect:

$$\frac{\Delta G}{G} = 2 \frac{\Delta v}{v} . \qquad (4.10.)$$

(e) The orientation factor.

Before theoretical values of the friction may be compared with experimental values it is frequently necessary to introduce an orientation factor to take into account the orientation relations between the direction of propogation of a stress wave and the various possible dislocation slip planes and directions. Also, many theoretical treatments employ shear stresses and shear strains, while experimentally longitudinal stress waves may be used, for example. Granato & Lücke (56) have considered the corrections necessitated by these effects. [See also ch. 7.12.]

4.2. Methods of Measuring the Damping.

(a) The torsion pendulum method.

This method requires a specimen in the form of a thin rod or strip which is then used as a suspension for an inertia member. The damping is determined by observing, either optically or with a capacitance strain gauge [Brown (61)], the rate of free decay of torsional oscillations. [Kê (47)]. A modification of the method in which the decay of velocity is measured instead has been given by de Morton, Lott & Stainsby (63). The torsion pendulum method is suitable for measurements in the approximate frequency range $0{\cdot}1\,c/s \rightarrow 15\,c/s$, and maximum strain amplitudes of about 10^{-4} may be used. The sensitivity of the method is limited by the background damping arising from losses in the apparatus, so very small damping, $Q^{-1} \ll 10^{-4}$, cannot be measured. An inverted torsion pendulum [Weinig (55)] apparatus has been described by Swartz (61), which enables decrements above 4.10^{-5} to be measured at maximum strain amplitudes in the range $2.10^{-7} \rightarrow 2.10^{-4}$. Simultaneous modulus measurements may be made, and a temperature range $80^{\circ}K \rightarrow 1000^{\circ}K$ may be used. A similar apparatus described by Okuda (63) enables measurements to be made between $4{\cdot}2\,^{\circ}K$ and room temperature. Measurements in the frequency range $10^{-1} \rightarrow 10^{-2}\,c/s$ have been made by direct measurement of hysteresis loops. [Roberts & Brown (60)].

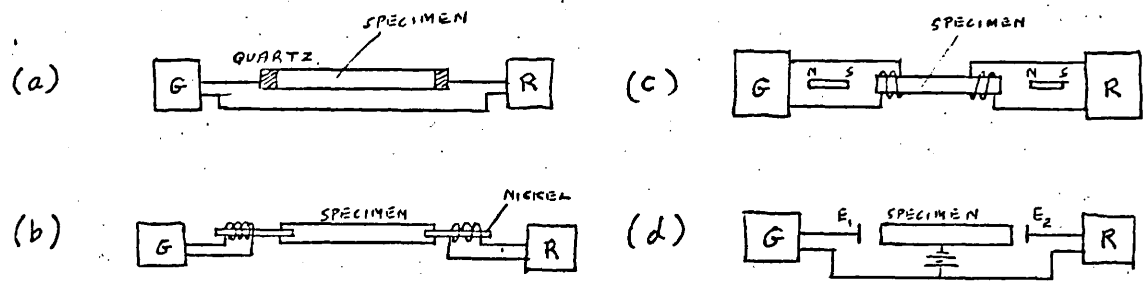

Fig. 4.1(a)-(d). SOME METHODS OF EXCITING LONGITUDINAL WAVES IN A ROD [AFTER GIACOMINI (56)]

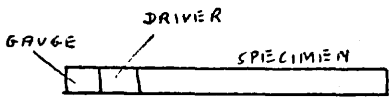

Fig. 4.2. ARRANGEMENT OF A MARX COMPOSITE OSCILLATOR.

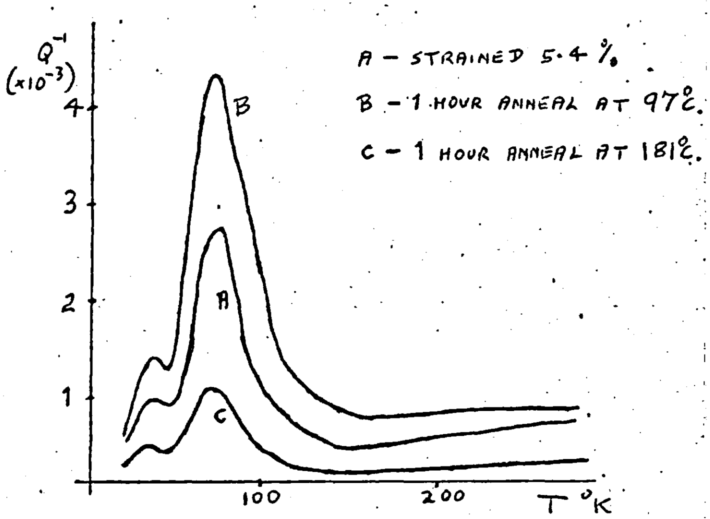

Fig. 4.3. INTERNAL FRICTION OF A Cu SPECIMEN AFTER STRAINING AND THEN ANNEALING. [AFTER NIBLETT & WILKS (55)].

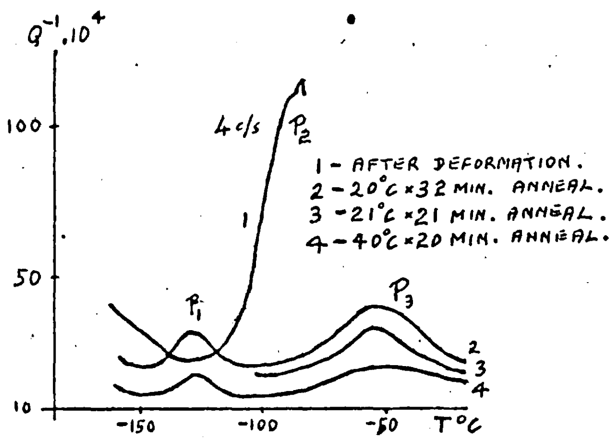

Fig. 4.4. THE PEAKS P_1, P_2 AND P_3 IN A GOLD SPECIMEN [AFTER OKUDA & HASIGUTI (63)].

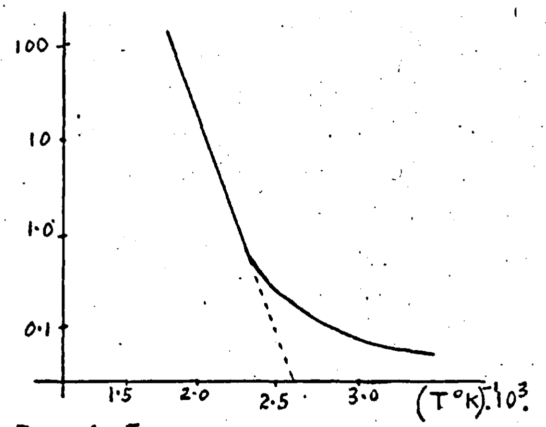

Fig. 4.5. Δ AS A FUNCTION OF TEMPERATURE [AFTER CHAMBERS (57)].

(b) Damped eigen vibration method. (Resonant bar technique)

The specimen, usually in the form of a bar or plate, is excited in one or more of its resonances, and the decay of the oscillations is measured. Very small damping, $Q^{-1} \geqslant 10^{-7}$, can be measured by this method. The frequency range in which the method is applicable is determined by the practical range in dimension of the sample, and is roughly 100c/s → 300Kc/s. Either longitudinal, torsional or flexural waves may be used. Fig. 4.1. illustrates some methods of exciting longitudinal vibrations in a rod, which for increased accuracy should be placed in vacuum.

Fig. 4.1. (a) illustrates the use of a quartz piezoelectric transducer [Quimby (25), Balmouth (34)]. The frequency of the driving voltage is made to very until the rod vibrates at resonance in the mode required. Another quartz crystal is connected to a detector to enable the conditions of resonance to be ascertained.

Many experimental methods are based on the three component piezoelectric resonator of Marx (51). In this arrangement an auxiliary quartz crystal is added to the piezoelectric resonator and serves as a strain gauge, as illustrated in Fig.4.2. Measurements of the decrement may be made virtually instantaneously. A modification of this arrangement by Baker & Carpenter (65) enables strain amplitudes in the range $10^{-10} \rightarrow 10^{-4}$ to be used.

In Fig.4.1.(b) the exitation and the detection are performed using two magnetostrictive transducers [Stanford (50)]. In Fig.4.1.(c) the driving force is obtained by interaction between an external magnetic field and eddy currents generated at one end of the rod by means of a suitable coil. [Zener, Rose & Randall (39)]. In Fig.4.1. (d) the excitation is obtained by electrostatic attraction between an electrode E_1 and one end of a metal rod specimen. [Jacobs & Bancroft (38)]. The detection is also electrostatic, based on the periodic variation of capacitance between the other end of the rod and a second electrode E_2. [Bruner & Mecs (63).]

A review of transducers used in the generation and detection of ultrasonic waves has been given by Barone (62). Systems for the automatic recording of internal friction measurements have been given by Kharitonov (61), Thompson & Glass (58).

(c) Pulse Methods.

A short pulse is radiated into the material under examination and detected after it has travelled a known distance, enabling the propagation velocity to be measured. The attenuation of the pulse may also be determined by comparing the transmitted and received pulses e.g. on an oscilloscope. Some versions of the pulse-echo technique have been used by Huntington (47), Roderick & Truell (52) and Chick, Anderson & Truell (60). The method is much used in the frequency range 1 Mc/s - 100 Mc/s. The strain amplitude may be easily varied, although it is usually quite small. Distortion of the pulse may arise due to scattering from the sides and end of a specimen, or effects arising from the coupling of the transducer to the specimen or from stresses in the specimen. A review of these and other spurious causes of change in pulse shape has been given by Redwood (65).

4.3. Some Typical Experimental Results.

(a) The Bordoni Internal Friction Peaks.

In a great many different annealed metals cold working is found to produce two characteristic peaks in the plot of internal friction against temperature around 80°K and 40°K, depending on the measuring frequency.

They are known as Bordoni peaks after Bordoni (47). The low temperature peak, first observed by Niblett & Wilks (55) is usually much the smaller. A typical example from the results of Niblett & Wilks (55) on copper is shown in Fig.4.3, which also shows the typical reduction of the damping upon annealing. These peaks are considered in chapter 5.1, and interpreted in terms of a relaxation process.

(b) The Hasiguti Internal Friction Peaks.

These are a group of perhaps three peaks, which have been observed by, amongst others, Okuda & Hasiguti (63) whose measurements on a gold specimen are shown in Fig.4.4. The peak labelled P_2 appeared at about 200°K after the specimen was deformed torsionally 16.4% at about 70°K. The peaks Labelled P_1 (140°K) and P_3 (220°K) appeared, and P_2 disappeared, after a 32 minute anneal at 20°C. These peaks are considered further in chapter 5.2, and are interpreted as relaxation peaks.

(c) The Internal Friction At High Temperatures.

This is a type of friction independent of strain amplitude observed at low strain amplitudes and relatively high temperatures, and is characterised by a rapid increase of decrement with temperature, according to

$$\Delta = R \exp\left(-\frac{E}{kT}\right), \tag{4.11.}$$

where R is a constant, and E an activation energy. This behaviour has been observed in both single crystal and polycrystalline specimens, but in the latter it is usually observed by grain boundary relaxation losses, (see chapter 3.10.) so only single crystal specimens will be considered. A typical result for aluminium is shown in Fig.4.5, where the exponential relation sets in at about 450°K. The activation energy calculated from the slope of the graph is about 0.9e.v., and this is typical of the values found for most metals. The friction has been found for copper and

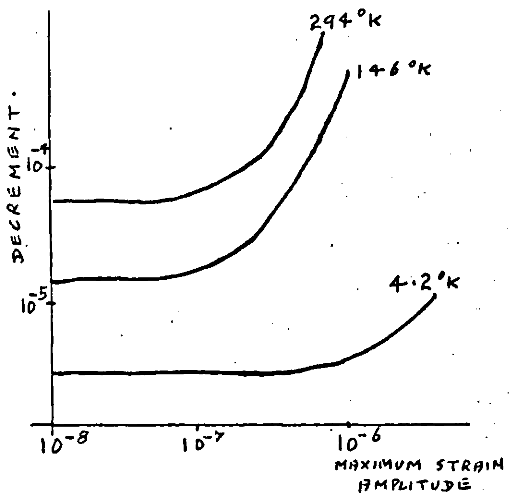

Fig. 4.6. INTERNAL FRICTION OF A Cu SINGLE CRYSTAL AT 40Kc/s [AFTER CASWELL (58)].

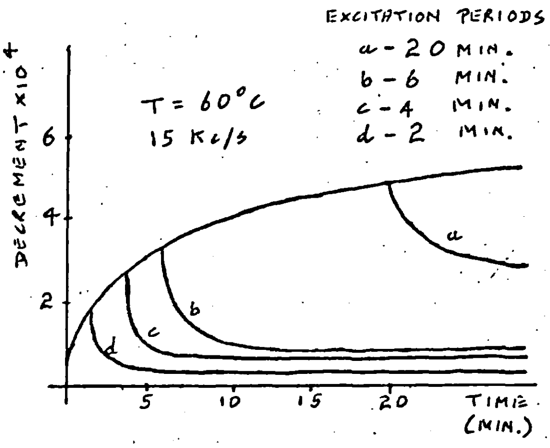

Fig. 4.7. INTERNAL FRICTION OF AN Al. SINGLE CRYSTAL EXCITED DIFFERENT LENGTHS OF TIME AT A CONSTANT STRAIN AMPLITUDE [AFTER CHAMBERS (57)].

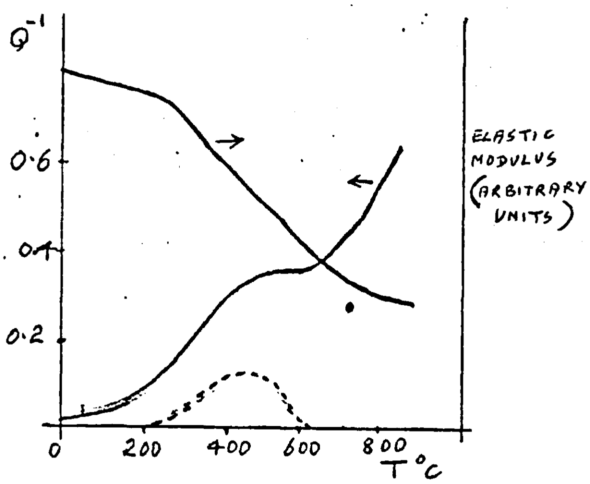

Fig. 4.8. FRICTION AND MODULUS CHANGE WITH TEMPERATURE. DOTTED LINE IS AN ANALYSIS OF THE PEAK. [AFTER KAMEL (61)].

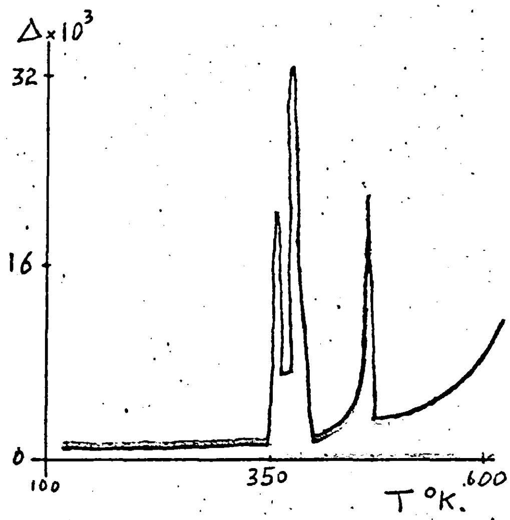

Fig. 4.9. INTERNAL FRICTION PEAKS IN Al. SINGLE CRYSTALS. [AFTER BIRNBAUM & LEVY (56)].

aluminium to decrease with increasing frequency at a rate slightly less rapid than the reciprocal of the frequency. Cold work is found to increase the damping considerably, especially in single crystals where the energy of activation itself increases with the amount of prestrain. This type of friction is considered further in chapter 5.3. Most theoretical treatments assume this friction arises by a relaxation process.

(d) Amplitude dependent friction at low and medium temperatures.

This is a type of friction common to all metals at low and medium temperatures. Fig.4.6. shows typical results obtained by CASWELL(58) in a lightly cold worked copper sample. The friction is also seen to increase with increasing temperature. The form of the curves in Fig.4.6. suggests that two different mechanisms are responsible for the friction. The decrement will accordingly be resolved into two components, Δ_I being the strain amplitude independent decrement observed at small stress amplitudes (see following section) and Δ_H the remaining strain amplitude dependent decrement. It is found that in general Δ_H increases with cold working but with large degrees of cold work shows a maximum. The presence of impurities is found to reduce this friction. The experimental evidence concerning the frequency dependence of Δ_H is indecisive, in some cases there is a small frequency dependence and in others none. The modulus defect $\left(\frac{\Delta G}{G}\right)_H$ and Δ_H are found to be roughly proportional to each other, the constant of proportionality varying from about 0.15 to 6 in different specimens. The damping is found also to be reduced by quenching from a high temperature and usually the faster the quench the greater the reduction.

Care must be taken when measuring the friction that time dependent effects are not causing errors. Fig.4.7. shows the results of Chambers(57) for the damping of aluminium as a function of time after excitation at a constant amplitude for 2,4,6 and 20 minutes. A damping of this nature which appears after a deformation (excitation) and anneals out with time either at the deforming temperature or a higher one, is known as the Köster effect. [Köster (40)]. This friction is considered further in chapters 6, 7 and 8.

(e) Amplitude independent friction at low strain amplitudes.

This is observed at low strain amplitudes and at temperatures below those at which the thermally activated friction of (c) above occurs. It is the component Δ_I of the preceeding section. When measuring this friction care must be taken since it is frequently small and background losses in the experiment may be significant, especially the thermoelastic losses (chapter 3.2.). Usually the friction increases monotonically with rising temperature although in general Δ_I does not seem to be a simple function of temperature. The experimental evidence regarding the frequency dependence of Δ_I is again inconclusive, some results showing a decrement proportional to frequency and others one independent of frequency. Small amounts of cold work are found to increase the friction and as with the amplitude dependent friction there is often a Köster effect. In general the effect of impurities is to reduce this component of the friction. Neutron irradiation is found to have a similar effect.

A theory of this type of friction will be developed in chapter 6.

(f) Miscellaneous Internal Friction Peaks.

Apart from the five characteristic types of damping noted above a number of miscellaneous peaks in the damping plotted as a function of temperature have been observed, which might be arising from a dislocation mechanism. Examples of such peaks will be given here, but they will be given no further attention.

Okuda (63) has observed a peak in gold below 15°K due to cold work, which might be associated with the motion of kinks along dislocation lines. Hasiguti, Igata and Kamoshita (62) have observed peaks apparently lying between the Bordoni peak and the lower Hasiguti peak, in measurements on aluminium.

Kessler (57) has observed a peak in the friction of germanium at 385°C, (see Fig.5.23.) which shifts its position to lower temperatures after the temperature cycle associated with a set of measurements. He proposes a relaxation mechanism involving the stress induced diffusion of impurity atoms located at sites which are inequivalent not by virtue of the basic crystal structure, (cf. chapter 3.9.) but by the strain field round an edge dislocation.

A peak observed in gold by Kamel (61) in the region of 450°C at a frequency of 25c/s is shown in Fig.4.8. together with the associated modulus G. Quenching from 1000°C to room temperature was found to increase the height of the peak considerably, but the temperature of the peak remained unchanged. The peak was observed to move to higher temperatures as the applied frequency was increased, and was associated with a relaxation process involving the thermally aided microcreep of pinned dislocation lines under the action of the applied alternating stress field. The behaviour of the peak after quenching suggests the defects involved are vacancies.

Filloux, Harper & Chambers (64) have made extensive measurements on two b.c.c. metals, Nb and Ta, in the temperature range 4°K - 500°K, at frequencies between 10^{-3} and 10^{5} c/s, maximum strain amplitudes between 10^{-8} and 10^{-3}, torsional bias stresses in the range 10^{-5} - 5.10^{-3} G and found nine separate peaks in the decrement, with associated modulus defects, one of them at around 8°K.

Other peaks are sometimes observed and are often not reproducible, making a systematic study difficult. Fig.4.9. shows the results of Birnbaum & Levy (56) for an aluminium single crystal. It was found in this experiment that the heat treatment during the first series of measurements was sufficient to remove the peaks completely. These and other miscellaneous peaks have been reviewed by Niblett & Wilks (60).

CHAPTER 5

Relaxation Losses

5.1. The Bordoni Peaks.

The existence of these peaks has already been noted in Chapter 4.3(a). Before presenting theoretical interpretations of these peaks, the behaviour of the peaks under different experimental conditions will be summerised.

(a) Experimental Observations of the Peaks.

(i) The effect of plastic deformation.

The peaks are absent in a perfectly annealed specimen and appear only when the specimen is subjected to cold work. Fig.5.1. shows the results of Caswell (58) for a copper single crystal. Cross-rolling, which activates a different set of slip planes, is seen to have a more pronounced effect on the main peak height than continued deformation above 3% in one direction. Measurements on single crystals have also been made by Briggs (55). Similar effects have been observed in polycrystalline specimens by Niblett & Wilks (57). The results of Caswell (58) suggest that the main peak moves to a slightly higher temperature with increasing cold work.

(ii) The effect of an anneal.

As mentionedabove the peaks are not observed in a fully annealed specimen. The actual annealing behaviour is rather complicated however. Fig. 5.2. shows the results of Carter & Wilks (63) taken on a polycrystalline aluminium specimen at 1 c/s. An annealed specimen was first strained 4.0% at 90°K and allowed to rest at this temperature for 20 hours, when the friction had decreased to the constant value

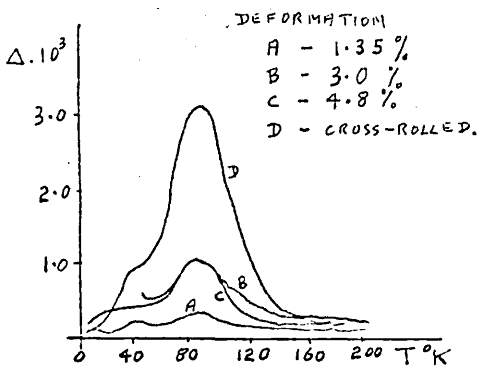

Fig. 5.1. THE EFFECT OF VARIOUS DEFORMATIONS ON THE BORDONI PEAK IN A Cu SPECIMEN [AFTER CASWELL (58)].

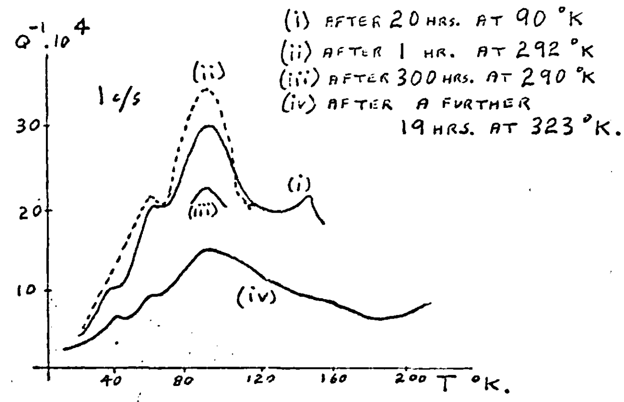

Fig. 5.2. ANNEALING BEHAVIOUR OF AN Al SPECIMEN [AFTER BAXTER & WILKS (63)].

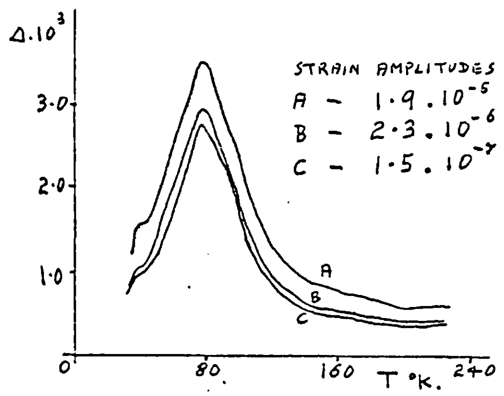

Fig. 5.3. STRAIN AMPLITUDE DEPENDENCE OF THE BORDONI PEAK IN Cu. [PARÉ (61)].

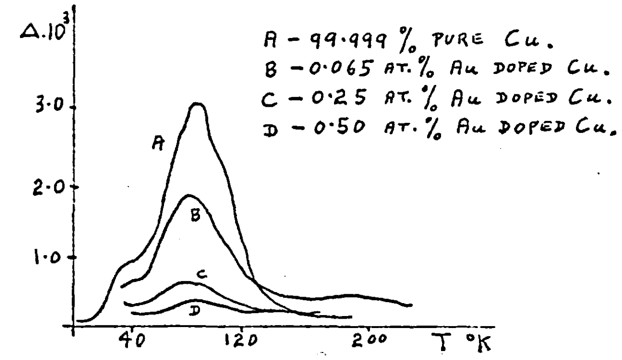

Fig. 5.4. INTERNAL FRICTION OF SEVERAL CROSS-ROLLED Au DOPED Cu CRYSTALS [AFTER CASWELL (58)]

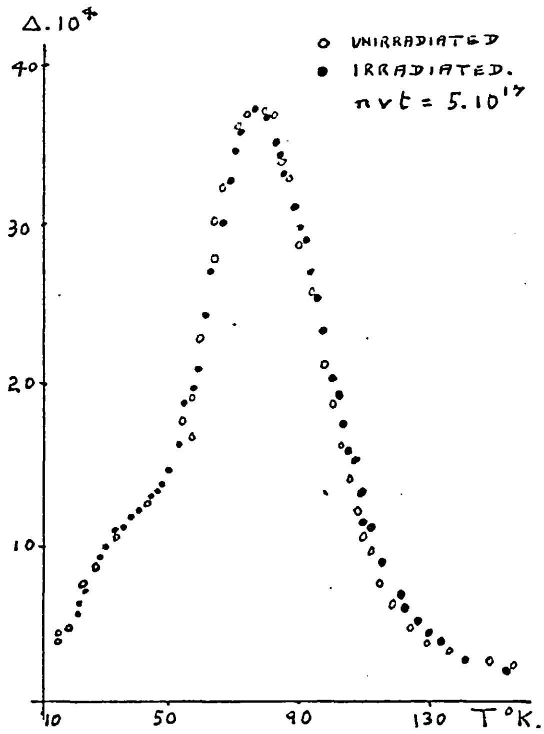

Fig. 5.5. FRICTION OF AN IRRADIATED AND UNIRRADIATED Cu SPECIMEN. EACH UNIRRADIATED POINT IS REDUCED BY 19·6 % [AFTER THOMPSON & HOLMES (59)].

corresponding to curve (i) in Fig.5.2. The main peak occurs at 95°K and two smaller peaks at approximately 66°K and 52°K. Another smaller peak occurs at about 148°K. The specimen was then annealed in stages to bring it up to room temperature. Annealing for one hour at 292°K increased the height of the main peak as shown by curve (ii). Further anneals at higher temperatures are seen to decrease the peak hight. These results indicate that at least two processes are involved in the annealing of the Bordoni peak in plastically deformed aluminium. A similar annealing behaviour has been observed in copper by Niblett & Wilks (59).

To remove the peak completely an anneal at a temperature just below the recrystallisation temperature of the specimen is required. This is a much higher temperature than that required to anneal out point defects [Niblett & Wilks (56)].

Measurements by Bordoni et al. (59), Caswell(58), Niblett & Wilks (59) and Baxter & Wilks (63) all indicate that the temperature at which the main peak occurs is lowered by around 5 to 10°K by annealing in the region of 200°K.

(iii) The dependence on strain amplitude.

The results of Niblett & Wilks (57), Sack (62), Paré (61) and Caswell (58) show that the strain amplitude dependence of the friction in the Bordoni peak region is not much different from that of the background (or annealed sample) friction, though the magnitude of the friction is higher at larger strain amplitudes. Fig.5.3. shows the results of Paré (61). In particular the temperature of the peak is seen to be unaffected.

(iv) The effect of purity.

The height of the Bordoni peak is greatly reduced by the presence of impurities. Fig.5.4. shows the results of Caswell (58) for a copper specimen which illustrate this effect. Caswell also observed that nickel, which has an atomic radius 2·5% greater than copper, was less effective in reducing the peak height than gold, which has an atomic radius 11·0% greater. The sensitivity of the peak height to impurity content is illustrated by the results of Niblett & Wilks (56), who found the peak height in pure copper to be reduced by a factor of ten when 0·0026% Bi and 0·032% P was added.

The main peak is also observed to move a few degrees towards a lower temperature when impurities are added, and at the same time it appears to become slightly broader [Niblett & Wilks (57), Caswell (58)].

Neutron irradiation appears to have a very similar effect on the Bordoni peaks as the presence of impurities. [Niblett & Wilks (60)] Fig.5.5. shows the measurements made by Thompson & Holmes (59) on a polycrystalline copper specimen before and after neutron irradiation. The two peaks have been brought into coincidence simply by reducing the unirradiated peak by 19·6%.

(v) The effect of frequency.

The peaks have been observed at frequencies from around 1c/s [Baxter & Wilks (63)] to several Mc/s [Bordoni et al. (59)]. If the Bordoni peaks arise from a simple relaxation process a graph of $\ln \omega$ against $\frac{1}{T_{PK}}$, where ω is the measuring frequency and T_{PK} the temperature at which the peak occurs, should give a straight line whose slope is equal to the activation energy E of the process, and whose intercept on the $\ln \omega$ axis gives the attempt frequency of the process (cf. equation 2.20.).

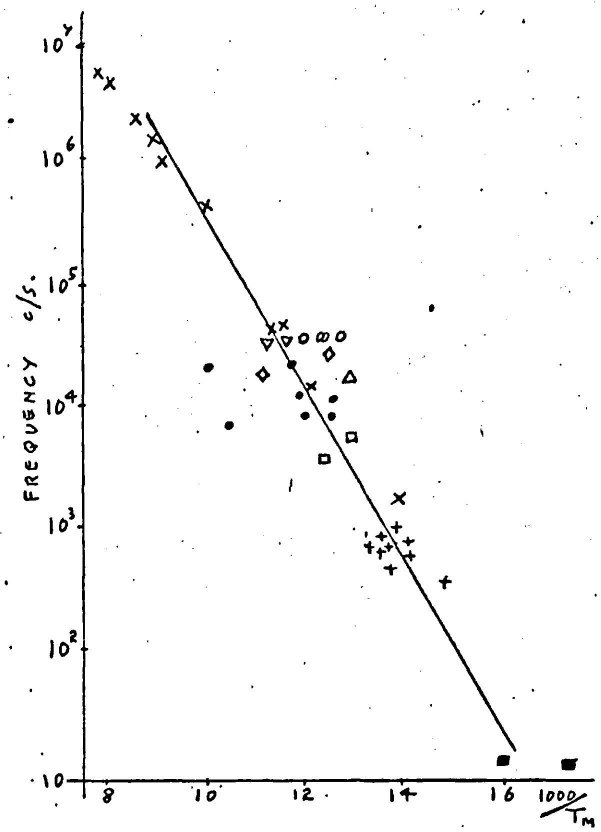

Fig. 5.6 FREQUENCY DEPENDENCE OF THE TEMPERATURE OF THE BORDONI PEAK IN COLD WORKED COPPER [AFTER NIBLETT (61)].

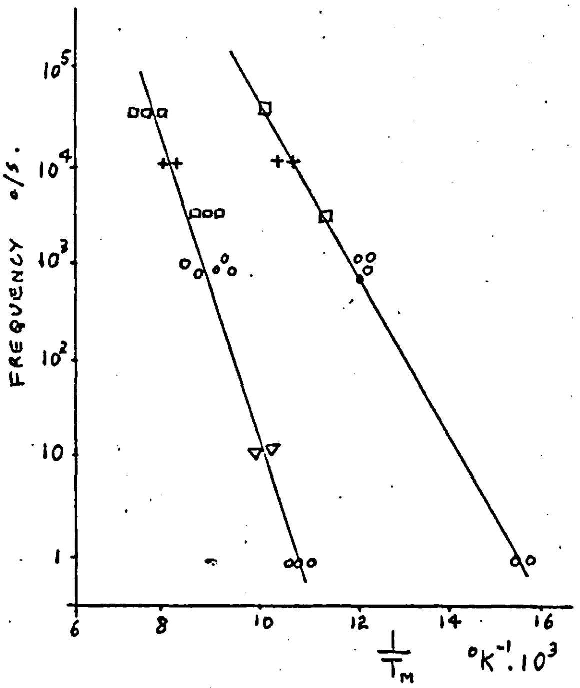

Fig. 5.7. FREQUENCY DEPENDENCE OF THE BORDONI PEAK IN Al. [AFTER BAXTER + WILKS (63)].

Niblett (61) has plotted such a graph, which is shown in Fig.5.6, using all the available experimental results on pure copper specimens with similar cold work treatments. The points show considerable scatter, which may arise because of differing amounts of deformation, degrees of purity and aging at room temperature, although Paré (61) has shown this is unlikely.

Fig.5.6. indicates an activation energy of about 0·14e.v. and an attempt frequency of about 4.10^{12} $sec.^{-1}$ Measurements by Bordoni et. al.(59) at frequencies in the range 1·8Kc/s to 6·5Mc/s indicate an activation energy of 0·122 ev. and an attempt frequency of $2{\cdot}4.10^{12}$ $sec.^{-1}$ but relatively impure copper specimens were used (0·12% Pb) which could account for the discrepancy between these two results. Measurements on a single pure specimen over a wide frequency range are really required.

Fig.5.7. shows similar results for Al compiled by Baxter & Wilks (63). A curve is plotted for both the main and subsidiary peak. Again the points show considerable scatter. An activation energy of 0·30ev. and an attempt frequency of 10^{16} $sec.^{-1}$ are found for the main peak,and corresponding values of 0·17ev. and $\sim 10^{13}$ $sec.^{-1}$ for the subsidiary peak, are calculated. These attempt frequencies seem rather high for any dislocation motion. However, the peaks appear to be too broad to represent a single relaxation process, and probably involve a distribution of activation energies or attempt frequencies, or both. Bordoni et al. (59) concluded from the shape of the peak at different frequencies that a distribution of attempt frequencies existed. Berry & Nowick (60) and Niblett (61) have also considered the effect of such distributions.

Niblett (61) has calculated the theoretical dependence of the width of the main Bordoni peak, $\Delta\left(\frac{1}{T}\right)$, on the peak temperature, T_M, for the case

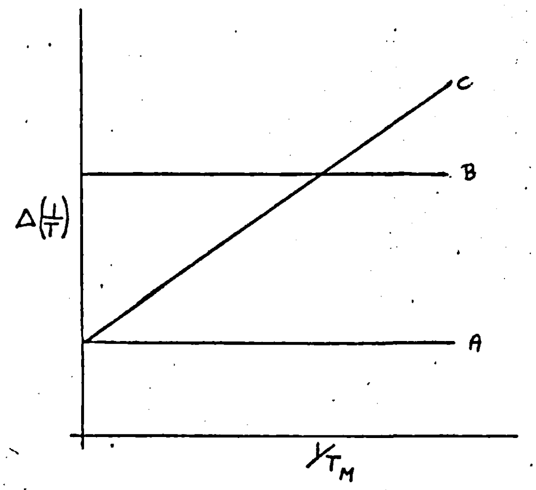

Fig. 5.8. THEORETICAL DEPENDENCE OF THE WIDTH OF THE BORDONI PEAK ON THE TEMPERATURE OF THE PEAK FOR:
A – SINGLE RELAXATION PROCESS
B – SINGLE ACTIVATION ENERGY
C – SINGLE ATTEMPT FREQUENCY.
[AFTER NIBLETT (61)].

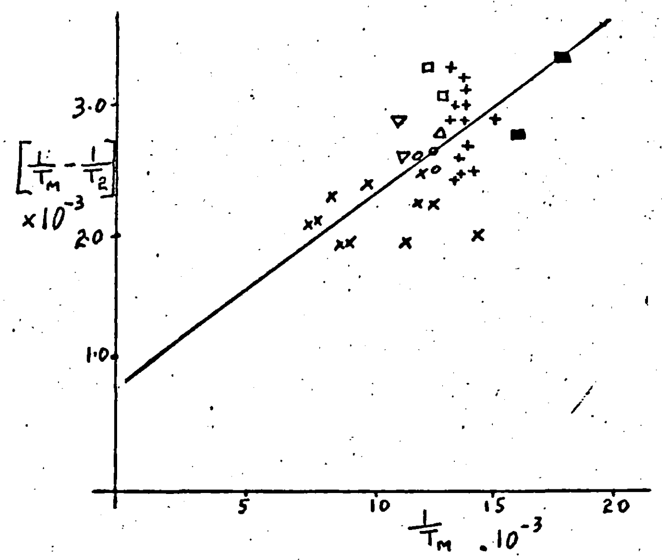

Fig. 5.9. EXPERIMENTAL DEPENDENCE OF PEAK WIDTH ON PEAK TEMPERATURE FOR THE RESULTS OF Fig. 5.6. [AFTER NIBLETT (61)].

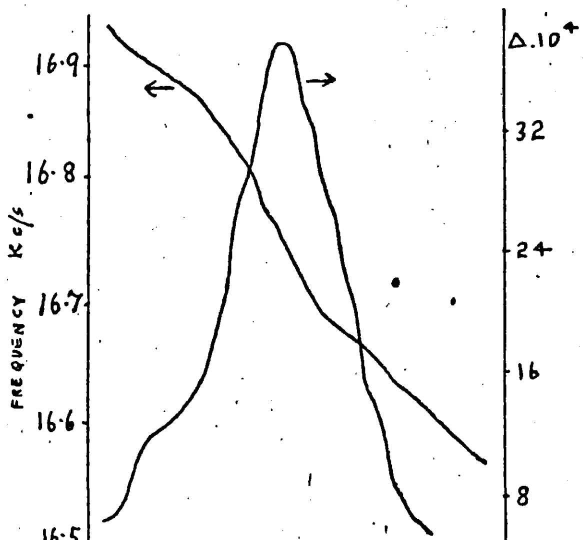

Fig. 5.10. DECREMENT AND RESONANT FREQUENCY OF AN IRRADIATED POLY-CRYSTALLINE Cu SPECIMEN [AFTER THOMPSON & HOLMES (59)].

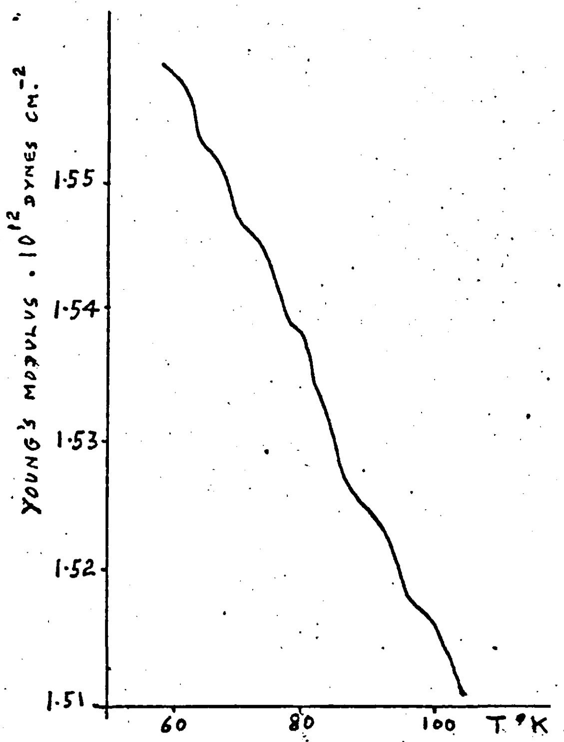

Fig. 5.11. A PLOT OF YOUNG'S MODULUS v.s. TEMPERATURE FOR A Cu CRYSTAL [AFTER THOMPSON & HOLMES (59)].

of,(A) a single relaxation process, (B) a single activation energy, but a distribution of attempt frequencies, and (C) a single attempt frequency, but a distribution in activation energies. The results of this calculation are illustrated in Fig.5.8. where the peak width $\Delta(\frac{1}{T})$ is plotted against $1/T_M$ and the lines A,B and C refer to the conditions above. The exact slope of the curve C, and the separation A and B depend on the breadth of the distribution assumed. Fig.5.9. shows the results of Fig.5.6. treated in this way. The peak width was taken as $\left(\frac{1}{T_M}-\frac{1}{T_2}\right)$, where T_2 is the temperature, greater than T_M, at which the friction has fallen to half its maximum value in order to eliminate the effect of the subsidiary Bordoni peak. The scatter of the experimental points is considerable, but a distribution in activation energies with a single attempt frequency seems slightly favoured. It is probable, however, that a complete description will have to introduce a range of both activation energies and attempt frequencies.

(vi) The modulus defect.

Simultaneous measurements of Youngs modulus, G, and the decrement in the region of the Bordoni peaks have been made by Thompson & Holmes (59), using the resonant bar technique and frequencies of 10 to 20 Kc/s. Fig.5.10. shows the results obtained for a neutron irradiated polycrystalline copper specimen. At the temperatures of the peaks the modulus curve is seen to have a complex step like structure. Fig.5.11. shows similar measurements on a similar but unirradiated and less cold worked crystal. The curve is seen to show considerable structure. The detail was found to decrease with increasing cold work. In the simple relaxation theory of Zener (48), abrupt decreases in the modulus are to be expected at temperatures at which peaks in the decrement appear also, cf. chapter 2.3(a). This again suggests, therefore, that the Bordoni peaks contain a number of superposed relaxation peaks.

(vii) Measurements in b.c.c. and hexagonal lattices.

So far only materials having a f.c.c. structure have been considered, and in fact most investigations have been on such materials. A review of the experimental data relating to f.c.c, b.c.c. and h.c.p. lattices has been given by Sack (62). In iron, a b.c.c. metal, a few experimental results have been obtained, but it is not possible to say definitely whether there is a Bordoni type peak. Chambers & Schultz (62) have studied the b.c.c. metals Nb, Ta, Mo and W, and found there exist two relatively broad thermally activated relaxation peaks in the internal friction versus temperature curves of plastically deformed specimens of these metals. The peaks are similar in some ways to the Bordoni peaks observed in copper. The activation energies are around 2 to 4 times larger than in copper, while the attempt frequencies tend to be slightly lower than in copper. The peaks also show a structure. The two classes of metal also show a difference in their response to annealing, the structure of the peaks in the b.c.c. metals being affected at anneal temperatures much below those required to produce similar effects in f.c.c. metals.

As for copper, the effect of impurities is to reduce the peak height and peak temperature. A thermal aging treatment at temperatures just under the recrystallisation temperature in Mo produces a large increase in the modulus measured at room temperature, but very little change in that measured at 5°K. This behaviour indicates that, contrary to the behaviour in copper, only a very small fraction of the dislocations in cold worked Mo are free to move at 5°K. Thus almost all dislocations in Mo must be thermally activated over barriers that are generally much larger than those found in the f.c.c. metals.

In the class of h.c.p. metals, magnesium has been studied by Tsui (61), and zinc by Read (40). Peaks are observed with essentially the same character as those appearing in f.c.c. metals.

Thus it is probable that the mechanism producing the Bordoni peaks in f.c.c. metals is operative in other metals also, although a definite decision cannot yet be made.

(viii) The Niblett and Wilks peak.

The behaviour of this peak, which appears on the low temperature side of the main Bordoni peak, is usually very similar to that of the main peak. For example, low temperature anneals cause the subsidiary peak to decrease in magnitude about as rapidly as the main peak, in copper, and even faster than the main peak, in gold [Okuda (63)]. While the Niblett & Wilks peak is normally smaller than the main Bordoni peak, Okuda (63) finds that in gold after a deformation in torsion, rather than tension, it is as large as the main peak. Brailsford (65) notes that while the main peak moves to slightly lower temperatures when impurities are added, the temperature of the subsidiary peak is apparently unchanged.

(b) Theoretical interpretations of the Bordoni Peaks.

The fact that the peak moves to higher temperatures at higher frequencies, and the apparent independence of the peak of strain amplitude, suggests a relaxation mechanism is responsible for the peaks. Since for a fixed applied frequency the temperatures at which the peaks occur are affected at most very little by cold working, the activation energy associated with the peak is independent of both the density of dislocations present and the separation of dislocation nodes. The activation energy seems also to be unrelated to the presence of point defects, since for a fixed frequency the temperatures of the peaks are largely independent of the concentration and nature of the impurities present. These experimental observations, together with the fact that the peaks anneal out at temperatures near the recrystallisation temperature of a specimen, which is far above the temperature at which point defects anneal out, suggest that an intrinsic dislocation mechanism is responsible for the relaxation; a mechanism which does not depend on a particular length of dislocation line, or on its interaction with impurity atoms. Seeger (55) & (56) and Seeger et al. (57) have proposed such a mechanism, in which short lengths of dislocation are thermally activated over the Peierls barrier [COTTRELL (53)] in a crystal.

(i) Seegers' theory.

Consider a length of dislocation lying parallel to one of the close packed directions of its glide plane. In order to move such a dislocation into an adjacent potential well without the aid of thermal energy, a shear stress must be applied normal to the dislocation equal in magnitude to the

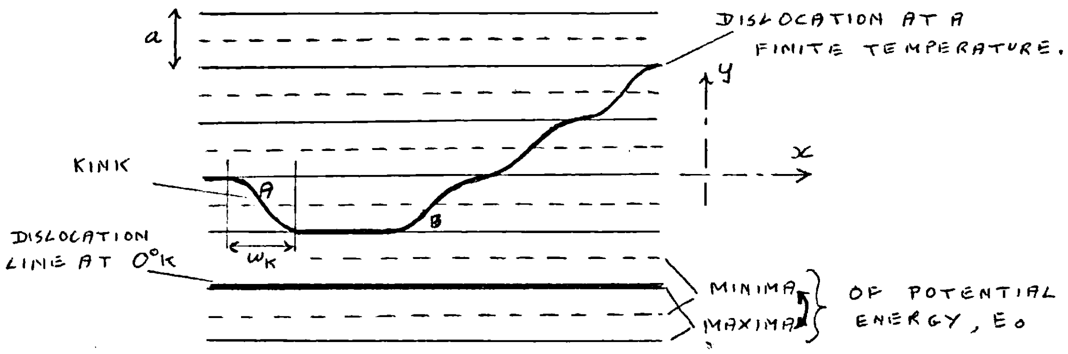

Fig. 5.12. THE POTENTIAL ENERGY SURFACE OF A DISLOCATION DUE TO THE PEIERLS STRESS.

Peierls stress at absolute zero, σ_p^o. However, at finite temperatures, a section of the dislocation line is set into transverse vibration in its slip plane by thermal stress waves, and in some cases the random action of thermal vibrations will be sufficient to drive part of the dislocation into a neighbouring potential valley in each cycle. If the resulting pair of kinks, A and B in Fig.5.12, attain a sufficient separation, d_{cr}, which depends on the applied stress, they may be pulled apart by the applied stress so that the whole dislocation moves to the neighbouring valley. The applied stress necessary to separate two kinks is much smaller than the Peierls stress, σ_p^o.

At separations less than d_{cr} the motion of the kinks is essentially reversible. Thus for an applied stress $\sigma < \sigma_p^o$ a dislocation line can move foreward by two processes, i) the sideways motion of kinks, ii) the formation of new pairs of kinks of opposite sign. The kink formation requires thermal energy, and so occurs with a temperature dependent frequency. If the frequency, f, of the applied stress is large compared with the frequency, ν, with which a pair of kinks in a dislocation is formed, kink formation contributes nothing to the strain and to the energy dissipation. If f is small compared with ν, the kinks are always in thermal equilibrium, and again no energy loss occurs. However, when the two frequencies are approximately equal, an internal friction results. The energy dissipation takes place as phonon radiation from accelerating dislocation lines.

To calculate the magnitude of the internal friction, the rate of formation, ν, of double kinks must be calculated. Seeger (55) used the Arrhenius equation [Zener (52)],

$$\nu = \nu_0 \exp\left(\frac{-H}{kT}\right), \qquad (5.1.)$$

where ν_0 is an attempt frequency, ie. the number of times a second the dislocation is in a favourable position for the formation of a bulge, and H is the activation energy for the formation of a bulge. Seeger took H to be just twice the additional energy, W_k, associated with a single kink in a dislocation which is otherwise parallel to a lattice direction, and ν_0 he took to be just the frequency of oscillation of a dislocation in a Peierls potential well. This treatment, however, gives only an approximate agreement with the experimental observations, (in particular the temperature of the peak is predicted to vary with strain amplitude), because equation (5.1.) is not applicable to the formation of bulges in dislocation lines. This equation is applicable, for example, to the motion, along a fixed path, of single atoms from an initial to a final state. However, a bulge in a dislocation extends over a 100 or more atoms, and a dislocation in changing from its initial state, ie. lying in a single potential well, to its final state, ie. containing two kinks which are sufficiently separated to be stable, does not pass through a well defined saddle point configuration, since there are a variety of ways by which the final state may be reached. Equation (5.1.) is therefore not applicable.

Seeger, Donth & Pfaff (57) have given a more thorough treatment of this problem using Donth's (57) statistical calculation of the rate of thermally activated kink formation, and a summary of their theory will be given here. The shape of a dislocation line, $y(x,t)$ (see Fig.5.12.) is to a good approximation determined by the equation [Seeger (56)]

$$E_0 \frac{d^2 y}{d x^2} - m \frac{d^2 y}{d t^2} = b\, \sigma_p^0 \sin \frac{2\pi y}{a} - b\sigma , \qquad (5.2)$$

where E_0 and m are the energy and mass per unit length of the dislocation, b is the Burgers vector of the dislocation, σ the resolved applied shear stress, and a the lattice parameter in the y-direction. Equation (5.2.)

leads to a kink energy, W_K, of the form

$$W_K = \frac{2a}{\pi}\sqrt{\frac{2ab\sigma_p^0 E_0}{\pi}} \quad , \tag{5.3.}$$

a kink width, ω_K, (see Fig.5.12.)

$$\omega_K = \left[\frac{\pi a E_0}{2b\sigma_p^0}\right]^{1/2} , \tag{5.4.}$$

and a critical kink separation, d_{CR}, under an applied stress, σ, $(\sigma << \sigma_p^0)$

$$d_{CR} = \frac{\omega_K}{\pi} \ln\left(\frac{16\sigma_p^0}{\pi\sigma}\right) . \tag{5.5.}$$

Donth shows that a solution of equation (5.2.) may be found in terms of normal modes of dislocation vibration, each characterised by an energy, W', per wavelength. In the case $W' \doteqdot 2W_K$ the dislocation vibrations are related to pairs of kinks of opposite sign. The exchange of energy between these modes is represented by a model in which particles, labelled by the coordinate W', diffuse under the influence of thermal stresses and radiation damping. The diffusion equation representing this process is solved, and finally the mean frequency, ν, with which a dislocation leaves the potential wells shown in Fig.5.12. is found, as a function of H and temperature, from the equations

$$\ln\left(\frac{\nu}{B_0}\right) = F_1(r, \alpha) \quad , \tag{5.6.}$$

$$B_0 = \frac{\pi^2 G b^2 k T}{32 \cdot a^2 v^2 m^{3/2} E_0^{1/2}} \quad , \tag{5.7.}$$

$$H = -\frac{d(\ln\nu)}{d(1/kT)} = kT F_2(r, \alpha) \quad , \tag{5.8.}$$

where v is the appropriate velocity of sound, and the functions F_1 and F_2 are shown in Figs.5.13(a) & 5.13(b). The parameters r and α are given by

$$r = \frac{2W_K}{kT} \quad , \tag{5.9.}$$

$$\alpha = 1 - \frac{\pi\sigma}{8\sigma_p^0} \quad . \tag{5.10.}$$

Using this result, Seeger et al. calculate the maximum decrement associated with the relaxation process, using a rate theory argument similar to that used by Mason (55), and find

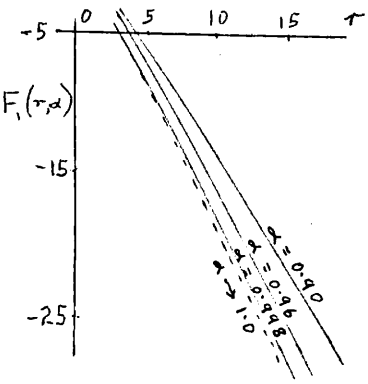

Fig. 5.13(a) THE FUNCTION $F_1(r,\alpha)$. IT IS RELATED TO THE FUNCTION $\Pi(r)$ OF DONTH (57) BY THE EQUATION $F_1(r,\alpha) = -\ln 2\pi\Pi(r)$.

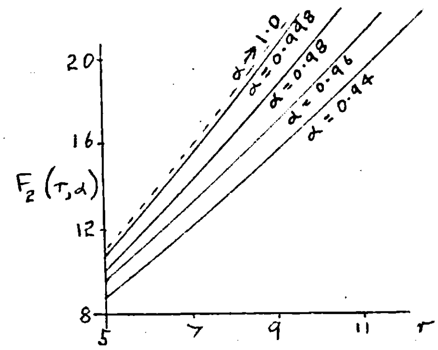

Fig. 5.13(b). THE FUNCTION $F_2(r,\alpha)$. IT IS RELATED TO THE FUNCTION $\Pi(r)$ OF DONTH (57) BY THE EQUATION $F_2(r,\alpha) = 1 + r\frac{d}{dr}\left[\ln \Pi(r)\right]$.

$$\Delta_{MAX.} = \frac{\pi}{Q_{MAX.}} = \frac{\pi p}{2(1+p)^{1/2}}, \qquad (5.11.)$$

where

$$p = \frac{2 N_0 a b^2 A G \omega_K}{kT}\left[\frac{d_{cR}}{3\omega_K} + 0.3\right]. \qquad (5.12.)$$

N_0 is the number of dislocation loops, of average length L, per unit volume, which contribute to the relaxation, and A is the area swept out by one dislocation during the process. The value of A cannot be specified exactly, but an upper and lower limit can be given. Providing $\frac{L}{a}$ is sufficiently large for the kink mechanism to operate, a lower limit of $\Delta_{MAX.}$ is given by taking $A = L a$ which corresponds to a dislocation moving one atomic spacing. An upper limit is obtained from the assumption that a dislocation sweeps out the maximum area compatible with the applied stress, the dislocation line tension, and the loop length, L. The upper limit of $\Delta_{MAX.}$ is then found to be

$$\Delta_{MAX.} = \frac{b^2 L^3 N_0 G \pi}{48 E_0} \doteqdot \frac{L^3 N_0 \pi}{24}. \qquad (5.13.)$$

(ii) A comparison of Seeger's theory with experiment.

This theory is found to account quite well for many of the observed features of the Bordoni peak. Equation 5.8. predicts an activation energy which is independent of stress amplitude, at least up to stresses for which $\alpha \doteqdot 1$. The theory also leads to reasonable values of N_0 and L.

Values of σ_p° calculated from the results of different investigators are found to be quite consistent, and in reasonably good agreement with theoretical predictions. [Seeger et al. (57)]

The subsidiary Bordoni peak may be accounted for in terms of a different type of dislocation, or dislocations on a different slip plane, with different values of σ_p° and activation energy. This is also in agreement with the observation that the main Bordoni peak contains several component peaks. The concept of several activation energies is also in agreement with the observation that the temperature of the main peak is slightly affected by cold work, annealing and irradiation, since these treatments may be expected to affect different dislocation systems in different ways. An overlapping spectrum of peaks would also explain why the above theory leads to a peak width of only about half that observed experimentally.

The theory also accounts qualitatively for the observed dependence of the peak height on cold work, annealing and impurity content. The initial increase in the peak height with cold work is associated with an increase in the number of dislocations. Both large amounts of cold work and the presence of impurities will decrease the average dislocation loop length, and hence, according to equation 5.13, the friction. The fact that the height of the peak sometimes increases on annealing before decreasing, is attributed to the reorientation of the dislocations present [BAXTER & WILKS (63)]. This may result in longer loop lengths, with a larger fraction of them lying along close packed directions and thus contributing to the internal friction.

(iii) Modifications to the Seeger-Donth theory.

The theory of Seeger & Donth has been modified by Lothe (60) & (63), who considers the recombination of kink pairs, of separation greater than d_{cr}, by diffusion. [Lothe & Hirth (59)] The kinks must reach a separation rather greater than d_{cr} in this case, before they may be considered as effectively separated. Seeger & Schiller (62) have calculated the rate of thermally activated kink formation using an approach differing from that of Donth (57). The formation of double kinks with the critical separation d_{cr} is regarded as a diffusion process. In this approach the interaction of kinks is considered. However, these modifications leave the original Seeger-Donth theory essentially unchanged.

Paré (61) has pointed out that some of the discrepancies between the Seeger-Donth theory and experiment may be resolved when the presence of internal stresses in a metal is considered. Seeger and Donth consider the probability of foreward jumps of a dislocation loop only, and neglect the probability of backward jumps. Paré finds that under certain conditions the two probabilities may be similar, leading to a very small Bordoni peak on the above theory. He finds there is a minimum stress, which is a function of loop length, which must be applied to a dislocation for the Bordoni peak to have a measurable height. The minimum value of this stress, corresponding to the longest loop lengths which are likely to occur, ie. in very lightly worked samples, is calculated to be $0{\cdot}01\sigma_p^\circ$. Since the peak has been observed using applied stresses less than $10^{-4}\sigma_p^\circ$, the stresses in question must be internal stresses. If then, the dislocations are under a total stress, internal and external, which is appreciable compared with σ_p°, then the activation energy given by equation 5.8. may well decrease as the applied stress is increased, even with a low applied stress. This leads to two effects. Firstly, there will be a distribution of internal stresses, and hence a distribution of activation energies, with a consequent broadening of the relaxation peak. Secondly, the variation of the peak temperature with applied stress will be much smaller than might otherwise be expected. This theory is also capable of explaining why components of the main Bordoni peak may be distinguished in lightly cold worked samples, but not in more heavily worked samples, for in the latter larger ranges in internal stresses might be expected.

(iv) Brailsford's theory.

A different account of the Bordoni peaks has been proposed by Brailsford (61), who considers dislocations which are not parallel to close packed directions, but at a small angle to them. Kinks are always present, therefore, in contrast to Seeger's model which assumes they are thermally activated. Brailsford considers the motion of a dislocation line in terms of the thermally activated motion of kinks, each only one or two lattice spacings wide, and thus emphasises the atomic nature of a dislocation. Thermal equilibrium is attained when the kink diffusion currents along the dislocation are zero, and the rates of generation and recombination of kink pairs are equal at each point in the dislocation. In contrast to Seeger, Brailsford assumes the rate of thermal generation of kinks is very small. The motion of a dislocation line under the influence of an applied stress is then regarded as a motion of the kinks towards one or other end of the dislocation line; ie. the equilibrium kink distribution is disturbed. The motion of kinks along a dislocation due to an applied stress, is illustrated in Fig.5.14.

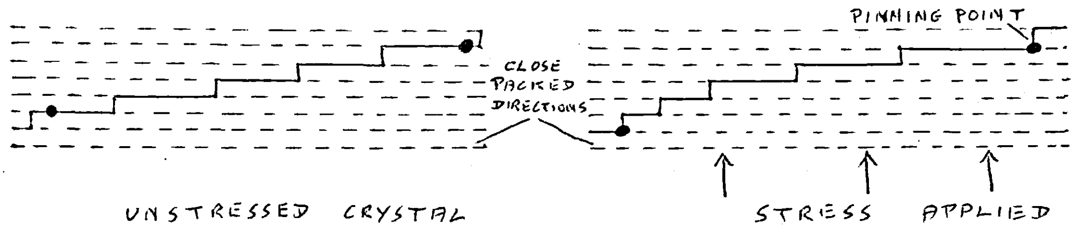

Fig.5.14. THE MOTION OF KINKS ALONG A DISLOCATION LINE DUE TO AN APPLIED STRESS [AFTER SOUTHGATE & ATTARD (63)].

When an oscillating stress is applied, a relaxation loss arises which has a maximum when the stress frequency, f, is given by

$$f = f_0 \exp\left(\frac{-H_k}{kT}\right) , \qquad (5.14.)$$

where f_0 is the attempt frequency, and H_k the activation energy for a kink to move one atomic spacing along a dislocation. A relaxation time, τ_D, characteristic of the motion of a length, L, of dislocation, may be defined in terms of the time kinks take to diffuse along the line under the action of a small harmonic time-varying stress. Brailsford finds $\tau_D \sim \frac{L^2}{D}$, where D is the diffusion constant for kink motion, given by

$$D = D_0 \exp\left(\frac{-H_k}{kT}\right) . \qquad (5.15.)$$

He also finds an expression for the decrement, which in contrast to that of Seeger's theory, is a function of dislocation loop length.

This theory is able to account for all the basic features of the Bordoni peaks. In addition, it predicts an attempt frequency, f_0, which is a function of dislocation length, and hence the specimen history. A unique value is nolonger expected, therefore. The theoretical peak width may be increased towards observed values by considering a distribution of dislocation lengths. This theory also leads immediately to an explanation of the slight shift of the temperature of the main peak with cold work or irradiation. The initial effect of cold work will be to increase L, and hence τ_D above. The peak therefore shifts to a higher temperature.

Similarly, the effect of irradiation will be to decrease L and hence to lower the temperature of the peak. The absence of the peak in well annealed specimens implies that in this state, dislocations are either absent, or lie almost entirely along close packed directions, with all the kinks condensed to form very large steps. These steps break up again into many kinks upon plastic deformation, the kink regeneration being completed at fairly low deformations, when the peak height should saturate, as is observed.

The low temperature subsidiary peak is attributed by Brailsford to pure screw dislocations, a view supported by the fact that while the main peak has its temperature lowered by impurities, the subsidiary peak remains unchanged.

An apparent fault with Brailsford's theory is his assumption that the relation $\mu kT = D$ where μ is a mobility and k Boltzmanns constant, is applicable to the kink motion. However, this is not the case, since the diffusion and stress induced kink motions are correlated. [Alefeld (65)]. The theory also assumes that kink motion is thermally activated, so very little dislocation motion by this mechanism should be possible at liquid helium temperatures. This is in contrast to the observations of Bruner & Mecs (63) and Druyvesteyn & Blaisse (62). Accordingly Brailsford (65) has modified his theory by including the effect of internal stresses, when the relaxation time τ_D above is found to be no longer the one determining the relaxation. Instead the relaxation is determined by the time τ_E which is a measure of time for any kink concentration in excess of the thermal equilibrium value to decay. It is the bowing out of dislocations under the influence of large internal stresses which gives rise to excess kink concentrations. The approach is found to predict a relaxation peak with the properties required to describe the main Bordoni peak, and also leads to a possible explanation of the subsidiary Bordoni peak. The ltter may arise by dislocations in crystal regions of small internal stress, when the relaxation r is determined by τ_D. The relative intensity of the two peaks should then depend on the mode of deformation, as is observed.

(v) Discussion.

The approach of Brailsford (65) leads to a theory very similar to Paré's (61) modification of the Seeger-Donth theory, and it is difficult to devise a clear-cut experimental test to distinguish between the two theories. However, if an accurate determination of the attempt frequency associated with the Bordoni peak yields a value in excess of $10^{-3}\omega_D$, where ω_D is the Debye frequency, then Brailsford (65) concludes that his mechanism cannot be operating. An investigation of whether or not the relaxation time associated with the peak is a function of dislocation length, should also help to decide between the two theories.

It should be possible to determine the importance of internal stresses by considering the Bordoni peaks in poly-crystalline materials. A small grain size material should show a well developed peak for smaller amounts of prestrain than a large grain sample, since there are presumably more regions of high stress concentration in the former. The observations of Thompson & Holmes (59) give weak support for this conclusion, while those of Hutchison & Hutton (58) appear to give no support. However, further experiments are required.

Measurements of Mecs & Nowick (65) on the modulus defect associated with the Köster effect are also relevant to this discussion. These authors find that a large fraction of the total modulus defect at room temperature corresponds to the Bordoni relaxation. This is difficult to understand in terms of Seeger's model, which assumes that only the small fraction of

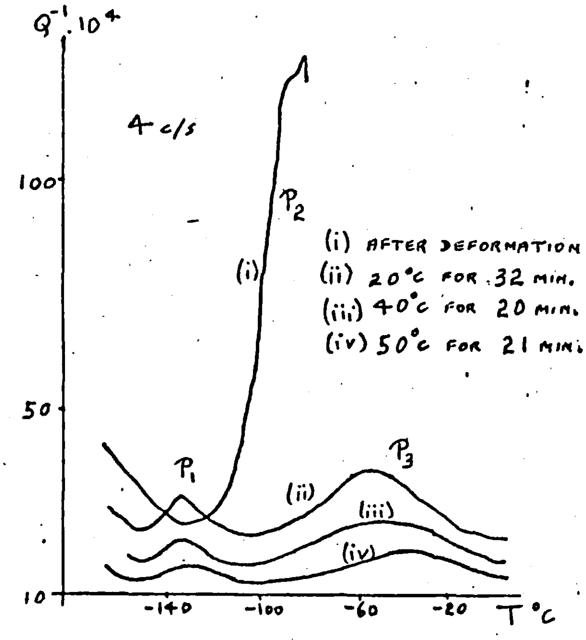

Fig. 5.15. DAMPING OF A Au SPECIMEN AFTER A DEFORMATION AND SUBSEQUENT ANNEALS. [AFTER OKUDA & HASIGUTI (63)].

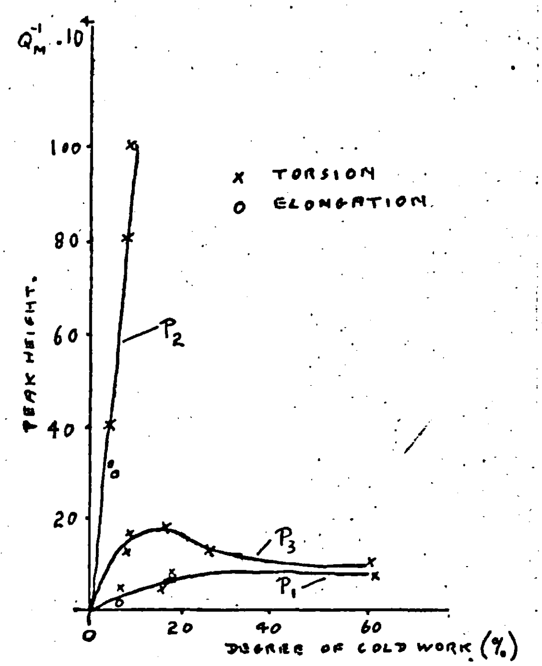

Fig. 5.16. PEAK HEIGHT V.S. DEGREE OF COLD WORK FOR A GOLD SPECIMEN [AFTER OKUDA & HASIGUTI (63)].

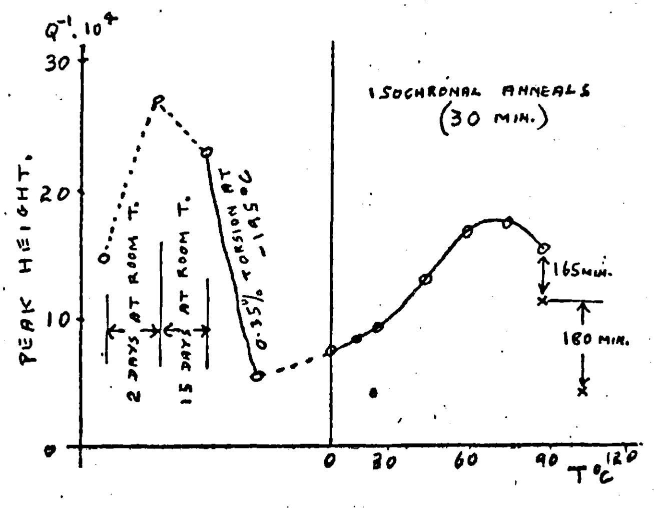

Fig. 5.17. CHANGE IN P_1 HEIGHT ON DEFORMING AND ANNEALING [AFTER KOIWA & HASIGUTI (63)].

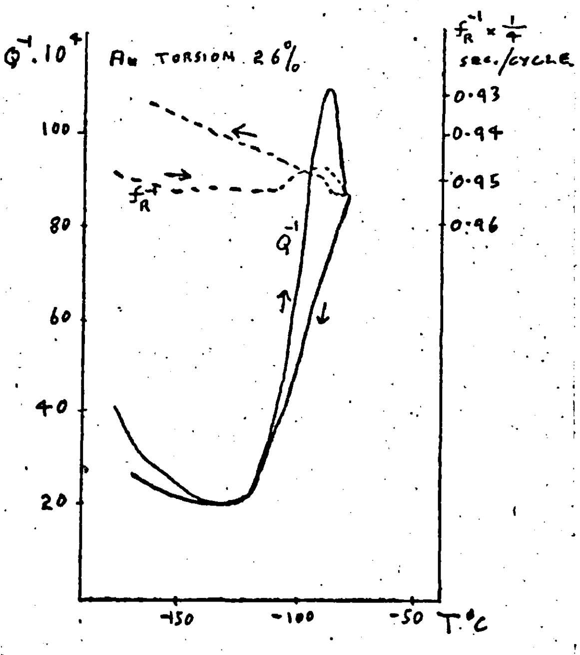

Fig. 5.18. FRICTION AND DYNAMIC MODULUS G ($f_R^{-1} \propto \sqrt{G}$) OF A Au SPECIMEN [AFTER OKUDA & HASIGUTI (63)].

dislocations present in a crystal which are parallel to a close packed direction, take part in the relaxation. However, this difficulty does not arise with Brailsford's theory, which claims that all dislocations with built in kinks contribute to the relaxation.

5.2. The Hasiguti Peaks P_1, P_2 and P_3.

(a) Experimental observations of the peaks.

As mentioned in chapter 4.3(b), a group of three peaks produced by plastic deformation are observed in the temperature range between 100 K and room temperature. They are at present not well understood, although mechanisms have been proposed to account for their occurrence. They are observed in both single crystal and polycrystalline specimens. These peaks have recently been studied in some detail by Hasiguti & Okuda (63), who have labelled them P_1, P_2 and P_3. The results of this investigation, which were essentially the same for both the copper and gold specimens used, will be summarised here. Fig. 5.15 shows the measurements of decrement as a function of temperature made on a polycrystalline gold specimen, deformed 16°4' by torsion at liquid nitrogen temperatures. A frequency of 4c/s was used. A peak, P_2, appeared on warming up the specimen after the deformation, curve (i), which began to decay around its peak temperature. An anneal for 32 minutes at 20°C caused P_2 to disappear completely, and the smaller peaks P_1 and P_3 to appear, curve (ii). P_1 and P_3 gradually disappeared upon annealing at temperatures above room temperature, curves (iii) and (iv). The maximum height of all the peaks increased with increasing deformation at first, then decreased or saturated at larger deformations, as shown in Fig. 5.16. It was found that if, after P_1 or P_2 had grown to almost maximum peak height, the specimen was further deformed at liquid nitrogen temperature, the height of these peaks was temporarily reduced; suggesting that the further deformation had at least partly destroyed the origin of the peaks. This effect was noted also by Koiwa & Hasiguti (63) whose results taken with a copper specimen are shown in Fig. 5.17. The measurements refer to the peak P_1, and show also the effect of 30 minute isochronal anneals on the height of the peak.

Hasiguti & Okuda (63) observe the peaks P_1 and P_3 (but not P_2) could also be produced by cold work at room temperature. The temperatures of the peaks were independent of the degree of deformation, but increased as the measuring frequency increased, as expected for a relaxation process. Fig 5.18 shows simultaneous measurements of reciprocal resonant frequency f_R (i.e. modulus) and internal friction in the region of P_2, for a gold specimen, twisted 26% at 70°K, after first warming up to about -75°C, and then cooling again. When no structral changes, e.g. dislocation displacements, take place in a crystal, the modulus should decrease, i.e. f_R should increase, with increasing temperature, and this change should be reversible. The results indicate structural changes are taking place. A discontinuity in f_R was also observed at about -10°C, about the temperature for the growth of P_1.

Quenching a specimen from 1000°C in such a way as to introduce the same number of vacancies as a deformation of a few% might introduce, did not give rise to any pronounced peaks. When this quenched specimen was deformed at 70°K, the results of internal friction measurements were essentially the same as shown in Fig.5.1.5. This behaviour is to be contrasted with that of the Bordoni peak. The annealing behaviour of P_1, P_2 and P_3 is also very different from that of the Bordoni peak, very much

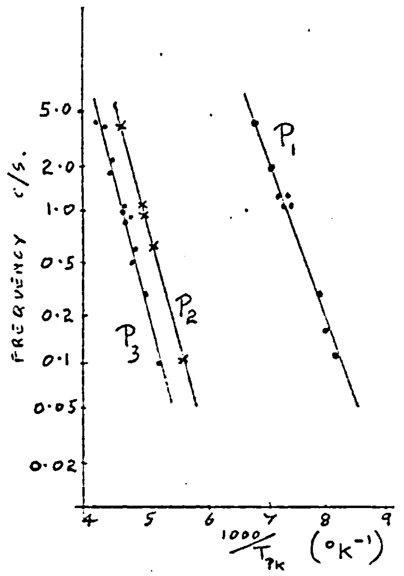

Fig. 5.19. FREQUENCY v.s. $1/T_{PK}$ FOR A GOLD SPECIMEN [AFTER OKUDA & HASIGUTI (63)].

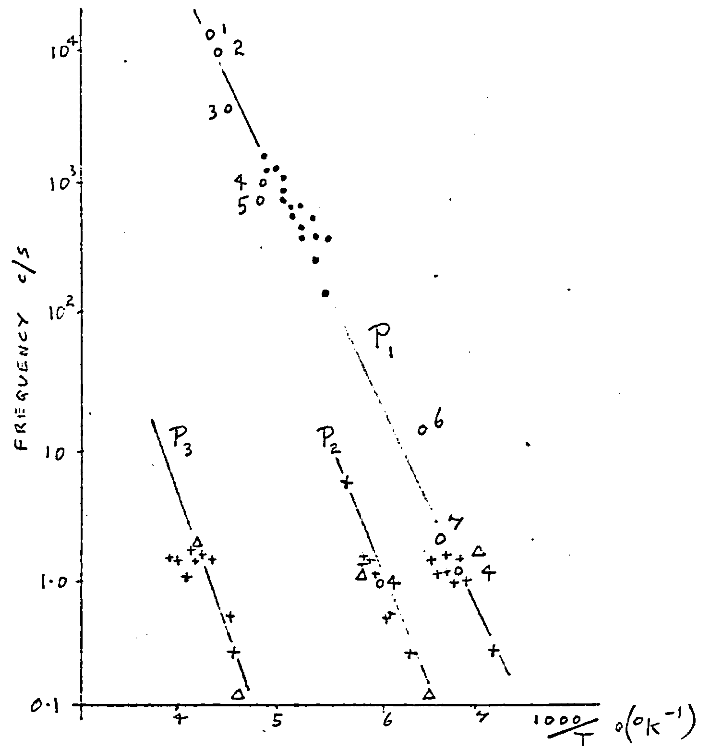

Fig. 5.20. FREQUENCY DEPENDENCE OF THREE PEAKS IN COPPER [AFTER KOIWA & HASIGUTI (63)].

MATERIAL	ACTIVATION ENERGY (e.V.)			ATTEMPT FREQUENCY (SEC⁻¹)		
	P_1	P_2	P_3	P_1	P_2	P_3
COPPER	0·32 (+)	0·35 (+)	0·45 (+)	10^{12} (+)	6.10^{11} (+)	8.10^{9} (+)
	~0·27 (Δ)	~0·3 (Δ)	~0·4 (Δ)	10^{12} (Δ)	10^{9} (Δ)	10^{10} (Δ)
	0·30 (•)			5.10^{10} (•)		
GOLD	0·22 (Δ)	0·34 (Δ)	0·36 (Δ)	2.10^{9} (Δ)	3.10^{9} (Δ)	3.10^{9} (Δ)

TABLE I. ACTIVATION ENERGIES AND ATTEMPT FREQUENCIES OF P_1 P_2 AND P_3 IN COPPER AND GOLD.

KEY TO RESULTS.

- o 1 THOMPSON & HOLMES (59).
- o 2 BRUNER (60).
- o 3 PARÉ (61).
- o 4 BAXTER & WILKS (62).
- o 5 NIBLETT & WILKS (60).
- o 6 NIBLETT (61).
- o 7 SWARTZ (62).
- • HASIGUTI, IGATA & KOIWA (62).
- + KOIWA & HASIGUTI (63).
- Δ OKUDA & HASIGUTI (63).

higher annealing temperatures than room temperature being required to remove the Bordoni peak. Okuda & Hasiguti also noted that the height of the Bordoni peak seemed to decrease slightly as P_2 appeared, and to increase again when P_2 disappeared.

Other investigations of these three peaks have been made by Niblett & Wilks (57), Thompson & Holmes (59), Paré (61), Niblett (61), Baxter & Wilks (62). Koiwa & Hasiguti (63) found that a preannealing treatment of a copper specimen greatly affected the height of the P_1 peak. The height of a P_1 peak in a fairly pure copper specimen, for example, was found to be small when the specimen had previously been annealed at 600°C. This may account for the small peaks observed by Baxter & Wilks (62), Bruner (60), Niblett & Wilks (57) and others.

All three peaks appear to be characterised by a well defined activation energy. Figs. 5.19 and 5.20 show the frequency dependence of the temperatures of the peaks P_1 P_2 and P_3 in gold and copper respectively, as measured by various authors. Table 1 gives the values of the activation energy and attempt frequency estimated by various authors for gold and copper.

(b) Theoretical interpretations of the peaks.

The sensitivity of the peaks to annealing treatment suggests that point defects are responsible in some way for the peaks, especially as the anneal is quickest at temperatures where point defects are expected to become mobile. That the peaks only appear after a deformation also suggests that point defects are involved and possibly dislocations also. The attempt frequencies given in Table 1 are more reminiscent of dislocation line vibration than of point defects, which would be expected to have an attempt frequency of the order of 10^{-15} c/s, which is characteristic of atomic motion. The fact that quenching, i.e. the introduction of vacancies, cannot alone produce the peaks, as cold working can, suggests dislocations are involved. The decrease in friction after an extra 0·35% deformation shown in Fig.5.17, also has a natural explanation if it is assumed that point defects and dislocations jointly give rise to the friction. The extra deformation pulls dislocations away from the point defects and lowers the friction.

Hasiguti & Okuda (63) have proposed a relaxation mechanism involving dislocations and point defects, a particular defect being responsible for each of the three peaks. The relaxation is considered to occur in the following way. A dislocation lying in a Peierls potential well containing a pinning point, has a certain probability of breaking away with the aid of thermal energy. When the dislocation has broken away, the defect will be attracted to it, and may pin it down before it returns to its original position. The maximum of the relaxation peak occurs when the frequency of the break-away and repinning process coincides with the applied stress frequency. Fig. 5.21 shows schematically the breakaway of a dislocation segment from a point defect by the formation of two kinks.

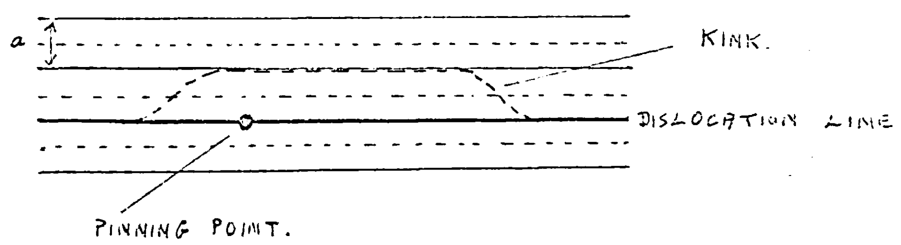

Fig. 5.21. SCHEMATIC DIAGRAM OF A DISLOCATION LINE PINNED DOWN BY A POINT DEFECT [AFTER HASIGUTI & OKUDA (63)].

Changes in peak height upon annealing and pre-annealing are attributed to changes in the dislocation configuration. Hasiguti and Okuda tentatively assign a vacancy, interstitial and divacancy to the peaks P_1, P_2 and P_3 respectively. This model requires an extremely small migration energy of a point defect adjacent to a dislocation compared with an ordinary migration energy of the same point defect without any influence of a dislocation strain field.

Schiller (64) has proposed a somewhat similar model.

Hasiguti (63) has considered the diffusion of dislocation kinks which are trapped by a point defect, and has shown that this can give rise to an internal friction peak of a relaxation type. The mathematical treatment is similar to the abrupt kink theory of the Bordoni peak proposed by Brailsford (61).

Hasiguti (65) has also considered the unpinning of Mott (52)-Friedel (63) type dislocation loops, which results in a relaxation peak similar in its final expression to the above dislocation-kink theory.

Koiwa & Hasiguti (65) have proposed a theory in which the peaks arise by a thermal unpinning of dislocations. This theory is found to account quite well for some of the characteristics of the P_1 peak observed in Cu. Koiwa and Hasiguti suggest that some of the difficulties encountered by their theory might be overcome by using the kink model of dislocation motion [Brailsford (61)], rather than the string model [Koehler (52).]

A somewhat different mechanism has been proposed by Bruner (60). Two partial dislocations, resulting from the dissociation of an edge type dislocation in a material of low stacking fault energy, will both have edge components. In the region of these partials there will be two equilibrium positions for a defect, where the strain fields combine to

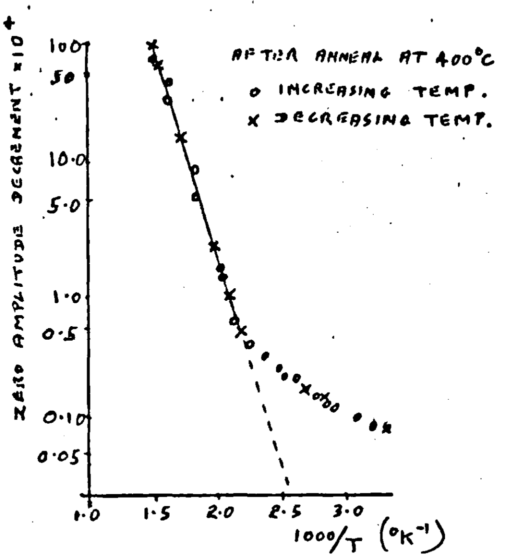

Fig. 5.22. FRICTION OF AN Al SINGLE CRYSTAL AS A FUNCTION OF TEMPERATURE [AFTER CHAMBERS (57)].

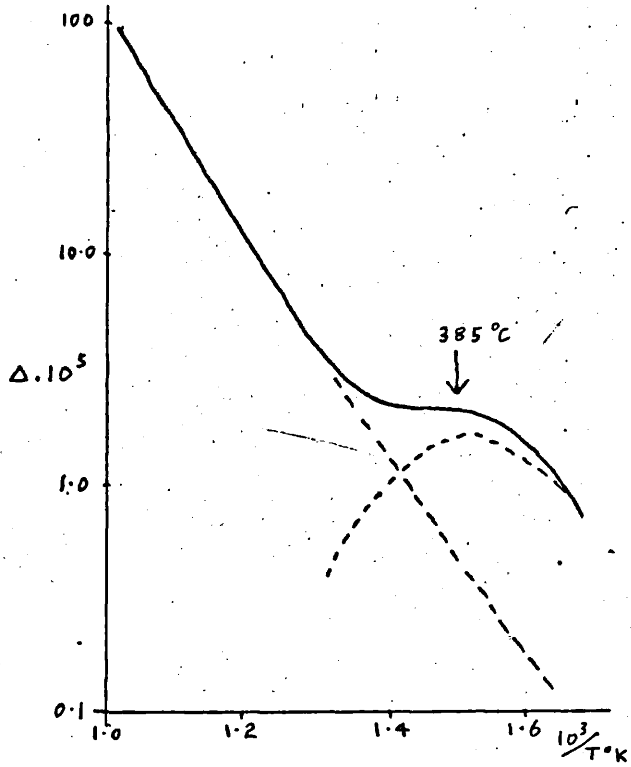

Fig. 5.23. DECREMENT v.s. 1/T FOR THREE SPECIMENS OF GERMANIUM [AFTER KESSLER (57)].

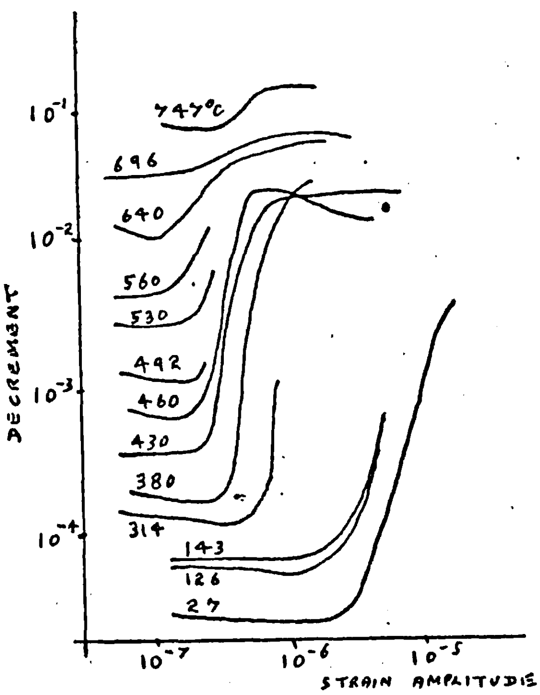

Fig. 5.24. FRICTION OF A Cu SINGLE CRYSTAL AS A FUNCTION OF STRAIN AMPLITUDE AT DIFFERENT TEMPERATURES (°C) AT 1450 c/s [AFTER KAMENTSKY (56)].

minimise the strain energy. Under the action of an applied stress the defect might move between the two equilibrium positions, giving rise to a relaxation loss. However, the separation of the partials [Seeger et al. (59)] is probably too great for a loss to occur at the low strain amplitudes, about 10^{-7} [Thompson & Paré (60)] at which the peaks have been observed. The peaks also occur in metals which probably do not have a low stacking fault energy. [Hasiguti, Igata & Kamoshita (62)]

5.3. The Friction at High Temperatures.

(a) Experimental observations of the friction.

We now consider the type of damping noted in chapter 4.3(c). At relatively high temperatures, that is well above room temperature, an amplitude independent internal friction, Δ , is observed at low strain amplitudes, which increases exponentially with temperature according to the relation

$$\Delta = A_0 \exp\left(\frac{-U_T}{kT}\right) , \qquad (5.16.)$$

where U_T is an activation energy, and A_0 is a constant. This loss was first observed by Kê (50) in some measurements on poly-crystalline materials. It was obscured to some extent by the presence also of grain boundary relaxation peaks. Reviews of this high temperature loss have been given by Mason (58) and Niblett & Wilks (60).

Some results obtained by Chambers (57), using an aluminium single crystal, are shown in Fig.5.22. The crystal was first annealed at 400°C. The exponential region is seen to begin at about 150°C. Fig.5.23. shows the results of Kessler (57) on a germanium single crystal, taken at 40Kc/s.

Above about 550°C the decrement increases exponentially with increasing temperature, while below this temperature a peak is observed [see chapter 4.3 (f)]. The curve above 550°C was found to be reproducible in subsequent measurements. Kamentsky (56) made an extensive study of this type of loss in copper, and Fig.5.24. shows some of his measurements of the friction as a function of strain amplitude. Here the exponential loss sets in at about 400°C. The friction is seen to be either almost constant, or to decrease slightly with increasing strain amplitude, when the latter does not exceed the critical value ϵ_c. Above ϵ_c the friction increases rapidly with strain amplitude. The value of ϵ_c is seen to decrease with increasing temperature, and is related to the breakaway of dislocations from pinning points [Kamentsky (56)]. To obtain reproducible measurements of the friction as a function of temperature, Kamentsky found it necessary to use only strain amplitudes below ϵ_c, and to allow the specimens to rest at each new temperature for several hours.

The activation energy calculated according to equation (5.16.) is found by Kamentsky to be between 0.5 ev and 2.0 ev for copper. Also for copper, Beshers (59) found a value of 1.0 ev below 500°C, and 0.8 ev above 500°C, while Chambers (57) and Birnbaum & Levy (56) both reported values of about 0.7 ev. For aluminium Friedel et al (55) found a value of about 1.6 ev, for magnesium Chambers (57) obtained a value of 0.7 ev, and for lead Weertman & Salkovitz (55) found an energy of 0.3 ev.

Doping copper single crystals with gold and nickel was found by Stevens (57) and Beshers (59) to reduce the magnitude of the friction at higher temperatures, but to leave the activation energy unchanged.

The frequency dependence of the friction has been investigated by

Kamentsky (56) and Friedel (55), who both found the friction to decrease with increasing frequency, f, not quite as rapidly as $\frac{1}{f}$.

At high temperatures Young's modulus is expected to decrease linearly with increasing temperature in the absence of a large internal friction. [Ludloff (40)]. The deviation from linearity when internal friction is present may therefore be used as a measure of the modulus defect associated with the friction. In this way Friedel et al (55) found that, for aluminium, the modulus defect had approximately the same temperature dependence as the decrement. However, Chambers (57) found, for the same material, a modulus defect with a somewhat smaller temperature dependence than the decrement, as did Kamentsky (56) for copper.

(b) Theories of the high temperature friction.

Birnbaum and Levy (56) have suggested that the friction arises because jogs on dislocations move under the influence of an applied stress and create vacancies or interstitials. The loss arises essentially by a relaxation process, for at low temperatures and low stresses there will be only a small probability of creating a defect and so a small friction, while at high temperatures defects will be created by thermal energy alone and again there will be no friction. Such a relaxation mechanism is capable of accounting for the observed frequency dependence, temperature dependence and the possibility of a maximum in the friction at high temperatures [Kamentsky (56)].

The wide range of activation energies reported for particular metals makes it difficult to associate the friction with a specific dislocation or point defect mechanism. However Schoeck, Bisogni & Shyne (64) have shown that the measured activation energy of the internal friction is not necessarily the same as the activation energy of the controlling dislocation mechanism but is usually much smaller. They allow for the fact that dislocations will normally be in a number of different geometrical configurations, and when displaced will be acted on by different restoring forces, because of distributions in line tension and internal crystal stresses. If there is a unique activation energy U_0 for the controlling dislocation mechanism, or a narrow spectrum of energies, then the measured activation energy, U, is found to be related to U_0 as:-

$$U = n U_0 , \tag{5.17.}$$

where n is a constant, over not too large a temperature range, whose value may be determined from the measured frequency dependence of the friction. Applying this theory to some measurements made on aluminium Schoeck, Bisogni and Shyne found activation energy of 1·4ev, which in fact is near to the energy of self-diffusion in aluminium, 1·35ev. [Federighi (59)]. The same measurements interpreted in terms of equation (5.16) yielded a range of activation energies (0·3ev to 2·0ev). An energy of 1·4ev also seems reasonable for the creation of a point defect.

Weertman (57) attempted to account for the friction in terms of thermally activated motion of dislocation loops through the stress field of randomly distributed impurity atoms. (see Chapter 7.3.) The viscous damping of the vibrating dislocation loops, is proportional to their velocity, which increases exponentially with temperature. Although the model predicts a friction inversely proportional to frequency, it is not expected to be applicable to very pure materials, in which, however, this loss is sometimes observed. This restriction arises because the dislocation displacements must be considerably greater than the wavelength of the stress field.

Mason (55) & (58) has proposed that the friction arises when two adjacent vibrating loops of dislocation break away from their common pinning point, with a subsequent irreversible exchange of energy between the two loops. However, the activation energy for this process should be of the order of 0.3ev, the interaction energy between a pinning point and a dislocation, which is rather lower than the measured values.

More measurements of the frequency dependence of this loss would be useful in testing the theories that have been proposed. A review of this loss has been given by Mason (58).

CHAPTER 6

A Theory of Dislocation Damping.

A theory to account for the types of damping introduced in chapter 4.3(d) and 4.3(e) will be given in this chapter, and then in chapter 7 the predictions of this theory will be compared with experiment.

6.1. Early Theories.

Early theories of the damping which results from dislocation motion were based on two ideas, proposed by Koehler (52) and Nowick (50).

Koehler regards the forced damped vibrations of a dislocation line, under the influence of an oscillating stress wave, as being analogous to the forced damped vibrations of a stretched string, energy being dissipated according to the damped resonance mechanism of chapter 2.3(b). The exact nature of the viscous like energy dissipation mechanism is not considered. The dislocation is assumed to be divided into segments by Cottrell pinning points [Cottrell (48)], and the equation of motion of such a segment is solved by Koehler for frequencies of vibration in the Kc/s range and below. In this way he obtains an expression for the decrement which is proportional to the frequency and the fourth power of the looplength. This theory is quite successful in accounting for the resonance type loss, Δ_I, at low frequencies and stress amplitudes. To account for the observed dependence of the component Δ_H of the decrement on strain amplitude at higher stress amplitudes, Koehler postulates breakaway of the dislocation segments from the pinning points when the tension in the dislocation exceeds the Cottrell binding force [Cottrell (48)]. The strain amplitude dependent loss is then associated with the increase in average dislocation loop length after breakaway. However, this theory predicts a loss proportional to frequency, in contradiction with much experimental evidence. Koehler also considers the effect of an exponential distribution, ie. random, of dislocation loop lengths on the strain amplitude independent decrement, Δ_I.

Nowick (50) has suggested a hysteresis mechanism for the strain amplitude dependent loss, predicting, therefore, a frequency independent decrement. The bowing out of loops under an applied stress is assumed to be restrained by potential barriers, eg. solute atoms, which prevent it from oscillating completely in phase with the stress. For each increment in stress, there is a corresponding number of dislocations which are torn loose and move rapidly to a point where the motion is again interrupted by a potential barrier. This sudden jump of the dislocation occurs at virtually constant stress and is accompanied by a small increment of non-elastic strain. Since this motion is not completely reversed upon removing the stress, a hysteresis effect arises.

This idea has been developed by Weertman & Salkovitz (55), using the theory of Mott & Nabarro (48) to describe the stress field associated with impurity atoms. An expression for the decrement at low stress amplitudes is derived, under the assumption that dislocation displacements of theorder of several atomic spacings may be obtained. At the low stress amplitudes considered, however, this is unlikely. [WHITWORTH (60)]. Weertman (55) has also solved the equation of Koehler for any frequency, but in a mathematical form which makes it difficult to describe the effect of the various experimental parameters upon the losses.

Koehler's theory has been modified with considerable success by Granato & Lücke (56). This theory is the starting point of many later theories, and will be considered now in some detail.

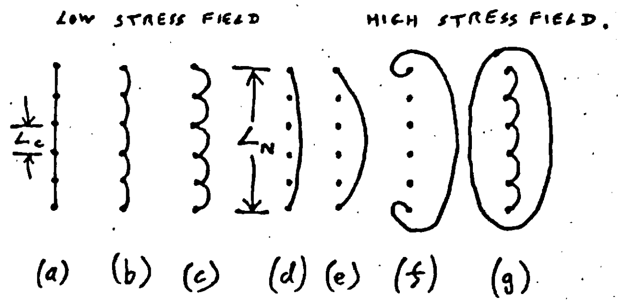

Fig. 6.1. SCHEMATIC ILLUSTRATION OF THE BOWING OUT OF A PINNED DISLOCATION LINE BY AN INCREASING APPLIED STRESS [AFTER GRANATO & LÜCKE (56)].

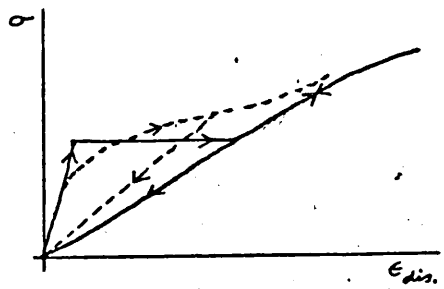

Fig. 6.2. STRESS-STRAIN RELATION CORRESPONDING TO THE MODEL OF Fig. 6.1. [AFTER GRANATO & LÜCKE (56)].

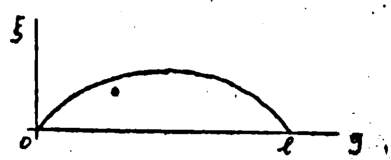

Fig. 6.3. A BOWED OUT DISLOCATION OF LENGTH ℓ. [AFTER GRANATO & LÜCKE (56)].

6.2. The Koehler-Granato-Lücke Theory.

(i) The model.

It is assumed that a pure single crystal contains, before deformation, a network of dislocations, [Mott (52)], which are pinned by two types of pinning point, of different strength. The stronger ones are assumed sufficiently strong to resist unpinning by a stress wave, and are associated with network junctions. They lead to major loop lengths L_N. The weaker pinning points may be unpinned when the applied stress overcomes the Cottrell binding force associated with the pinned dislocation, and give minor loop lengths ℓ. It is assumed that the ratio $\frac{L_N}{L_c}$ is greater than about 5, where L_c is the average minor loop length, ℓ.

If an external stress is now applied at right angles to a network length, there will be, in addition to an elastic strain, a dislocation strain, caused by the minor loop lengths bowing out, as illustrated in Fig.6.1. For zero applied stress, the length L_N is pinned down as in Fig.6.1(a). With increasing stress, the dislocation segments bow out, Fig.6.1(b) & (c), until the breakaway stress is reached, Fig.6.1(d), when a large increase in dislocation strain results, for no increase in stress. At higher stresses , the stress-dislocation strain law is determined by the length L_N, and not L_c. Further increases in stress cause the dislocation to bow out further, Fig.6.1(e), until multiplication by the Frank-Read (50) mechanism is possible, Fig.6.1(f), and an irreversible plastic strain results, Fig.6.1(g). In Fig.6.2. the corresponding stress-strain law is illustrated. The dashed curve would result if there were a distribution of minor loop lengths.

Two losses are considered, a dynamic (damped resonance) and hysteretic loss.

(ii) The dynamic loss.

This is due to the dynamic nature of the measurement. Because the forced motion of the dislocation is opposed by some damping mechanism, there is a phase lag between the stress and strain, giving a resonance type loss. To find the decrement and modulus defect felt by a stress wave, Granato-Lücke first obtain the equation of motion

$$\frac{\partial^2 \sigma}{\partial x^2} - \rho \frac{\partial^2 \epsilon}{\partial t^2} = 0 , \qquad (6.1.)$$

where ρ is the density of the material, and x the coordinate in the direction of displacement of the dislocation loop.

The strain, ϵ , has two components, an elastic strain, ϵ_{el} , and a dislocation strain, ϵ_{dis}, the latter arising from the dislocation motion. The elastic strain is given, as in equation (2.1.), by

$$\epsilon_{disel.} = \frac{\sigma}{G} . \qquad (6.2.)$$

If $\xi(y)$ is the displacement of the dislocation loop, of length ℓ, from its equilibrium position at a point given by the coordinate y , as shown in Fig.6.3. then the average dislocation displacement is given by

$$\bar{\xi} = \frac{1}{\ell}\int_0^\ell \xi(y)\, dy . \qquad (6.3.)$$

A more exact expression has been given by Koehler & DeWit (59).

The dislocation strain produced by a loop of length ℓ in a unit cube of material, is then given by [Koehler (52)] $\xi \ell a$, where a is the lattice parameter. If Λ is the total length of moving dislocation, then

$$\epsilon_{dis.} = \frac{\Lambda a}{\ell}\int_0^\ell \xi(y)\, dy . \qquad (6.4.)$$

Equations 6.1. to 6.4. may be combined to give

$$\frac{\partial^2 \sigma}{\partial x^2} - \frac{\rho}{G}\frac{\partial^2 \sigma}{\partial t^2} = \frac{\Lambda \rho a}{\ell}\frac{\partial^2}{\partial t^2}\int_0^\ell \xi\, dy . \qquad (6.5.)$$

The equation of motion of a pinned down dislocation loop, is taken as that used by Koehler (52)

$$A\frac{\partial^2\xi}{\partial t^2} + B\frac{\partial\xi}{\partial t} - C\frac{\partial^2\xi}{\partial y^2} = b\sigma \ , \qquad (6.6.)$$

where $\xi = \xi(x, y, t)$. A is the effective mass per unit length, the term in B is the damping force per unit length, the term in C gives the force per unit length due to the effective tension in a bowed-out dislocation, and the term on the right is the force per unit length exerted on the dislocation by the external shearing stress. The constants are given by $A = \pi\rho b^2$; $C = \frac{2Gb^2}{\pi(1-\nu)}$, where ρ is the density of the material, b the Burger's vector, G the shear modulus, and ν is Poisson's ratio. [Koehler (52)].

The equations (6.5.) and (6.6.) are then solved, subject to the boundary conditions that the displacement at the pinning points is zero, by considering a trial solution of the form

$$\sigma = \sigma_0 \exp(-\alpha x)\exp\left[i\omega\left(t - \frac{x}{v}\right)\right] . \qquad (6.7.)$$

This is chosen such that σ is periodic in time, and also independent of y , implying that the dislocation is normal to the stress wave-front, and that displacements are small. This trial solution leads to

$$\xi = 4b\sigma\sum_{n=0}^{\infty}\frac{1}{(2n+1)}\sin\left[\frac{(2n+1)\pi y}{\ell}\right]\frac{\exp i(\omega t-\delta_n)}{\left[(\omega_n^2-\omega^2)^2+(\omega d)^2\right]^{1/2}} , \qquad (6.8.)$$

with the substitutions

$$d = \frac{B}{A} , \qquad (6.9.)$$

$$\omega_n = (2n+1)\frac{\pi}{\ell}\left(\frac{C}{A}\right)^{1/2} , \qquad (6.10.)$$

and

$$\delta_n = \tan^{-1}\frac{\omega d}{\omega_n^2-\omega^2} . \qquad (6.11.)$$

ω_0 is the fundamental resonant frequency of the dislocation loop, and ω_n is the n^{th} harmonic frequency. At frequencies less than ω_0, which is typically $\sim$100 Mc/s it is a good approximation to consider only the first term in the expansion of equation (6.8.), the others decreasing as $\left(\frac{1}{2n+1}\right)^6$. Using this approximation, ξ and σ satisfy equation (6.5.)

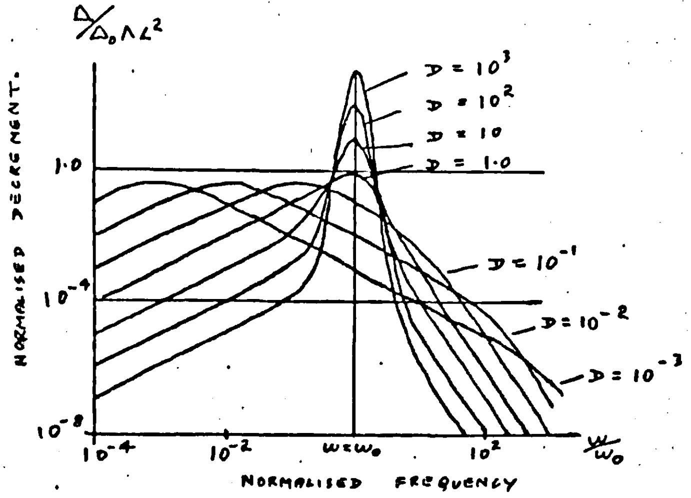

Fig. 6.4. FREQUENCY DEPENDENCE OF THE DECREMENT FOR VARIOUS VALUES OF THE DAMPING CONSTANT, AND FOR A δ-FUNCTION DISTRIBUTION OF LOOP LENGTHS [AFTER GRANATO & LÜCKE (56)].

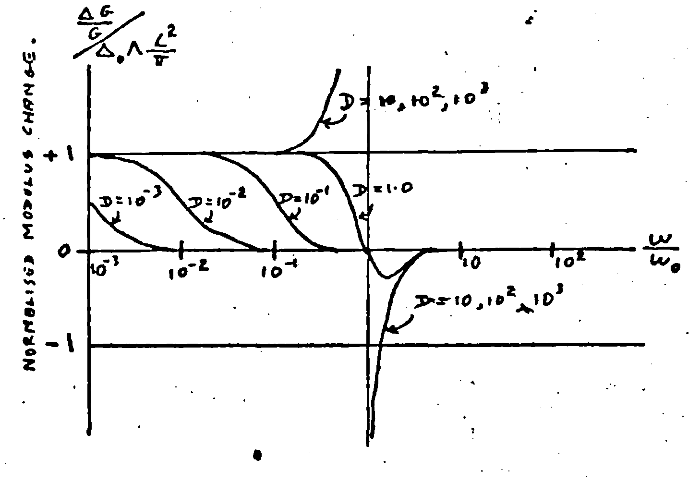

Fig. 6.5. THE FREQUENCY DEPENDENCE OF THE % CHANGE IN MODULUS [AFTER GRANATO & LÜCKE (56)].

and equation (6.6.) if

$$\alpha(\omega) = \frac{1}{v}\frac{4Gb^2}{\pi^4 C}\omega_o^2\Lambda L^2\frac{\omega^2 d}{(\omega_o^2-\omega^2)^2+(\omega d)^2}, \qquad (6.12.)$$

$$v(\omega) = v_o\left[1-\frac{4Gb^2}{\pi^4 C}\omega_o^2\Lambda L^2\frac{\omega_o^2-\omega^2}{(\omega_o^2-\omega^2)^2+(\omega d)^2}\right], \qquad (6.13.)$$

where $\alpha(\omega)$ is the attenuation, $v(\omega)$ the velocity of the stress wave,

$$v_o = \sqrt{\frac{G}{\rho}}, \qquad (6.14.)$$

and

$$\omega_o = \frac{\pi}{L}\left(\frac{C}{A}\right)^{\frac{1}{2}}. \qquad (6.15.)$$

The attenuation $\alpha(\omega)$ results from the component of displacement out of phase with the applied stress, and the velocity change, $\Delta v = v_o - v(\omega)$, from the component in phase with the stress. $v(\omega)$ is the measured velocity, and v_o the velocity corresponding to the true elastic modulus. If the decrement and modulus defect are given by (Chapter 4.1.)

$$\Delta(\omega) = \alpha(\omega).2\pi\frac{v}{\omega}, \qquad (6.16.)$$

$$\frac{\Delta G}{G} = 2\frac{\Delta v}{v}, \qquad (6.17.)$$

then one finds

$$\Delta(\ell) = \frac{8Gb^2\Lambda L^2}{\pi^3 CD}\left[\frac{\Omega}{(1-\Omega^2)^2+\left(\frac{\Omega}{D}\right)^2}\right], \qquad (6.18.)$$

$$\frac{\Delta G}{G} = \frac{8Gb^2\Lambda L^2}{\pi^4 C}\left[\frac{1-\Omega^2}{(1-\Omega^2)^2+\left(\frac{\Omega}{D}\right)^2}\right], \qquad (6.19.)$$

where $D = \frac{\omega_o}{d}$ and $\Omega = \frac{\omega}{\omega_o}$. The dependence of Δ and $\frac{\Delta G}{G}$ on Ω are shown in Fig.6.4. and Fig.6.5. where values of the damping constant, B, have been chosen in the range 5.10^{-3} to 5.10^{-5}; L ranging from 10^{-3} to 10^{-6} cm; and $\Lambda = 10^{7}$ cm. The following features are noted:

(a) The frequency response has two main branches, depending on whether the damping is large, $D \ll 1$, or small, $D \gg 1$. For very small damping the response is linear for frequencies up nearly to the resonant frequency, passes through a maximum whose sharpness depends on the smallness of the damping, and then decreases like the inverse third power of the frequency. For large damping, the initial response is linear up to a maximum value which occurs at a frequency less than ω_o. It then decreases as $\frac{1}{\omega}$

through the resonant frequency range, and finally decreases as $\frac{1}{\omega^3}$.

(b) The resonant frequency depends only on L, C, A.

(c) The maximum loss occurs at ω_o for small damping, and at $\frac{\omega_o^2}{d}$ for large damping.

(d) Near the resonant frequency, the loss is inversely proportional to the damping.

(e) From a consideration of reasonable values for L and B, the loss is expected to be important mainly in the Mc/s region.

(iii) The effect of a distribution of loop lengths.

In equation (6.18.) both $\frac{1}{D}$ and Ω are proportional to L, so Δ depends on L^4 and might therefore be expected to be sensitive to the distribution of loop lengths. So far a δ-distribution has been assumed. However, Granato & Lücke find that the qualitative results are little changed by using different distributions, except in that the large increase in damping near the resonant frequency becomes less marked. It is found that to a good approximation an effective loop length may be used, which is larger than the average because the fourth power dependence of attenuation on loop length gives more weight to long loop lengths. A general rule is

$$L^i_{eff.} = (i+1)!\, L^i \, . \qquad (6.20.)$$

Granato & Lücke calculate the effect of an exponential distribution of loop lengths on the decrement, using Koehler's (52) expression for the number of loop lengths between ℓ and $\ell + d\ell$

$$N(\ell)\, d\ell = \frac{\Lambda}{L^2} \exp\left(\frac{-\ell}{L}\right) d\ell \, , \qquad (6.21.)$$

which holds if the concentration ofpinning points isnot too large. The new expressions for Δ and $\frac{\Delta G}{G}$ are found to be

$$\Delta = \frac{8 G a^2}{\pi^5 C^2} \Lambda L^4 5! B \omega \left[1 + \frac{2.6.7. L^2 A \omega^2}{\pi^2 C} - \frac{6.7.8.9. L^4 B^2 \omega^2}{\pi^4 C^2} \right] , \qquad (6.22.)$$

$$\frac{\Delta G}{G} = \frac{8 G a^2}{\pi^4 C} 3! \Lambda L^2 \, , \qquad (6.23.)$$

where it has been assumed $\frac{\omega}{d} \ll 1$.

(iv) The stress amplitude dependent hysteretic loss.

This loss arises because in the unloading part of the stress cycle (e)→(a) in Fig.6.1. the long loops collapse elastically along a path determined by the long loop length, resulting in a hysteresis loss. This hysteresis loop is different from the ones considered in chapter 2, in that the curve passes through the point $\sigma = 0$, $\epsilon = 0$ twice per cycle (Fig.6.2.) Granato & Lücke estimate this loss for frequencies in the Kc/s region and below, when the dynamic loss may be neglected and the frequency function $F(\Omega) \doteqdot 1$, where

$$F(\Omega) = \left[(1-\Omega^2)^2 + \left(\frac{\Omega}{D}\right)^2 \right]^{-\frac{1}{2}}. \tag{6.24.}$$

The shearing strain produced by a loop of length ℓ is then found to be

$$\epsilon_{dis.} = \sigma_0 \exp(-\alpha x) \frac{\Lambda\, 8 b^2 \ell^2}{\pi^4 C} \left[\cos(\omega t - kx - \delta) \right] F(\Omega). \tag{6.25.}$$

If the slight variation of the stress over the sample dimensions is neglected and the damping is small, one obtains

$$\epsilon_{dis.} \doteqdot \frac{8 b^2 \sigma_0}{\pi^4 C} \cos(\omega t).\, \ell^3. \tag{6.26.}$$

The distribution of loop lengths as a function of stress must now be considered. Initially this is exponential (random) but as breakaway proceeds the distribution changes, and is thus a function of stress.

The maximum force exerted on an impurity atom by an anchored dislocation during a cycle is [Koehler (52)],

$$F_M = \pi C (\phi_1 - \phi_2) = \frac{\pi \sigma_0 b}{2} (\ell_1 + \ell_2), \tag{6.26A.}$$

where πC is the loop tension [Mott & Nabarro (52)], ϕ_1 and ϕ_2 are the angles made by loops of length ℓ_1 and ℓ_2 at the impurity when maximum displacement occurs. These angles are measured to the unstressed position of the dislocation. Breakaway occurs when this force is larger than the Cottrell binding force, which is given by [Cottrell (48)],

$$F \doteqdot \frac{4 G \epsilon' b^4}{z^2} \quad , \tag{6.27.}$$

where ϵ' is the difference in atomic radii divided by the atomic radius of the solvent atom, and z is the distance of the impurity atom from the dislocation axis. Breakaway will occur now if $\ell_1 + \ell_2$ is greater than $\mathcal{L}$, where

$$\mathcal{L} = \frac{\pi . F_M}{4 b \sigma} \quad , \tag{6.28.}$$

and F_M is the maximum value of the binding force obtained. The breakaway process is catastrophic, since the loop length after breakaway will always be greater than before breakaway.

At high stresses the distribution function becomes a δ-function, where all network lengths, L_N, are assumed equal:

$$N_0(\ell) d\ell = \frac{\Lambda}{L_N} \delta(\ell - L_N) \, d\ell \, . \tag{6.29.}$$

For intermediate stresses, where only partial breakaway has occured, the distribution function is taken to be

$$N'(\ell) d\ell = \begin{cases} \frac{\Lambda}{L_c^2} \exp\left(\frac{-\ell}{L_c}\right) J(\mathcal{L}, L_c, L_N) \, d\ell, & [0 \le \ell < \mathcal{L}] \quad (6.30a.) \\ \frac{\Lambda}{L_N} \delta(\ell - L_N) \, M \, d\ell \, , & [\mathcal{L} \le \ell < \infty] \quad (6.30b.) \end{cases}$$

where M is the fraction of network lengths in which breakaway has occured, and J is determined by the condition that after breakaway loops join the δ distribution ie: Λ is constant. Namely

$$\Lambda = \int_0^\infty \ell \, N'(\ell) \, d\ell \, . \tag{6.31.}$$

Granato & Lücke find

$$J = \left[1 - (q+1) \exp(-q)\right]^{n-1} \tag{6.32.}$$

$$M = 1 - \left[1 - (q+1) \exp(-q)\right]^{n} \, , \tag{6.33.}$$

where $n = \frac{L_N}{L_c} - 1$ is the average number of loop lengths in a network length, and

$$q = \frac{\mathcal{L}}{L_c} = \frac{\pi F_M}{4 b L_c \sigma} = \frac{\Gamma}{\sigma} \, . \tag{6.34.}$$

The following approximations are made, which are valid in the early stages of breakaway when n is large,

$$M \doteqdot n(q+1)\exp(-q), \tag{6.35.}$$

$$J \doteqdot 1 - n(q+1)\exp(-q). \tag{6.36.}$$

So far $\mathcal{L}$, and hence σ, has been assumed constant. If σ varies with time, then a finite time will elapse before the distribution readjusts itself. This time is governed by the speed with which atoms in a dislocation can move, and is very small. In fact the distribution can be regarded as following the stress instantaneously up to frequencies of the order of several hundred Mc/s. The distribution function for the quarter cycle of increasing stress is determined by the instantaneous value of the stress. For the quarter cycle when the stress is decreasing, the distribution $N_2'(\ell)d\ell$ is unchanging and corresponds to the distribution at the maximum stress σ_0 achieved in the first quarter cycle. Thus the final form of the distribution function is

$$N'(\ell)d\ell = \begin{cases} N_1'(\ell)d\ell = \begin{cases} \frac{\Lambda}{L_c^2}\left[1-n\left(\frac{\Gamma}{\sigma}+1\right)\exp\left(\frac{-\Gamma}{\sigma}\right)\right]\exp\left(\frac{-\ell}{\sigma}\right)d\ell, & 0\leq\ell\leq\mathcal{L} \quad (6.37a.)\\ \frac{\Lambda}{L_N}\,\delta(\ell-L_N)\,n\left(\frac{\Gamma}{\sigma}+1\right)\exp\left(\frac{-\Gamma}{\sigma}\right)d\ell, & \mathcal{L}\leq\ell<\infty \quad (6.37b.)\end{cases}\\ N_2'(\ell)d\ell = \begin{cases} \frac{\Lambda}{L_c^2}\left[1-n\left(\frac{\Gamma}{\sigma_0}+1\right)\exp\left(\frac{-\Gamma}{\sigma_0}\right)\right]\exp\left(\frac{-\ell}{L_c}\right)d\ell, & 0\leq\ell\leq\mathcal{L} \quad (6.37c.)\\ \frac{\Lambda}{L_N}\,\delta(\ell-L_N)\,n\left(\frac{\Gamma}{\sigma_0}+1\right)\exp\left(\frac{-\Gamma}{\sigma_0}\right)d\ell, & \mathcal{L}\leq\ell<\infty \quad (6.37d.)\end{cases}\end{cases}$$

where $\sigma = \sigma_0(x)\cos(\omega t - kx)$.

The dislocation strain for increasing stress, $\epsilon_{1\,dis.}$ and for decreasing stress, $\epsilon_{2\,dis.}$, may now be calculated, using $N'(\ell)d\ell$ and equation (6.26.)

$$\epsilon_{1\,dis.} = \int_0^\infty \ell^3\,\frac{8b^2\sigma_0}{\pi^4 C}\cos(\omega t).\,N_1'(\ell)d\ell, \tag{6.38.}$$

$$\epsilon_{2\,dis.} = \int_0^\infty \ell^3\,\frac{8b^2\sigma_0}{\pi^4 C}\cos(\omega t).\,N_2'(\ell)d\ell. \tag{6.39.}$$

These expressions are evaluated by Granato & Lücke for the early stages of breakaway when q is large, and used to calculate the energy lost per cycle, according to

$$\Delta W = 2\int_0^{\sigma_0} \left(\epsilon_{1\,lin.} - \epsilon_{2\,lin.}\right) d\sigma \quad . \tag{6.40.}$$

Using as a definition of the decrement

$$\Delta = \Delta W \frac{G}{\sigma_0^2} \ , \tag{6.41.}$$

the strain amplitude dependent decrement is found to be

$$\Delta_H = \frac{8 G a^2}{\pi^4 C} \Lambda L_N^2 \left(\frac{L_N}{L_c}\right) \left[\frac{\Gamma}{\sigma_0} - 1 + \ldots\right] exp\left(\frac{-\Gamma}{\sigma_0}\right) , \tag{6.42.}$$

or

$$\Delta_H = \frac{8 G a^2 \Lambda L_N}{\pi^4 C L_c} \frac{\Gamma}{\sigma_0} exp\left(\frac{-\Gamma}{\sigma_0}\right) , \tag{6.43.}$$

for low values of $\frac{\sigma_0}{\Gamma}$.

Granato & Lücke find a modulus defect of the same form as the decrement, the two being related by a constant r of the order of unity, as

$$\Delta_H = r . \left(\frac{\Delta G}{G}\right)_H \quad . \tag{6.44.}$$

At high frequency the expression for Δ must be multiplied by a factor $1 + \frac{\pi \omega d}{\omega_{oN}^2}$ and that for $\left(\frac{\Delta G}{G}\right)_H$ by $1 + \frac{\pi \omega d \cdot L_c}{\omega_{oN}^2 \ L_N^5}$ where ω_{oN} is the resonant frequency of the network lengths.

(v) Discussion.

The maximum displacement of a dislocation loop of reasonable length cannot be greater that a few atomic spacings, over which distance the Cottrell binding force does not vary all that much, so the concept of breakaway becomes suspect.

The theory so far has neglected the possibility of thermally assisted unpinning, and must therefore be considered to apply only at absolute zero. An extension to finite temperatures is made in chapter 6.4.

The point defects have been assumed to be randomly distributed along a dislocation line. It is possible however, that there exists an elastic repulsive force between neighbouring impurities, in which case the correct distribution function might be nearer a δ-function. Also it has been assumed there are no impurities in the region surrounding the dislocation, which might interfere with a brokenaway or bowed out dislocation.

The theory given above is also applicable only to the case of single crystals. A generalisation to the case of polycrystals has been given by Kharitonov (63).

The network length L_N has been assumed constant, while it should really be distributed exponentially. This is not a serious omission, however, since as already explained, the effect of an exponential distribution may be included by using an effective loop length. The quantity n, the number of minor pins between two major pins, should also have a distribution of values. The probability of a given value will be given by a Gaussian distribution about the mean value $n = \frac{L_N}{L_c} - 1$. The actual decrement will be given by the sum of terms with different n values. However, when n is large the mean value of n gives very nearly the whole sum.

6.3. Rogers' Extension To The Granato-Lücke Theory.

The dynamic loss was calculated assuming that no breakaway took place. Rogers (62) has recalculated the dynamic decrement using a loop length distribution function which is stress amplitude dependent during that part of a cycle when the stress is increasing. The expression he finds for Δ contains two terms Δ_c, a contribution from minor loops which have not broken away, and Δ_N, a contribution from loops which have completely broken away. Thus

$$\Delta_c = \frac{8 G a^2 \Lambda L_c^4 5! B\omega}{\pi^5 C^2}\left[1 - \exp\left(\frac{-\Gamma}{\sigma_0}\right)\sum_{m=0}^{5}\frac{1}{m!}\left(\frac{\Gamma}{\sigma_0}\right)^m\right]\left[1 - \left(\frac{\Gamma}{\sigma_0}+1\right)\exp\left(\frac{-\Gamma}{\sigma_0}\right)\right]^{n-1}, \qquad (6.45.)$$

$$\Delta_N = \frac{8 G a^2 \Lambda B\omega L_N^4}{\pi^5 C^2 F_N^2}\left\{1 - \left[1 - \left(\frac{\Gamma}{\sigma_0}+1\right)\exp\left(\frac{-\Gamma}{\sigma_0}\right)\right]^n\right\}, \qquad (6.46.)$$

where

$$F_N^2 = \left(1 - \frac{\omega^2}{\omega_{0N}^2}\right)^2 + \frac{\omega^2 B^2}{\omega_{0N}^4 A^2}. \qquad (6.47.)$$

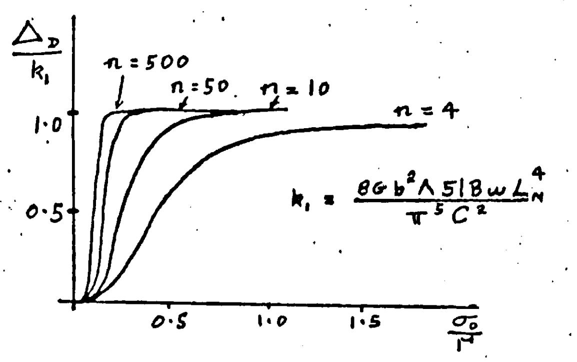

Fig. 6.6. Amplitude dependent dynamic loss for several n (i.e. L_c) values [after Rogers (62)].

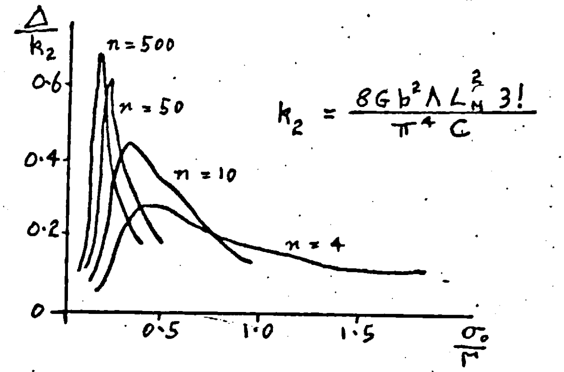

Fig. 6.7. Combined dynamic and break-away loss for several n (i.e. L_c) values [after Rogers (62)].

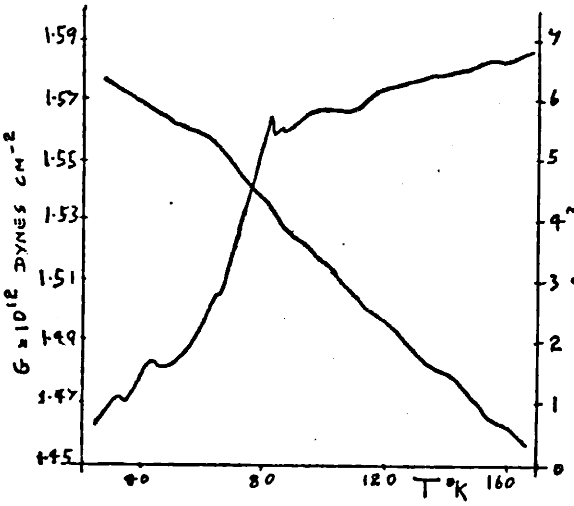

Fig. 6.8. Young's modulus and decrement versus temperature of a copper crystal [after Thompson & Holmes (59)].

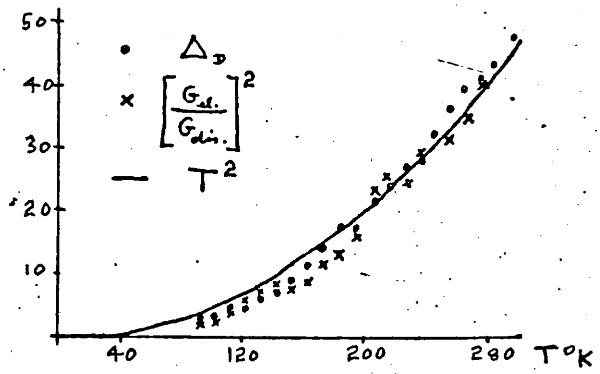

Fig. 6.9. Plots of Δ_D, $\left[\frac{G_{el}}{G_{dis}}\right]^2$, T^2 v.s. T for a copper crystal [after Thompson & Holmes (59)].

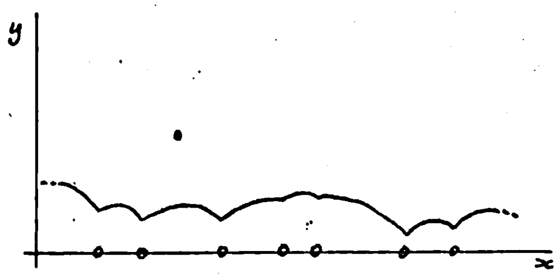

Fig. 6.10. Possible equilibrium configuration of a pinned dislocation under stress [after Teutonico, Granato & Lücke (64)].

At frequencies such that $\omega \ll \omega_N$, F_N becomes unity, and at high n or high $\frac{\sigma_0}{\Gamma}$, the term Δ_N is expected to dominate $\Delta_>$, which then becomes

$$\Delta_> \approx \Delta_N = \frac{8 G a^2 \Lambda B 5! L_N^4}{\pi^5 C^2} \left\{ 1 - \left[1 - \left(\frac{\Gamma}{\sigma_0} + 1 \right) \exp\left(\frac{-\Gamma}{\sigma_0} \right) \right]^n \right\} . \qquad (6.48.)$$

The amplitude dependent dynamic decrement is shown if Fig.6.6. for several mean values of n after a further correction has been made for a distribution in n values.

The contribution of Δ_c to $\frac{\Delta_>}{k_1}$ has a maximum value at $\sigma_0 = 0$ of 0·0625 for $n = 1$, and is smaller for higher n.

Rogers also extends the Granato-Lucke calculation of the amplitude dependent hysteretic decrement to larger strain amplitudes. The breakaway loss for several values of n is shown in Fig.6.7. An interesting feature is the presence of a low stress amplitude maximum. When the damping shown in Fig.6.6. and Fig.6.7. is combined to give the total damping, a peak appears at quite low stress amplitudes. A peak might be expected by considering equation (6.41.), for at a sufficiently high stress for breakaway to be complete, the numerator becomes constant, while the denominator may still increase. It is unfortunate that in the region of $\frac{\sigma_0}{\Gamma}$ usually employed experimentally ie:0→0·2, both the amplitude dependent dynamic and hysteretic decrements have the same form. The theory also suffers from quite strict limitations on the relative values of the parameters $\frac{\sigma_1}{\Gamma}$ and n.

6.4. Extension Of The Theory To Finite Temperatures.

So far the theory has been developed neglecting thermally aided unpinning, and is applicable strictly only at 0°K. In fact, if τ is the relaxation time for thermally aided unpinning, given by

$$\tau = \frac{1}{\nu} \exp\left(\frac{u}{kT} \right) , \qquad (6.49.)$$

where ν is an attempt frequency, typically $\sim 10^{10}$ c/s, and U is an interaction energy between a pinning point and dislocation, typically 0·10 ev., then τ is $\sim 10^{-8}$ sec. at room temperature. This corresponds to a thermal unpinning frequency NOT much greater than those frequently used in damping experiments.

Clearly thermally induced effects must be considered. It should be noted that the temperature dependence of the constants β and C is not sufficient to account for the temperature dependence of the damping. [See chapter 8.]

Thompson & Holmes (59) have proposed a model accounting for thermal effects on the basis of their experiments on copper. They find that the damping may be divided into a relaxation component and a background component, the character of the latter being different in the temperature region I (<150°K) and the region II (150°K → 300°K). In region I, a strong tendency is found for relaxation peaks to be followed by a rapid rise in the background component, Fig. 6.8., and the following model is proposed to explain this.

For small stresses and temperatures, below the relaxation peak dislocations are principally trapped in potential wells by Peierls forces. As the temperature rises kink formation is possible and the relaxation component rises by Seeger's (56) mechanism. As the temperature rises above the temperature of the relaxation maximum, transition of dislocation segments to the next trough becomes much easier, and dislocations begin to move between troughs more in phase with the stress and the relaxation component decreases. However, it now becomes relatively probable for kinks to be formed from the second to third trough, and very soon a bowing out mechanism is possible, as postulated by Granato & Lücke. The background component is thus expected to increase quite rapidly with temperature on the high temperature side of the relaxation peak. If unpinning is not allowed, however, then at a given frequency and stress a maximum contribution to the damping from a loop of given length is expected. A levelling off of the decrement at higher temperatures is in fact seen in Fig. 6.8. With increasingly cold worked specimens Niblett & Wilks (60) find the decrement decreases, as would be expected on this model, since the cold work decreases the loop lengths. Thompson & Holmes (59) find from an analysis of their results that the number of dislocation segments available for bowing, assuming no unpinning, is temperature dependent with an activation energy of twice Seeger's kink energy, as the model requires. In the temperature range II, a second component of the background friction becomes significant. See Fig. 6.9. This component is negligible in region I. It is found that the decrement, and the square of the ratio of the elastic to the dislocation modulus, $\left(\frac{G_{el.}}{G_{dis.}}\right)^2$ that is the dislocation contribution to the strain, show a very similar temperature dependence, increasing as T^2. In Fig. 6.9. only a scale factor has been used to bring the two curves into coincidence. This suggests that the average free lengths of dislocation increase with temperature i.e. thermally activated unpinning.

No satisfactory theory has yet been given to describe the increase of the dynamic loss with temperature. Leibfried (57) has considered the thermal motion of dislocation lines, ~~and in particular the thermal motion~~

~~of dislocation lines~~, and in particular the thermal forces on dislocation pinning points.

Friedel (63) considers the role of thermal activation in the pinning of dislocations by impurities, in two extremes, (a) random solid solutions, (b) dilute Cottrell clouds. For the latter case, which should be applicable to a fairly pure crystal, well annealed and at low temperatures, Friedel finds a decrement increasing exponentially with strain amplitude, and increasing exponentially also with temperature, as

$$\Delta \simeq A \exp\left[\frac{-(U_0 - \epsilon G V)}{kT}\right], \tag{6.50.}$$

where U_0 is an activation energy, and V is an activation volume.

Teutonico, Granato & Lücke (64) have considered the thermally aided unpinning of dislocations in some detail, and their approach will be summarised here.

The model used is the same as that of the previously given Koehler-Granato-Lücke theory. A possible equilibrium configuration of a pinned dislocation under stress is shown in Fig.6.10. The equation of motion of the dislocation line, equation(6.6.) now contains two extra terms, however,

$$A\frac{\partial^2 y}{\partial t^2} = \sigma b + C\frac{\partial^2 y}{\partial x^2} - B\frac{\partial y}{\partial t} - \sigma_P b - \rho(x)\frac{dE}{dy}. \tag{6.51.}$$

The force $\sigma_P b$ arises from the motion of the dislocations over the Peierls barrier, and in the present discussion is neglected under the assumption that no dislocations run parallel to a close packed direction. The term in $\rho(x)\frac{dE}{dy}$ represents the force on the dislocation due to pinning agents, and is the one to be considered. Assuming low frequencies so that the inertial and viscous forces are unimportant, equation(6.51.) becomes

$$C\frac{\partial^2 y}{\partial x^2} - \rho(x)\frac{dE}{dy} + \sigma b = 0. \tag{6.52.}$$

The interaction energy between a pinning point and a dislocation and the associated force is found by approximating the Cottrell force to a linearised triangle force, as in Fig.6.11. Equation (6.52.) is then

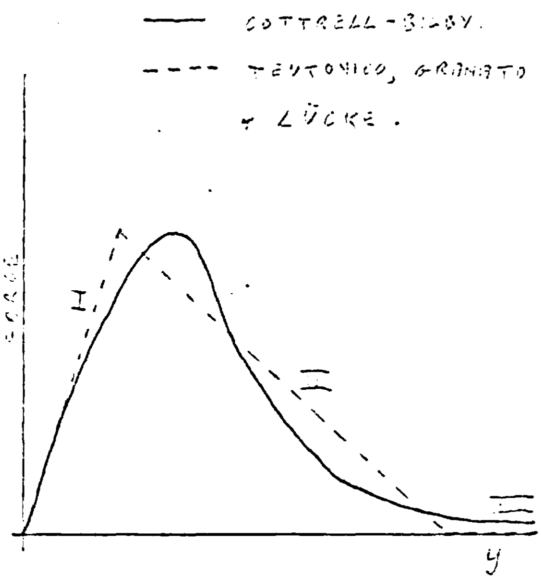

Fig. 6.11 THE FORCE SEPARATION CURVE USED TO REPRESENT THE PIN DISLOCATION INTERACTION [AFTER TEUTONICO, GRANATO & LÜCKE (64)].

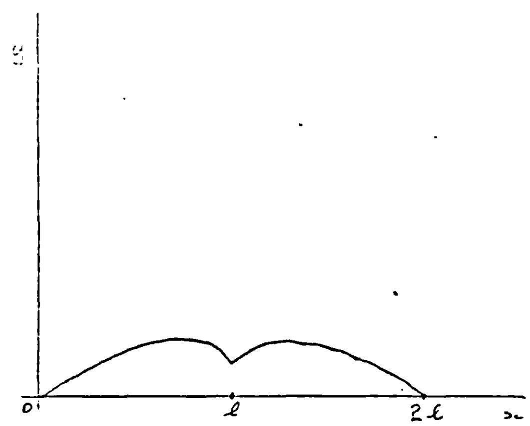

Fig. 6.12. EQUILIBRIUM CONFIGURATION UNDER STRESS OF A DISLOCATION WITH A SINGLE PINNING POINT AT ITS MID-POINT [AFTER TEUTONICO, GRANATO & LÜCKE (64)].

solved for two limiting cases. Firstly for the case of a dislocation with a single pinning point at its centre, and secondly for a continuous uniform distribution of pinning points. This latter case is equivalent tosmearing out the pinning points along a dislocation line. Although

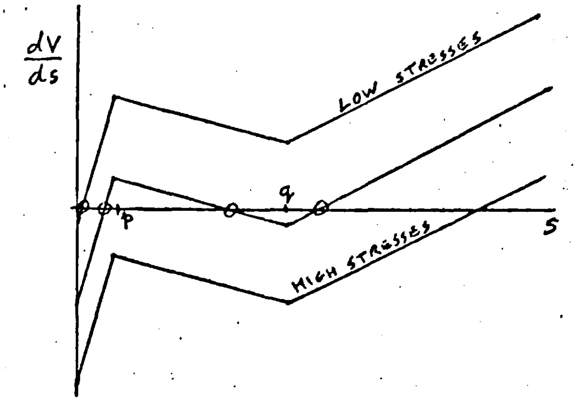

Fig. 6.13. PLOTS OF $\frac{dV}{ds}$ vs. s FOR THREE STRESS LEVELS [AFTER TEUTONICO, GRANATO + LÜCKE (64)].

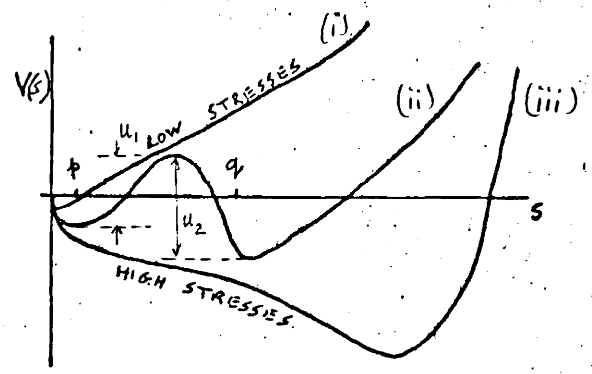

Fig. 6.14. THE THREE POTENTIAL CURVES CORRESPONDING TO THE FORCE CURVES OF Fig. 6.13. [AFTER TEUTONICO, GRANATO + LÜCKE (64)].

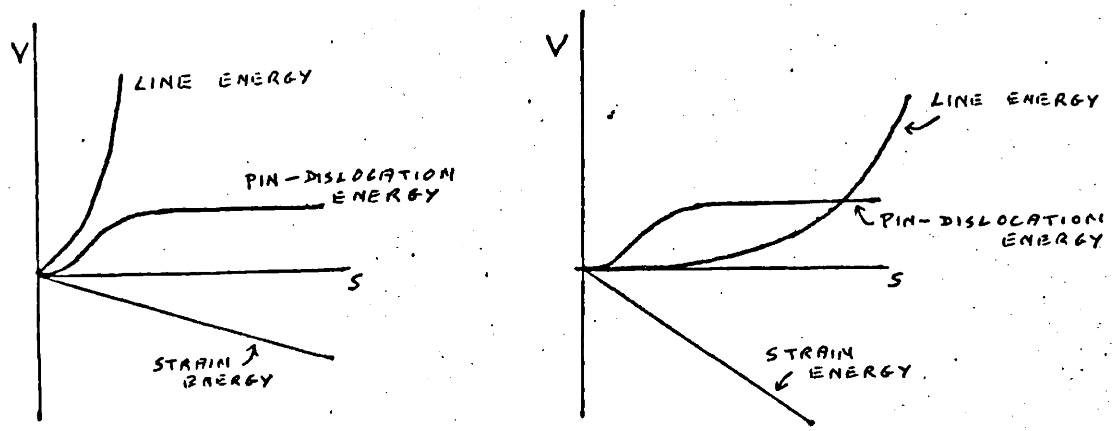

(a) SHORT LOOPS.

(b) LONG LOOPS.

Fig. 6.15. CONTRIBUTIONS TO THE TOTAL ENERGY, V, IN THE CASE OF SHORT AND LONG LOOPS [AFTER TEUTONICO, GRANATO + LÜCKE (64)].

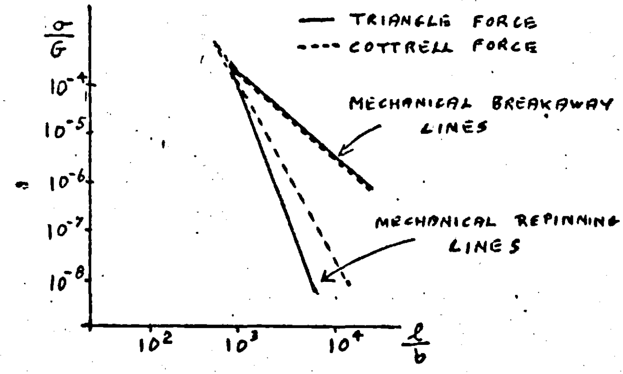

Fig. 6.16. A PLOT OF STRESS V.S. LOOP LENGTH FOR THE DOUBLE LOOP. [AFTER TEUTONICO, GRANATO + LÜCKE (64)].

Teutonico, Granato & Lücke solve equation (6.52) for both cases, and find expressions for the decrement and modulus change, the results are qualitatively the same for both. The solution for a single pinning point only will be considered here. The equilibrium configuration under stress of a dislocation with a single pinning point at its mid-point is shown in Fig. 6.12. The potential energy, V, of this dislocation line has three components: the line energy, the pin-dislocation interaction energy, and the strain energy. An expression for $\frac{dV}{ds}$, the change of V with s, where s is the distance of the dislocation from its pinning point, is found for each of the three regions of the triangle force (see Fig. 6.11.), leading to three possible equilibrium values of s ($\frac{dV}{ds} = 0$).

These are denoted by s_{I} , s_{II} and s_{III} where the subscript refers to the appropriate region of the triangle force. However, the solutions for the equilibrium configuration of the dislocation corresponding to each of these s values exist only when the s value, determined by the parameters of the problem, falls in the corresponding force region. This is illustrated in Fig. 6.13.

At low stresses there is seen to be only one possible position of equilibrium, at intermediate stresses three, and at high stresses again only one. In fig. 6.14. is plotted the potential energy against displacement s. It is seen that at low and high stresses there is only one equilibrium position, corresponding to a pinned and unpinned state respectively. At intermediate stresses there are two stable positions, seperated by a saddle point. The physical interpretation of this is as follows. For a dislocation to break away at absolute zero a sufficiently high stress must be applied for the potential energy hill to disappear cf. curve (iii). The threshold stress, σ_1, at which breakaway occurs is that used in the Granato-Lücke theory. When finite temperatures are introduced it becomes possible for the dislocation to overcome the potential barrier at much lower stresses, so long as there is a second potential minimum into which it may jump, cf. curve (ii). Since this second minimum does not exist for all stresses, we have the important result that even for thermal breakaway a stress threshold exists.

In the discussions so far it has been assumed that the dislocation loops are of reasonable length, say $> 100\,b$. For shorter loop lengths it is found that there is no stress at which there is more than one potential minimum. This behaviour can be understood by considering Fig.6.15. For short loops, Fig.6.15(a), the line energy term dominates the energy function at all values of s, and the concept of breakaway does not apply. For long loops, Fig.6.15(b), however, this term dominates only at large values of s. Thermal breakaway is possible, therefore, for sufficiently long loop lengths and stresses in the range $\sigma_2 < \sigma < \sigma_1$, where σ_2 is the stress at which the second potential minimum first appears, called the mechanical repinning stress. The activation energy for jumping in each direction is shown in Fig.6.14. U_1 has its maximum value when the stress is σ_2, and decreases to zero at the mechanical breakaway stress σ_1. U_2 is zero at the mechanical repinning stress σ_2, and has its maximum at the mechanical breakaway stress σ_1. Fig.6.16. which summarises these results, shows the variation of a normalised stress, $\frac{\sigma}{G}$, with a normalised loop length, $\frac{\ell}{b}$. The region of thermal breakaway is shown bounded by the mechanical repinning and breakaway lines. The dotted lines show results obtained using an exact expression for the Cottrell binding force. It must be remembered, however, that the latter is itself an approximation.

So far only the conditions for breakaway and the nature of the breakaway have been considered. Before an expression for the decrement can be calculated, the rate at which thermal breakaway and repinning take place must be considered.

Let f' represent the fraction of dislocations in the second potential minimum i.e. broken away. The rate at which dislocations leave this state is given by $-f'\nu_2 \exp\left(\frac{-U_2}{kT}\right)$, where ν_2 is an effective attack frequency associated with the vibration (thermal) of the dislocation in the direction of the energy barrier. Similarly the rate at which dislocations enter the second minimum from the first is $(1-f')\nu_1 \exp\left(\frac{-U_1}{kT}\right)$. These rates apply only in the stress region where two minima exist. However, a single rate equation true for all stresses may be constructed if E_1 and E_2 are defined,

$$E_1 = \begin{cases} \infty & \sigma < \sigma_2 \\ U_1 & \sigma_2 < \sigma < \sigma_1 \\ 0 & \sigma > \sigma_1 \end{cases} \qquad E_2 = \begin{cases} 0 & \sigma < \sigma_2 \\ U_2 & \sigma_2 < \sigma < \sigma_1 \\ \infty & \sigma > \sigma_1 . \end{cases}$$

The rate equation is then

$$\frac{df'}{dt} = (1-f')\nu_1 \exp\left(\frac{-E_1}{kT}\right) - f'\nu_2 \exp\left(\frac{-E_2}{kT}\right). \qquad (6.53)$$

Granato, Lücke, Teutonico & Schlipf (64) have calculated the effective jump frequencies ν_1 and ν_2 using the statistical mechanical treatment of absolute rate theory. Equation (6.53) may be solved for $f'(t)$ in the three stress regions, and using expressions for the mean displacement of the dislocation in pinned and unpinned states, the contribution of dislocations in these states to the total dislocation strain may be found. This may then be used in expressions for the decrement and modulus change.

However, the expressions for the decrement and modulus defect found in this way while explicit, are too complicated to be used directly for comparision with experimental results.

The treatment for a symmetric double loop given above leads to results of the same form when applied to an assymmetric loop and to a continuously pinned loop as Teutonico, Granato and Lücke show. Now, if the density of pinning points is made such that the effective loop length is the same as the loop length used in the symmetric loop length solution, then the two approaches become equivalent and the activation energy for breakaway as a function of stress should be the same. The agreement, however, is found to be very poor, even with short loop lengths, and it is concluded that (a) the activation energies for breakaway are not adequately described by the continuous pinning approximation and (b) the problem of cooperative thermal activation of breakaway from several individual pinning points should be studied. This is important because breakaway from a first pinning point may eventually lead to breakaway from all other pinning points in the network length.

The thermally aided unpinning of a dislocation has recently been considered further by Koiwa & Hasiguti (35).

CHAPTER 7

A Discussion of the Koehler-Granato-Lücke Theory.

In this chapter some selected experimental results will be discussed in terms of the Koehler-Granato-Lücke theory (hereafter referred to as the K.G.L. theory). Where certain aspects of the damping are not accounted for by this theory, other models or modifications of the K.G.L. theory will be introduced. The conditions under which the different theories are expected to hold will be indicated.

7.1. The Frequency Dependence of the Damping.

(a) The hysteretic loss.

The K.G.L. theory predicts a decrement independent of frequency, cf. equation(6.42.) The experimental evidence is inconclusive, but seems to support this.[Niblett & Wilks (60)] Measurements by Kamentsky (56) on copper single crystals at various harmonics in the Kc/s range are somewhat scattered, but appear to show a tendency for the strain amplitude dependent decrement to increase with increasing frequency. However, as Nowick (50) has pointed out, such an effect may be due to the structure sensitivity of the measurements, since at different harmonics different parts of a specimen are excited. Measurements on annealed single crystals of lead by Hiki (58) at both 64Kc/s and 192Kc/s are shown in Fig.7.1. No dependence on frequency is observed, although the strain amplitude dependence of the friction in these measurements does not agree well with the K.G.L. theory.

(b) The dynamic loss.

Here the K.G.L. theory predicts a decrement proportional to frequency below the Mc/s frequency range, with a maximum decrement in the Mc/s range near the dislocation resonant frequency. This high frequency behaviour

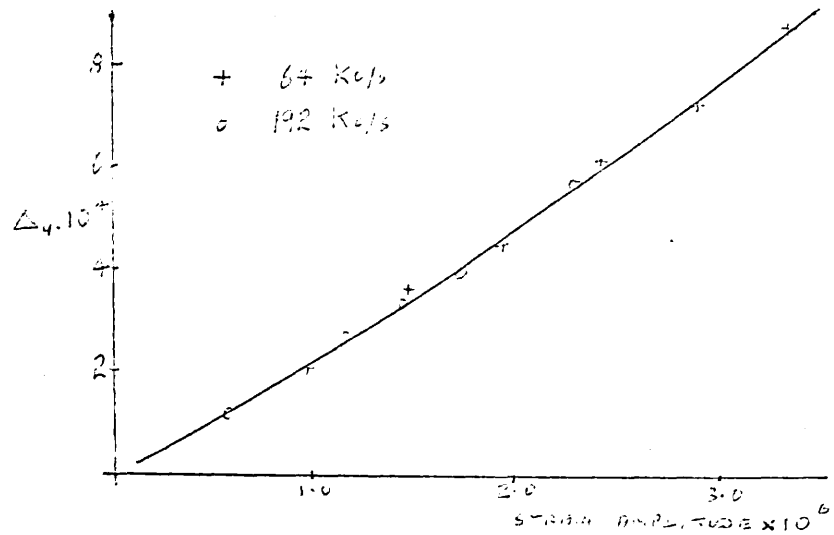

Fig. 7.1. AMPLITUDE DEPENDENT FRICTION OF A Pb SINGLE CRYSTAL MEASURED AT TWO FREQUENCIES [AFTER HIKI (56)].

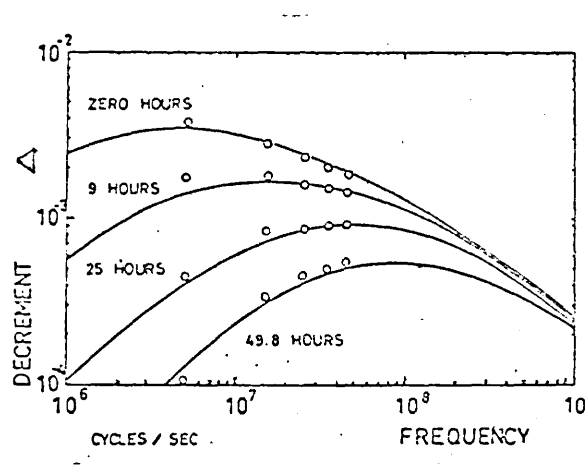

Fig. 7.2. DECREMENT AS A FUNCTION OF FREQUENCY FOR SEVERAL IRRADIATION TIMES. THE SOLID CURVES ARE PREDICTED BY AN ANALYSIS BASED ON THE K.G.L. THEORY [AFTER STERN & GRANATO (62)].

will be discussed first.

(i) The high frequency behaviour of the dynamic decrement.

This has been investigated for copper by Stern & Granato (62). The K.C.L. theory predicts, at high frequencies, a decrement of the form

$$\Delta_I = \Omega \Delta_0 \Lambda L^2 \frac{\omega \tau}{1+\omega^2 \tau^2} , \qquad (7.1.)$$

where $\tau = \frac{BL^2}{\pi^2 C}$. This decrement has a maximum value, Δ_{IM}, given by

$$\Delta_{IM} = \frac{\Omega \Delta_0 \Lambda L^2}{2} , \qquad (7.2.)$$

at a frequency, ω_M, where

$$\omega_M = \frac{1}{\tau} = \omega_0^2 \frac{A}{B} = \frac{\pi^2 C}{BL^2} . \qquad (7.3.)$$

For frequencies much greater than ω_M, the decrement should decrease as $\frac{1}{\omega}$, so that the attenuation, α, takes the limiting value α_∞, where

$$\alpha_\infty = \frac{4 \Omega G b^2 \Lambda}{\pi^2 B} , \qquad (7.4.)$$

which is seen to be independent of the dislocation loop length.

Stern and Granato measured the attenuation as a function of both loop length and frequency over the frequency range 5Mc/s to 45Mc/s in pure copper, by irradiating with γ-rays. Typical results are shown in Fig.7.2. The maximum in the decrement moved to continuously higher frequencies as the irradiation progressed. The amplitude of the maximum decreased with irradiation. They found also that the orientation dependence was consistent with the dislocation damping model, in that only shear stresses in dislocation slip systems were effective in producing damping. The maximum in damping moved to higher frequencies at lower temperatures, consistent with resonance under conditions of large damping.

Similar results were obtained by Alers & Thompson (61), who were able to fit the K.C.L. theory to their results. Stern and Granato were unable to do this immediately, because the maximum was broader than the theory predicted.

Also it should be possible to generate the curves for all irradiation times (see Fig.7.2.), by sliding one maximum along its upper asymptote, since α_∞ is independent of loop length and only the latter should be affected by irradiation. However, Stern and Granato were unable to do this. They resolve this difficulty by postulating the presence of two different dislocation systems. The observed curve is then the resultant of two individual ones that move along parallel asymptotes, at different rates, as irradiation proceeds. Thompson & Paré (60) have also found evidence for a two dislocation system from measurements in the Kc/s region.

(ii) The low frequency behaviour of the dynamic decrement.

The experimental evidence available on the low frequency behaviour of the dynamic decrement is inconclusive, but in general appears not to support the K.G.L. theory. Typical results by Takahashi (56) on polycrystalline copper, made at room temperature and frequencies between 1 and 10Kc/s, show a decrement almost independent of frequency. The magnitude of the friction observed by Weinig & Machlin (56) in polycrystalline 99·999% copper, at a frequency of about 1c/s, is as great as many values obtained in the Kc/s range, indicating a decrement independent of frequency.

A number of mechanisms have been proposed to account for the weak frequency dependence of the dynamic decrement in the low frequency region, some of which will be considered here.

Wilks (59) has suggested that a larger value of Δ_I may be obtained at low frequencies, as a result of thermally aided unpinning of a dislocation line. This increases the average dislocation loop length, L, and, since Δ_I is proportional to L^4 on the K.G.L. theory, the decrement increases. If breakaway takes a time $\tau = \nu_0^{-1} \exp\left(\frac{E}{kT}\right)$, where ν_0 is an attempt frequency, and E an activation energy, the condition for breakaway is $\frac{1}{\omega} \gg \tau$. This condition will hold at low frequencies, when the decrement will become a function of $\frac{1}{\omega}$, and its frequency dependence is suppressed. However, if this mechanism is operating, the decrement should be strongly temperature dependent, which is not often observed in practice.

Blistanov & Shaskol'skaya (64) have attempted to correct the frequency dependence of Δ_I using the micro-creep idea of Cottrell (53). It is assumed that a pinning point can move, under the influence of the attractive force exerted on it by a dislocation, and follow a dislocation which is moving under an applied stress. This behaviour is illustrated in Fig.7.3, which shows the displacement of a dislocation segment under the action of a periodic stress during one cycle. Continuous lines represent the displaced position of the dislocation, and dashed lines its original position. The displacement of a dislocation line is now the geometrical sum of the pinning point displacement, ξ_P, and the dislocation displacement, ξ_d'. This replaces the quantity ξ_d in the K.G.L. theory. The decrement is then calculated to be

$$\Delta_I = \Lambda \Delta_0 \eta^2 \left[\frac{\omega d}{(\omega_0^2 - \omega^2) + \omega^2 d^2} + \frac{A}{A_2} \cdot \frac{\pi d_1}{\omega(\omega^2 + d^2)} \right], \qquad (7.5.)$$

which at low frequencies, ie. $\omega \ll \omega_0$, reduces to

$$\Delta_I = \Omega \Lambda \Delta_0 \eta^2 \left[\frac{\omega d}{\omega_0^2} + \frac{A}{A_2} \frac{\pi}{\omega d_1} \right]. \qquad (7.6.)$$

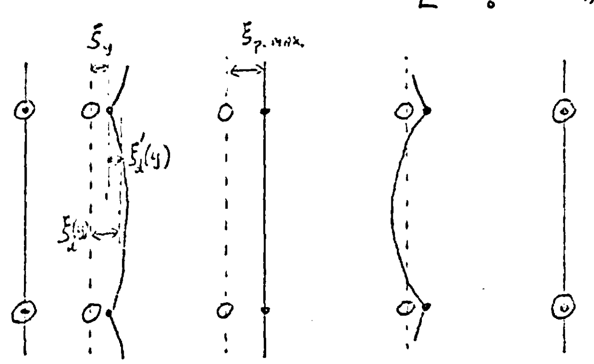

Fig. 7.3. DIAGRAM OF THE DISPLACEMENT OF A DISLOCATION SEGMENT UNDER THE ACTION OF A PERIODIC STRESS [AFTER BLISTANOV & SHASKOL'SKAYA (64)].

The first term on the R.H.S. is the K.G.L. term, the second represents the effect of micro-creep, and is seen to become important at low frequencies. The point at which the frequency dependence departs from linearity is determined by the ratio $\frac{A}{A_2}$, and by B and B_1. When reasonable values of the parameters are assumed, this is around 100c/s. Thus at low frequencies Δ_I may be quite large, as a result of the mobility of point defects. The predicted frequency dependence is not observed, however, over any large frequency range, but a distribution in the values of A_2 and d_1, associated with different types of pinning point, may account for the observed dependences. The activation energy of the frictional process is about half the activation energy of diffusion of a point defect, so that the theory should apply only when assemblies of defects form the pinning points.

The weak dependence of Δ_I on frequency suggests that a hysteresis mechanism, such as that proposed by Nowick (54), is responsible for the damping, giving a decrement independent of frequency. This idea has been taken up by Weertman & Salkovitz (55), who consider the effect of random impurities on the motion of a dislocation. In the K.G.L. model, point defects appear only on dislocation lines, and after breakaway the dislocation motion is limited only by line tension. In the Weertman-Salkovitz model, a dislocation line is initially unpinned, and when a stress is applied it moves in a hysteretic fashion over the potential barriers associated with random defects. The critical stress necessary to overcome such impurity barriers is calculated, according to Mott & Nabarro (52), to be $\mu\epsilon' c \ln\left(\frac{1}{c}\right)$, where μ is the shear modulus, ϵ' the fractional difference in size between solvent and solute atom, and c is the concentration of impurities. If a

is the atomic spacing, the stress field will have an average wave-length of a/b. Weertman & Salkovitz calculate the energy lost by a length of dislocation oscillating over such potential barriers, and derive expressions for the decrement and modulus change from which semi-quantitative comparisons with experiment may be made. In many cases a decrement of the correct order of magnitude is predicted, but the model is theoretically unsound since it requires that a coherent length of dislocation, (a length capable of moving independently of other lengths), should oscillate with an amplitude at least equal to the wave-length λ of the stress field, ie. a/b. At even quite high stress amplitudes, and for the maximum coherent length of dislocation, ie. that corresponding to a Frank-Read source, the displacement is only of the order of a.

The requirement that the pinning of the dislocation is negligible under zero applied stress, also restricts the application of the model.

(c) Ultrasonic harmonic generation.

Recently the generation of a second and higher harmonic of an ultrasonic wave in a solid has been considered. These harmonics are related to the second and higher order terms in the stress-strain relation for a nonlinear solid. This nonlinearity may arise from two causes, the anharmonicity of the lattice forces, and the nonlinear nature of dislocation displacements. In most metals, dislocation displacements are expected to occur and to contribute to the nonlinearity for static bias stresses lower than those required to affect the lattice anharmonicity. The loss from the fundamental ultrasonic wave by second harmonic generation is, however, small. Hikata, Chick & Elbaum (63) & (65), have calculated that, for a 10Mc/s wave, assuming reasonable values for dislocation and lattice parameters, the amplitude of the second harmonic wave is about three orders of magnitude smaller than the amplitude of the fundamental wave, at a static bias stress of about 10^6 dynes/cm. The dislocation contribution to harmonic generation has been considered also by Breazeale & Thompson (63), Suzuki, Hiki & Elbaum (64), Brailsford (64) and Alefeld (65).

7.2. The residual, low stress amplitude component of the decrement.

It is generally found that at least part of the damping at low stress amplitudes cannot be accounted for by the dynamic loss mechanism according to equation (6.22.). This loss would be completely suppressed by a sufficiently high pinning point density on the dislocations, but Beshers(55) has found that, by addition of Au to Cu, the damping in the Kc/s region does not decrease below a value of about 10^{-4}. Similar results have been found by Weinig & Machlin (56) in the lc/s region, and by Fiore & Bauer (64). Rogers' modification to the K.G.L. theory (cf. chapter 6.3.), is capable of predicting a constant decrement of this magnitude at low strain amplitudes and high pinning point densities. However, this decrement should also decrease to a very low value at a sufficiently low strain amplitude. Although this theory may account for some of the experimental results, it is unlikely that sufficiently low strain amplitudes have not been reached in some experiments.

An alternative damping model, incorporating the features of both the K.G.L. model and the hysteresis model of Weertman & Salkovitz (55), has been proposed qualitatively by Celli (62), which may account for this residual damping. Celli's model is considered in chapter 7.3(ii).

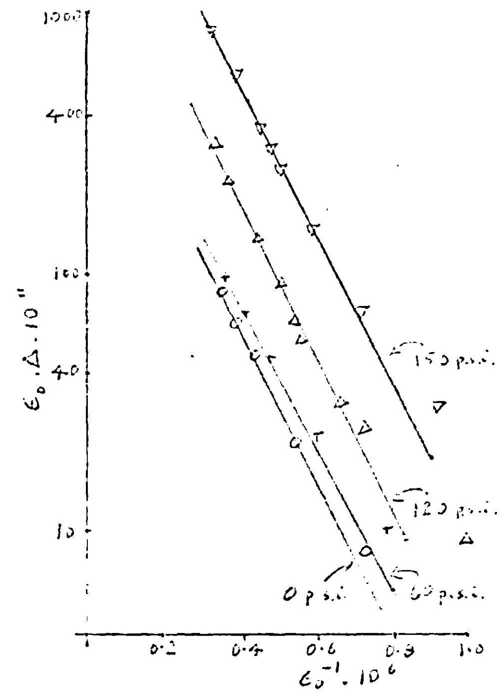

Fig. 7.4. The measurements of Reid (41) on a copper single crystal at several deformations treated by Granato & Lücke (56).

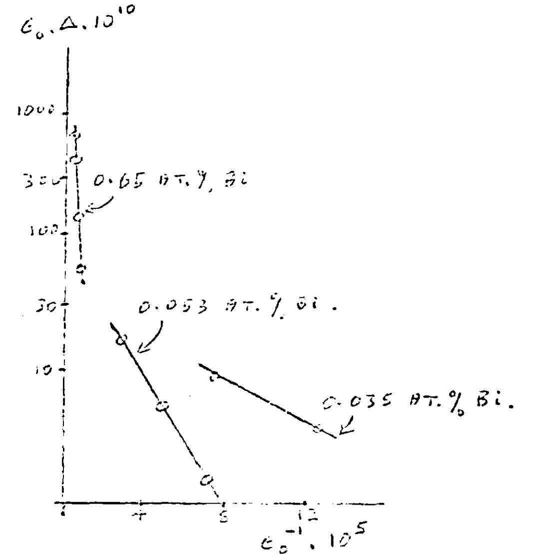

Fig. 7.5. Data of Weertman & Salkovitz (55) plotted as $\ln(\Delta \epsilon_0)$ vs. ϵ_0^{-1} [after Granato & Lücke (56)].

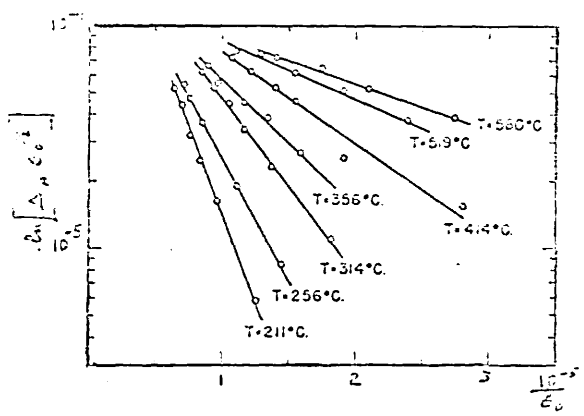

Fig. 7.6. K.G.L. plots for a Cu-Ge alloy at different temperatures [after Fiore & Bauer (64)].

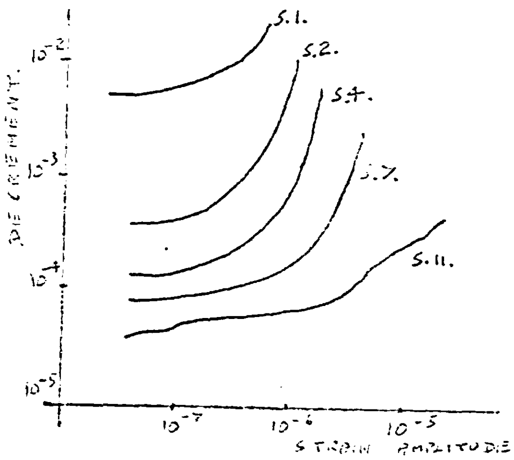

Fig. 7.7. Strain amplitude dependence of the damping for several neutron doses [after Thompson & Paré (65)].

7.3. The Strain Amplitude Dependence of the Friction.

(i) According to the K.G.L. theory, strain amplitude dependent data are describable by the function, (equation 6.43)

$$\Delta_H = \frac{C_1}{\epsilon_0} \exp\left(\frac{-C_2}{\epsilon_0}\right) , \qquad (7.7.)$$

where

$$C_2 = \frac{K\epsilon' a}{L_c} , \qquad (7.8.)$$

$$C_1 = \frac{\Omega \Delta_0 \Lambda L_N^3 K \epsilon' a}{\pi L_c^2} . \qquad (7.9.)$$

In fact if ϵ_0 varies over the specimen, a further integration is necessary to find Δ_H. For example, standing waves in a thin rod yield [Fiore & Bauer (64)]

$$\Delta_H = A_1 \Lambda L_N^3 \sqrt{\frac{2}{\pi A_2 L_c^3 \epsilon_0}} \exp\left(\frac{-A_2}{L_c \epsilon_0}\right) . \qquad (7.10.)$$

A useful way to test this theory is to plot a graph of $\ln(\Delta_H \epsilon_0)$ against $\frac{1}{\epsilon_0}$ which, according to equation (7.7.), should yield a straight line, with slope C_2 and an intercept on the $\ln(\Delta_H \epsilon_0)$ axis of C_1.

The experimental evidence in favour of such a relation has been considered by Granato & Lücke (56), and the agreement in general is found to be quite good. In particular, the measurements of Read (41), on 99.998% copper single crystals after successive static loads of 0, 60, 120, 150p.s.i. when plotted as above, yield straight lines with the same slope but different intercepts, as shown in Fig.7.4. The loading should affect mostly the dislocation density, Λ, which will change the intercept, C_1, but will hardly affect L_c, so the slope should remain constant. The slope of a K.G.L. plot should be proportional to the concentration of impurities. Fig.7.5. shows the results of Weertman & Salkovitz (55) for lead single crystals, with up to 1% Bi, at room temperature. These plots are seen to give straight lines over the limited range of ϵ_0 involved, the slopes varying with concentration in roughly the predicted manner. Similar experiments have been performed by Weinig & Machlin (56), Takahashi (56) and Caswell (58). Weinig & Machlin's results give quite good straight lines, but the slope varies only slightly with $\frac{1}{L_c}$, in contrast with the graphs of Weertman and Salkovitz. Takahashi made measurements on polycrystalline copper containing small quantities of Al, Zn or P, and found his results could be fitted to an expression of the form

$$\Delta_H = \beta \, \epsilon_0^{\alpha} \; , \qquad (7.11.)$$

with the value of α increasing from about 1·0 for pure copper to about 2·5 for copper containing 1·0% of Zn or P. A relation of this form was observed also by Nowick (50), Panseri et al. (62) and Kharitonov (63). Caswell's results also yield curved plots of $\ln(\Delta_H \epsilon_0)$ against $\frac{1}{\epsilon_0}$, again in contradiction with the K.G.L. prediction.

Fiore & Bauer (64) have made measurements on Cu-Ge single crystals with composition varying from 0·005 to 0·5 atomic per cent. Ge. Specimens were excited in their fundamental longitudinal mode at 80Kc/s, and at temperatures in the range 200°C to 600°C. Equation (7.10.) is relevant here. When the decrement is plotted as a function of strain amplitude, three regions of different strain amplitude behaviour are found, which will now be considered in turn.

(a) The strain amplitude dependent region.

Fig.7.6. shows a plot of $\ln(\Delta_H \epsilon_0^{\frac{1}{2}})$ against $\frac{1}{\epsilon_0}$ for measurements made at different temperatures. The plots are seen to be linear. Values of L_c calculated from the slopes are given in Table II. If c is the impurity pinning point concentration, which varies with temperature according to

$$c = c_0 \exp\left(\frac{U_B}{kT}\right) \; , \qquad (7.12.)$$

where U_B is the activation energy for the breakaway of a dislocation from a pinning point, and c_0 is the impurity pinning point concentration at 0°K, then L_c should vary with temperature as

$$L_c = \frac{a}{c} = \frac{a}{c_0} \exp\left(\frac{-U_B}{kT}\right) . \qquad (7.13.)$$

Fiore and Bauer find that equation (7.13.) describes the increase of L_c with temperature, and the decrease with c_0, which they observe (Table II). The calculated values of L_c, ranging from 4.10^{-8} cm. to 1.10^{-5} cm, appear reasonable, since they lie in the range of 2.10^{-8} cm. for a continuously pinned dislocation, and about 5.10^{-4} cm. for an impurity free dislocation. Also, the values of U_B calculated from L_c and c_0 are in agreement with predictions [Flinn (62)]. The values of ΛL_N^3 may be calculated from the intercepts on the $\frac{1}{\epsilon_0}$ axis and the values of L_c. The dislocation density, Λ, is assumed to be 5.10^{5} cm.$^{-2}$ and reasonable values of L_N are then obtained, (see Table II). The values of the parameter $\frac{L_N}{L_c}$ are seen to fall within the range of validity of the K.G.L. theory.

ALLOY	ATOMIC % Ge.	TEMPERATURE °C	U_B eV.	L_c cm.	L_N cm. [$\Lambda = 5.10^5$ cm^{-2}]	Δ_D	B [K.G.L] dyne.sec.cm.$^{-2}$	B [Rogers] dyne.sec.cm.$^{-2}$
A	0.54	454	0.27	$6.4.10^{-8}$	$1.1.10^{-4}$			
B	0.12	462	0.26	$3.8.10^{-7}$	$1.6.10^{-4}$	$1.0.10^{-4}$	2.10^{5}	$1.0.10^{-3}$
C	0.05	441	0.30	$3.9.10^{-7}$	$2.4.10^{-4}$	$1.0.10^{-4}$	3.10^{5}	$3.0.10^{-3}$
D	0.009	454	0.30	$2.4.10^{-7}$	$3.9.10^{-4}$	$2.3.10^{-3}$	1.10^{4}	$3.0.10^{-3}$
E	0.0057	530	0.27	$1.1.10^{-5}$	$7.5.10^{-4}$	$3.1.10^{-3}$	5.10^{1}	$0.4.10^{-3}$
E	0.0057	519	0.27	$8.5.10^{-6}$	$6.5.10^{-4}$	$2.2.10^{-3}$	5.10^{1}	$0.3.10^{-3}$
E	0.0057	414	0.25	$4.9.10^{-6}$	$5.7.10^{-4}$	$2.0.10^{-3}$	6.10^{2}	$0.7.10^{-3}$
E	0.0057	356	0.26	$3.8.10^{-6}$	$2.3.10^{-4}$	$1.6.10^{-3}$	1.10^{3}	$0.8.10^{-3}$
E	0.0057	314	0.23	$2.4.10^{-6}$	$4.6.10^{-4}$			
E	0.0057	256	0.25	$1.8.10^{-6}$	$4.2.10^{-4}$			
E	0.0057	211	0.24	$1.3.10^{-6}$	$4.0.10^{-4}$			

TABLE II [AFTER FIORE & BAUER (54)].

(b) The strain amplitude independent region.

The K.G.L. theory predicts an amplitude independent decrement Δ_D of the form

$$\Delta_D = A_0 B L^4 \Lambda , \qquad (7.14.)$$

where

$$\frac{1}{L} = \frac{1}{L_N} + \frac{1}{L_c} . \qquad (7.15.)$$

Difficulties arise because the parameters L_N, L_c, Λ and B are unknown. Fiore and Bauer , however, use the values of L_N and L_c calculated above for the amplitude dependent decrement, and assume a value of Λ. A value of Δ_D is obtained assuming the residual decrement,(see ch. 7.2.), to be the minimum observed value of the total decrement. Values of B may then be calculated, and are shown in Table II. The calculated values of B are not at all constant, nor do they agree with the theoretical value of 10^{-4} dyne sec. cm.$^{-2}$ for pure copper [Mason (60)]. The validity of the K.G.L. theory is therefore questionable. A further discrepancy arises when the Cu-Ge alloy is dilute, ie. $L \doteqdot L_c$, and Δ_D is about 10^{-3}. Using Mason's value of B , the minimum value of L is found to be about 7.10^{-5} cm. compared with an impurity spacing of 10^{-6} cm, assuming there is no impurity clustering. Since impurities may be expected to gather preferentially on dislocations, L_c is probably less than 10^{-6}.

Rogers' modification to the K.G.L. theory can however describe these results. According to equation (6.48.)

$$\Delta_D = A_0 B \Lambda L_N^4 . \qquad (7.16.)$$

Thus the relevant loop length is not necessarily determined by the impurity spacing, but by the network length L_N, and the values of L_N in Table II are seen to be greater than 7.10^{-5} cm. Also shown in Table II are values of B calculated from equation (7.16.) assuming the edge dislocation

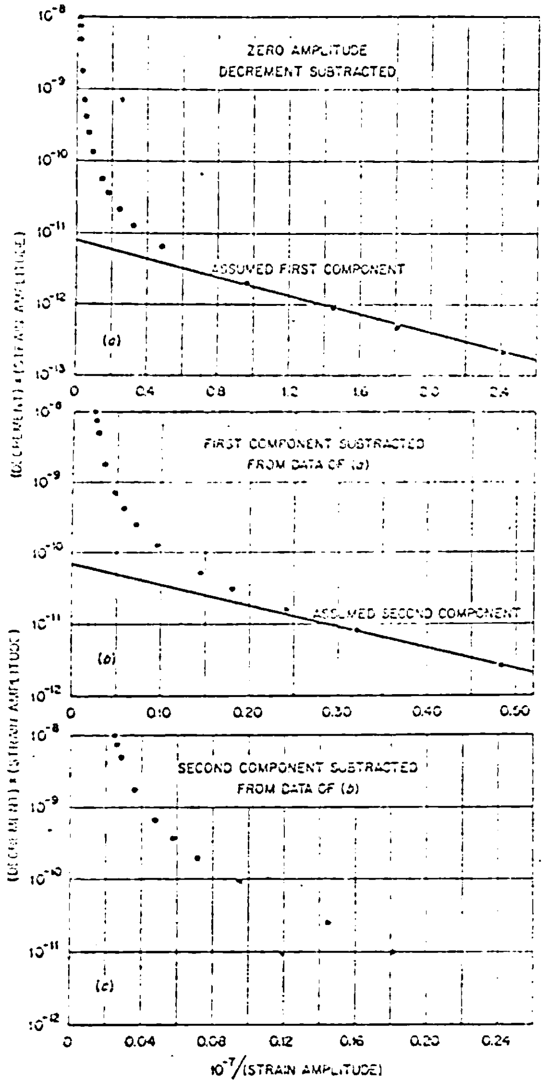

Fig. 7. 8. K.G.L. Plots for dose level 5.7. of Fig. 7.7. [after Thompson & Paré (65)].

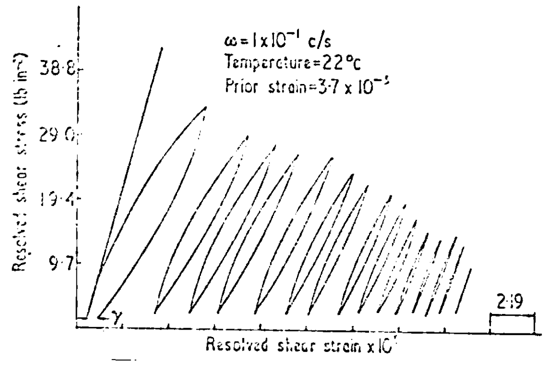

Fig. 7. 9. Hysteresis loops in zinc single crystals [after Roberts & Brown (62)].

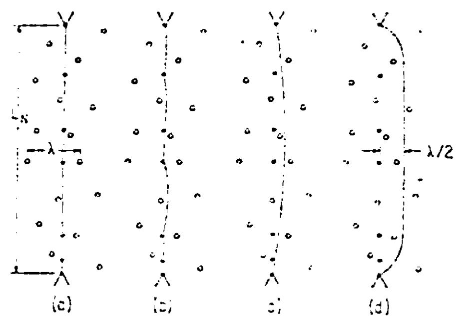

Fig. 7. 10. The K.G.L. model modified by restoring effect of impurities near dislocation [after Swartz & Weertman (61)].

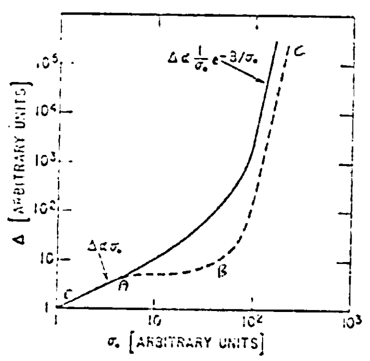

Fig. 7. 11. The dependence of the damping Δ on the stress amplitude σ_0 [after Swartz & Weertman (61)].

density is the same as that of the screw dislocations. The values of B are in quite good agreement with the predicted value of Mason (60), which should describe both edge and screw dislocations.

(c) The plateau region.

A region of constant decrement at large stresses, or when the ratio $\frac{L_N}{L_c}$ tends to unity, is observed by Fiore and Bauer, and is predicted by Rogers' modification to the K.G.L. theory. This behaviour may be understood also from a simple physical argument. The decrement may be written [equation(4.8.)]

$$\Delta = \frac{\Delta W}{2W} , \qquad (7.17.)$$

where ΔW is a measure of the energy dissipated in pulling a dislocation away from the strain field of a point defect. After a certain separation, the strain field felt by the dislocation becomes small, and further dislocation displacement is not accompanied by an increase in ΔW. However, W increases continuously with dislocation displacement. A maximum is therefore expected in the decrement. This behaviour is expected at high temperatures and/or low concentrations of defects, because the solute atmosphere round a dislocation will then be least dense, and the net attractive potential smallest.

Thompson & Paré (65) have investigated the breakaway stress in copper, at 100°C, as a function of fast neutron irradiation. Fig.7.7. shows the measured decrement variation with strain amplitude after different radiation doses. The friction is seen to decrease, and the breakaway stress to increase, with irradiation. Fig.7.8(a) shows a K.G.L. plot of $\ln(\Delta_H \epsilon_0) / \frac{1}{\epsilon_0}$ for these results. The plot is curved, and is not, therefore, in agreement with the K.G.L. theory. In Fig.7.8(b) and 7.8(c) an attempt has been made to separate out any components due to several dislocation systems, by subtracting the straight line portion of the graphs. The resulting graph, however, shown in Fig.7.8(c), is seen to be almost as curved as in Fig.7.8(a). It is also found that the slopes of the curves at low maximum strain amplitudes remain nearly constant with radiation dose, while the intercepts decrease with increasing dose. According to the K.G.L. theory, such a slope and intercept behaviour implies that the density of unbreakable, or network, pinning points increases with dose, while the density of breakable pinning points remains constant. Since the theory requires the loop length ratio $\frac{L_N}{L_c}$ to be greater than about 5, it is not known whether the theory is even applicable here.

Instead of using the K.G.L. theory, Thompson and Paré apply an analysis of their own, based on the curves of Fig.7.8, which leads to a relation between dislocation loop length and irradiation time. They then find that the loop length tends to a constant value at high doses, an effect not observed previously, [Thompson & Holmes (56), Thompson & Paré (60)] possibly because of the high temperatures used in the present experiment, or because high background damping masked the effect in previous experiments. The loop length behaviour observed by Thompson and Paré might be accounted for if the predominant radiation defects were vacancies, with a tendency to form clusters. After a certain time, the clusters already present would tend to grow and develop into strong network pins, while no new cluster would be formed to change the loop length.

The experiment described above also has application to the study of the yield point and hardening mechanism in copper. The former is related to the unpinning of dislocations, and hence to the breakaway stress, while the latter is a function of the number of pinning points present.

In fact internal friction measurements enable the hardening to be evaluated at stress and dose levels smaller than are possible in tensile tests. [Young (62), Blewitt (60), Diehl (62), Fischer (62)]

A feature of the K.G.L. theory is the prediction of an asymmetric hysteresis loop (see Fig.6.2.). However, Roberts & Brown (62) in measurements on zinc single crystals in the frequency range 10^{-1} to 10^{-2} c/s, found symmetric hysteresis loops, as shown in Fig.7.9. Other features of the results are, however, described quite well by the K.G.L. theory, and Roberts and Brown suggest the theory fails to describe the shape of the hysteresis loop since it neglects thermally aided unpinning effects.

(ii) Other models to account for the damping.

In contrast to the results of Fiore and Bauer (64) which appear to substantiate the K.G.L. theory to a large extent, other results such as those of Takahashi (56), Caswell (58), and Niblett & Wilks mentioned above, give nonlinear plots of $\ln(\Delta_H \epsilon_0) / \frac{1}{\epsilon_0}$. Often data which approach the K.G.L. amplitude dependence at high strain amplitudes, vary with strain amplitude slower than expected at lower strain amplitudes. [Caswell (58)] Two theories will be introduced here which attempt to resolve these difficulties.

(a) The model of Swartz and Weertman.

Swartz & Weertman (61) have proposed a hysteresis mechanism, similar to those discussed in chapter 7.1, to explain the above results. The theory is limited, however, to a specific metal-impurity system. The K.G.L. model is modified firstly by assuming that the pinning force, F, of dislocations to impurity atoms, arising from an elastic interaction, depends on the orientation of the dislocation line. Secondly, it is assumed that once a dislocation line has broken away, its motion may be limited by the stress field of neighbouring atoms rather than by its line tension. This behaviour is illustrated in Fig.7.10. in which, (a) shows the position of a pinned dislocation under zero applied stress, (b) its position under a small stress, (c) its position under maximum applied stress, when its motion is line tension controlled, as in the F.G.L. theory, and (d) its position under maximum applied stress, when its motion is impurity controlled. The latter case implies an impurity stress field varying rapidly over the distance the dislocation is displaced.

Swartz and Weertman calculate the mean dislocation displacement corresponding to Fig.7.10(c), which is a function of the applied stress, and also the mean dislocation displacement corresponding to Fig.7.10(d), which is independent of the applied stress. They then calculate the corresponding decrements which, in the approximation of small applied stress, are for the line tension limited case

$$\Delta_1 \doteqdot \frac{N L_N^3 b \sigma_0}{9\pi F_0} , \tag{7.18.}$$

where $F = F_0 \sin\alpha$, and α is the angle between the dislocation and its Burgers vector, b. For the impurity limited case,

$$\Delta_2 = \frac{\beta N b L_N}{\pi C^{1/3} \epsilon} . \tag{7.19.}$$

At a particular stress the smaller of these two decrements is applicable, since it involves the smaller dislocation displacement, ie. breakaway distance. The stress necessary to unpin a dislocation is, by Cottrell's theory [Cottrell (53)], approximately equal to the stress necessary for the dislocation to overcome the Mott-Nabarro (48) potential barrier associated with the same impurity. Thus an impurity originally pinning a dislocation cannot limit its motion after unpinning, so two types of pinning point are needed. If both interstitial impurities, which interact strongly with both edge and screw type dislocations, and substitutional impurities which interact only with edge type, are present, then the interstitials may pin strongly a dislocation of partly screw and partly edge character, while the substitutionals may pin the same dislocation only weakly. At very low stresses, such a dislocation may break away from substitutional pins and move hysteretically over neighbouring substitutionals, its displacement being line tension controlled, and the decrement will be proportional to stress. At higher stresses, this dislocation may reach neighbouring interstitials, and its motion will be impurity limited. The decrement then becomes independent of applied stress. At still higher stresses, complete unpinning occurs, and both decrements, Δ_1 and Δ_2, depend exponentially on the stress, as in the K.G.L. model. This behaviour is illustrated in Fig.7.11. and compared with the K.G.L. theory.

Pure edge dislocations remain pinned by both impurity types, and so do not contribute to the hysteretic decrement at low stresses. Pure screw dislocations have only one type of pinning point, so the theory is not applicable. The model is expected to be applicable, however, to metals with a low stacking fault energy, in which partial dislocations having both screw and edge character are produced.

The decrement of equation (7.10.) is seen to have the amplitude dependence of Takahashi's results, equation (7.11.), and the curve OABC of Fig.7.11. fits better the results of Caswell (58), at low strain amplitudes.

(b) The model of Celli.

Celli (62) has proposed a damping model to replace that of K.G.L. in the low strain amplitude region, where plots of $\ln(\Delta_H \epsilon_0) / \frac{1}{\epsilon_0}$ are often curved. The new model is also able to account for the residual, amplitude

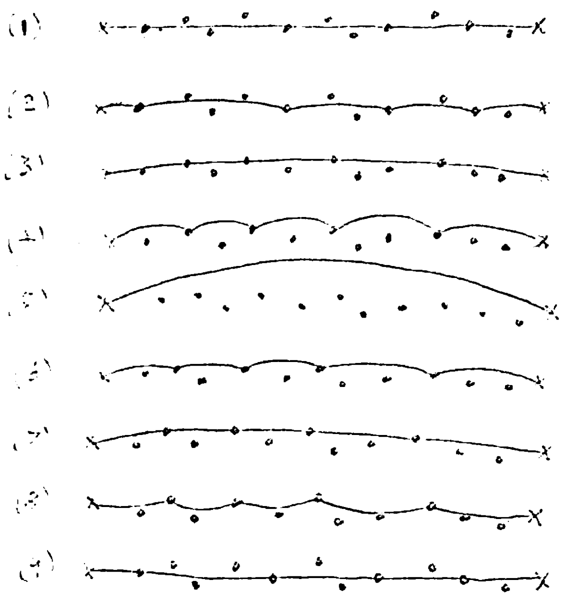

Fig. 7.12. Successive positions of a dislocation segment when an alternating stress is applied. [After Gelli (62)].

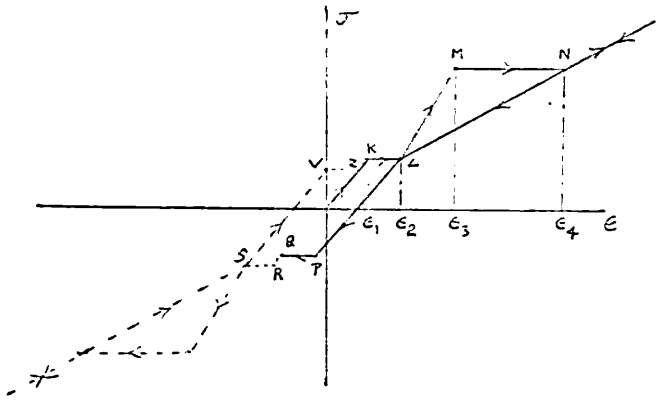

Fig. 7.13. Stress-strain curve during a cycle of an alternating applied stress. Solid lines correspond to that part of the motion illustrated in Fig. 7.12. [After Gelli (62)].

independent, damping considered in chapter 7.2. The main difference between the two models is that Gelli postulates an almost random distribution of impurities round a dislocation, while the K.G.L. model assumes the pinning points lie exactly on the dislocation. When the density of impurities is sufficiently great, the following modifications to the K.G.L. theory should arise.

The equilibrium position of a loop length L_N is not determined uniquely by the position of the major (network) pinning points, but several configurations of the dislocation may be possible, corresponding to different selections of pinning points from the available atoms. A corresponding number of energetically equivalent positions therefore exist for the dislocation, as illustrated in figure 7.12(1) & 7.12(3). In Fig.7.12(2) a dislocation segment is shown bowing out with no break-away under an applied stress. This behaviour will give rise to an amplitude independent decrement as in the K.G.L. theory. However, the distance L_c between two pinning points is now no longer proportional to $\left(\frac{1}{c}\right)^{\frac{1}{3}}$, but to a higher power of $\frac{1}{c}$, since L_c is now generally greater than the mean separation of impurity atoms. The amplitude independent decrement does not therefore decrease with the fourth power of L_c as in the K.G.L. theory. Also, when the atmosphere is dense enough, the critical break-away stress for static hysteresis is quite low, since the difference in energy between successive energy levels should be lower the higher the impurity density.

At low stresses the movement of a dislocation from the position shown in Fig.7.12(1) to that of Fig.7.12(3) is accompanied by a hysteresis loss of a type not considered by K.G.L. The hysteresis loop corresponding to successive dislocation positions illustrated in Fig.7.12(1), (2), (3), (7), (8), (9) is shown in portion K L P Q R S V Z of Fig.7.13. Only for higher strain amplitudes, Fig.7.12(4), (5), (6) does break-away occur in the K.G.L. manner, giving rise to portion L M N of Fig.7.13. Four critical strain amplitudes $\epsilon_1, \epsilon_2, \epsilon_3, \epsilon_4$ are indicated in Fig.7.13. For a maximum strain amplitude ϵ_0 such that $\epsilon_0 \leq \epsilon_1$ the loss is of a dynamic nature, giving rise to a decrement Δ_{I1}. When $\epsilon_1 < \epsilon_0 \leq \epsilon_2$ an amplitude dependent decrement Δ_{H1} arises. When $\epsilon_2 < \epsilon_0 \leq \epsilon_3$ a second dynamic loss arises Δ_{I2}, and when $\epsilon_3 < \epsilon_0 \leq \epsilon_4$ a second K.G.L. type hysteretic decrement Δ_{H2} arises. Thus in the general case of $\epsilon_0 \leq \epsilon_4$ the total decrement is given by

$$\Delta = \Delta_{I1} + \Delta_{H1} + \Delta_{I2} + \Delta_{H2} . \tag{7.20.}$$

The Takahashi type dependence of the decrement on ϵ_0 (equation 7.11) may be associated with Δ_{H1}. Thus

$$\Delta_{H1} = \beta \, \epsilon_0^{\alpha} , \tag{7.21.}$$

where α and β are constants, while

$$\Delta_{H2} = \frac{C_1}{\epsilon_0} \exp - \frac{C_2}{\epsilon_0} , \tag{7.22.}$$

after K.G.L.

The model of Celli thus incorporates the important features of two previous models. A dislocation is pictured as being surrounded by a Cottrell atmosphere, in the central region of which energy is dissipated in a way similar to that proposed by Weertman & Salkovitz, and in the external region of which the K.G.L. mechanism is applicable. The internal region is expected to vanish gradually when decreasing the impurity content.

Celli (62) has performed experiments on Al and obtained results which appear to follow a law of the type described by equation(7.21) at low amplitudes, and of the type described by eq.(7.22) at higher amplitudes.

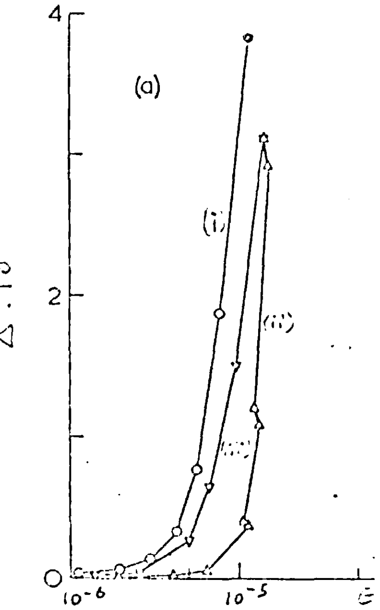

Fig. 7.14. Damping in an NaCl crystal deformed 0.2% before annealing at 102°C (i) after the anneal (ii) and on repeating the measurements (iii). [After Whitworth (60)].

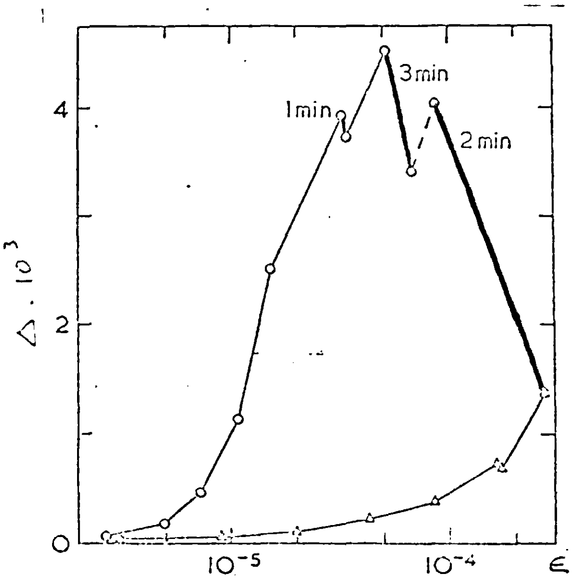

Fig. 7.15. Internal friction at high amplitudes of an NaCl specimen lightly deformed in compression [After Whitworth (60)].

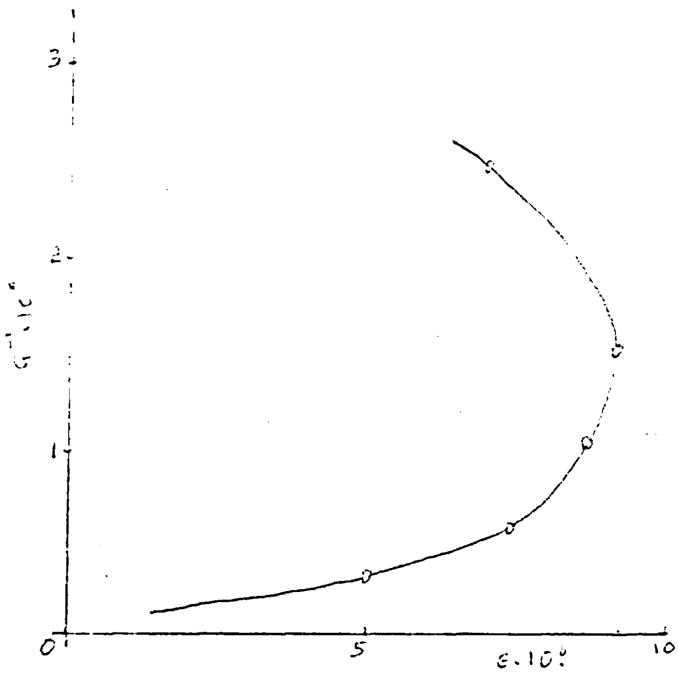

Fig. 7.16. Damping of an Al single crystal at 126°K [After Birnbaum (55)].

Numbers indicate order in which measurements were made.

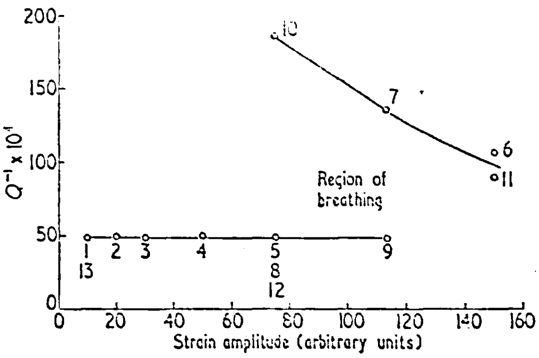

Fig. 7.17. Friction of a Cu specimen at 90°K showing 'breathing'. [After Baxter + Wilks (62)].

(iii) Effects observed at high strain amplitudes.

These effects fall roughly into six categories of behaviour.

I) After vibration in the strain amplitude dependent region, the damping at lower amplitudes is sometimes increased above its original value. [Beshers (59) and Whitworth (60)]. Whitworth's results for a NaCl crystal with 0·2% prestrain are shown in Fig.7.14. where curves 1, 2, 3 were plotted respectively before an anneal, after the anneal and after plotting 2. The increase in damping seen in curve 3 cannot be explained by the generation of new dislocations (see II below), so the loop length must be increasing. This phenomenon cannot be explained by the K.G.L. theory, which requires dislocations to return to their original position after break-away. Nowick's hysteresis model is applicable, however, where the stress field associated with pinning centres is short ranged.

II) The damping is found to be reproducible in the amplitude dependent region until some critical stress is exceeded, when it increases rapidly with stress. Subsequently the damping is increased at all lower stresses. [Mason (56), Whitworth (60)]. Whitworth performed simple etching experiments, which showed a large increase in the number of dislocations present in certain slip planes after the critical stress had been exceeded.

III) In some fatigue tests on specimens at 10 - 1,000 c/s the damping is found to decrease after vibration at high strain amplitudes. [Wadsworth (57) Broom & Ham (59), Whitworth (60)]. Some typical results of Whitworth are shown in Fig.7.15. At high strain amplitudes the decrement decreases at constant stress (thick lines) and a subsequent repetition of the measurements (dashed line) shows the decrement is everywhere lower. No completely satisfactory mechanism has been proposed, but the generation of vacancies by interacting dislocations, or the movement of dislocations to highly pinned positions, are possibilities.

IV) As the driving force applied to a specimen is increased, the amplitude of resonance rises to a maximum, and then starts to fall, as shown in Fig.7.16. This leads to a double valued decrement versus strain curve, as found by Birnbaum (55) and Whitworth (60).

V) The damping rises with increasing strain amplitude, but when the strain is subsequently reduced, the damping continues to rise, [Hiki (58)].

VI) When the internal friction of a specimen is being measured by the resonant bar technique, a periodic fluctuation in the amplitude of vibration of the specimen is sometimes observed, while the driving voltage is held constant. [Takahashi (52), Kessler (57) and Baxter & Wilks (62).] This phenomenon has been called 'breathing' by Baxter & Wilks, whose results on a Cu specimen vibrated at 780 c/s and at 90°K are shown in Fig. 7.17. In the region of breathing, the friction is seen to be double valued, while beyond this region the friction decreases. That breathing will occur if a specimen shows a friction of the form of Fig.7.17. is readily seen, for if the strain amplitude is increased a little beyond ϵ_2 the friction increases and if the applied voltage is held constant the amplitude of vibration of the specimen will decrease. If this new amplitude is below ϵ_1 the magnitude of the friction will decrease, and the amplitude of oscillation will build up again, the cycle then repeating itself.

If the strain amplitude is large enough to unpin a dislocation completely, the K.G.L. theory predicts that the friction will decrease if the strain amplitude is further increased. Such behaviour is observed in

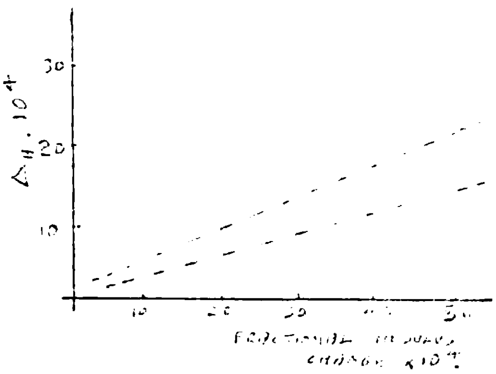

Fig. 7.18. Change in modulus associated with Δ_H in several Al single crystals. Measurements at temperatures between 20°C and 200°C were found to lie between the two dotted lines [after Chambers (57)].

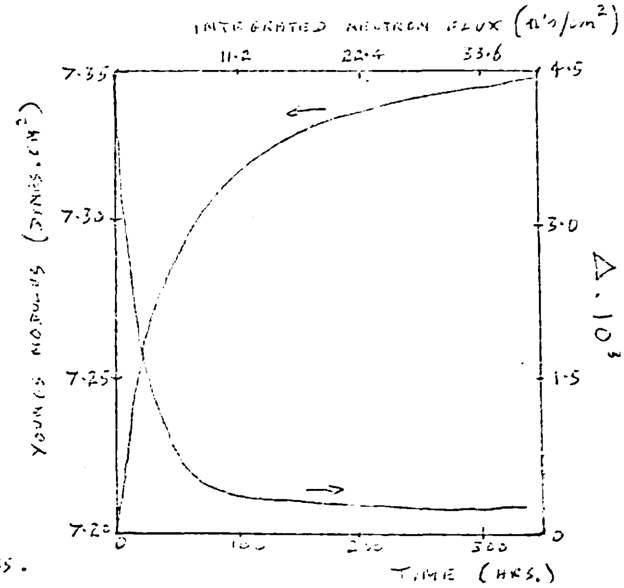

Fig. 7.19. Youngs modulus and Δ as a function of irradiation time for a copper specimen [after Thompson & Holmes (56)].

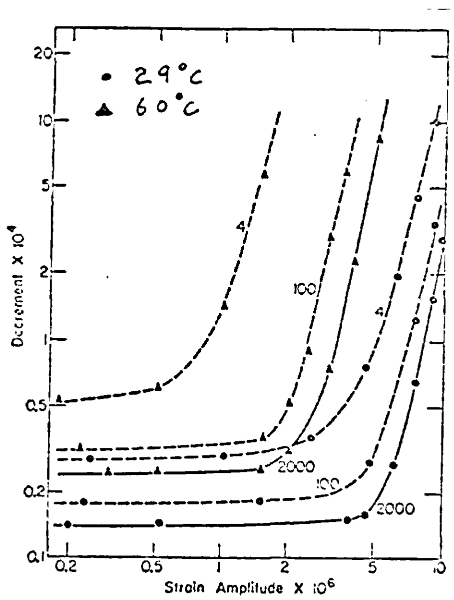

Fig. 7.20. Instantaneous decrement vs. strain amplitude as a function of time. Numbers indicate time in minutes after end of a 20 min. excitation [after Chambers & Smoluchowski (60)].

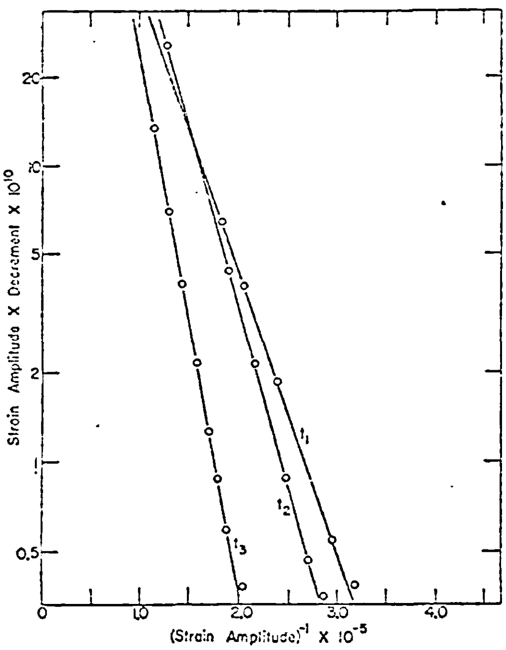

Fig. 7.21. K.G.L. tests as a function of time t after start of decay at 60°C. t_1 = 12 min. t_2 = 15 min. t_3 = 60 min. [after Chambers & Smoluchowski (60)].

Fig.7.17. The sudden increase in damping may also be accounted for in terms of the K.G.L. model, if the distribution of loop lengths approximates to a δ-function rather than an exponential function. However, another condition for breathing is that some time lag be present, so that the strain amplitude falls quite appreciably before the friction returns to its lower value. This may be interpreted by postulating two types of impurity in the specimen, one which unpins and repins a dislocation each half cycle and is associated with the large damping above the breathing region, while the other type is such that a dislocation once free does not repin again until the amplitude of oscillation has fallen considerably. The former impurity must be immobile, as postulated by K.G.L, while the second may have a low energy of migration and after break-away will diffuse away from the dislocation, returning sometime later when the amplitude of vibration of the dislocation is much reduced.

7.4. The Modulus Defect.

The modulus defect associated with amplitude dependent damping is, according to the K.G.L. theory, related to Δ_H as

$$\Delta_H \doteqdot r\left(\frac{\Delta G}{G}\right)_H , \qquad (7.23.)$$

where r is a constant expected to be about unity. Fig.7.18 shows the results of Chambers (57) on Al single crystals at various temperatures in the range 20°c to 200°c. The experimental points lie somewhere between the dotted lines, giving an approximately constant value for r of about 0.4.

Kamentsky (56) found, for different dilute copper alloys, constant values of r between 0.15 and 6.0. Fiore & Bauer (64) find for Cu-Ge alloys values of r between 0.9 and 1.2 .

The ratio r should not, according to the K.G.L. theory, show any orientation dependence. In fact it is found to have almost exactly the orientation dependence expected for Δ_H alone [Niblett & Wilks (60)].

7.5. The Effect of Irradiation.

Dienes (52) has predicted changes in the modulus of an irradiated material resulting from changes in the lattice parameter near radiation induced defects. The results of Thompson & Holmes (56), however, indicate that such effects are negligible compared with the pinning effect on dislocation segments of defects induced by neutron irradiation. Fig.7.19. shows Thompson and Holmes' measurements of the decrement Δ_Y and Young's modulus G, as a function of radiation time, for a copper single crystal. Neither the high order of magnitude of the modulus change, nor the presence of a saturation effect at high doses, are in favour of Dienes' mechanism, while the observed decrement and modulus changes can be explained, at least at low stresses, if radiation induced defects restrict the oscillatory motion of dislocation segments and reduce the plastic strain. The effect of neutron radiation on the damping in copper has been investigated also by Barnes et al. (58).

Increasing the pinning point density on a dislocation in this manner provides a useful way of studying the breakaway stress in strain amplitude dependent friction (see ch.7.3.), and also of studying the loop length dependence of internal friction. The latter study requires a relationship between radiation dose and dislocation loop length.

If γ defects are produced per unit time in a crystal containing a total dislocation length Λ, then the number, n, of pinning points on dislocations at a time t is given by

$$n = \frac{\Lambda}{L_o} + f_d \gamma t = \frac{\Lambda}{L(t)}, \qquad (7.24.)$$

where L_o is the original average loop length, f_d is the fraction of defects which end up on a dislocation, and L is the average loop length at a time t. Equation (7.24.) leads to the general relation [Koehler (52)]

$$L = \frac{L_o}{1+\beta t}, \qquad (7.25.)$$

where $\beta = \frac{f_d \gamma L_o}{\Lambda}$. Time dependent effects due to defects diffusing to dislocations have been neglected here (see ch.7.6.).

By measuring a decrement as a function of γ-irradiation time in copper in the Mc/s frequency range, Stern & Granato (62) obtained results which they could interpret using the relation above, and found, in accordance with the G.L. theory, a dynamic decrement proportional to the fourth power of loop length, L, a maximum decrement proportional to L^2, and a frequency corresponding to the maximum decrement proportional to $\frac{1}{L^2}$.

Thompson & Holmes (56), whose results were shown in Fig.7.10, derive expressions for a decrement and modulus defect as a function of irradiation time which contain terms similar to the R.H.S. of equation (7.25.). They find their results indicate a decrement proportional quite accurately to L^4, and a modulus defect proportional to L^2.

Evidence of the L^4 dependence in NaCl has been found by Granato, Hikata, & Lücke (58), in whose experiment the change in loop length was related to the recovery of the damping with time after a plastic deformation. (see chapter 7.6.)

Although the loop length behaviour of the above experiments appears to follow the G.L. theory for the dynamic decrement quite well, other authors [Takahashi (56)] have found a decrement depending on a rather smaller power of the loop length than four, especially in rather impure specimens. It is interesting to note that the hysteretic damping theory of Swartz & Weertman (61) mentioned in chapter 7.3. predicts a decrement proportional to L for impurity limited motion, and L^3 for line tension limited motion, at low stress amplitudes. The very specific model employed in this theory may be applicable to some of these experimental results. The theory of Celli [see ch.7.3(ii)] also leads one to expect a decrement proportional to a power of the loop length somewhat less than four.

Evidence in favour of the loop length dependence of the hysteretic decrement of the K.C.L. theory has also been given by Fiore & Bauer (64).

Some effects of electron radiation in copper have been considered by Lomer & Niblett (62), and of deuteron radiation in W by Muss & Townsend (62).

7.6. Time Dependent Effects.

The change in damping with time during irradiation has been mentioned in chapter 7.5. The present section is concerned with recovery effects after a specimen has been treated in some way, eg. a small plastic deformation. A decrement showing a time dependent recovery is known as the Köster effect [Köster (40)]. The recovery usually takes place much faster than the recovery of most other mechanical properties, such as hardness, X-ray line broadening, yield limit etc. Three mechanisms have been proposed to account for this effect. (i) A rearrangement of dislocations, (ii) annihilation of dislocations, (iii) pinning of dislocations. Experimental evidence will be shown to favour the pinning mechanism.

Chambers & Smoluchowski (60) have measured the strain amplitude

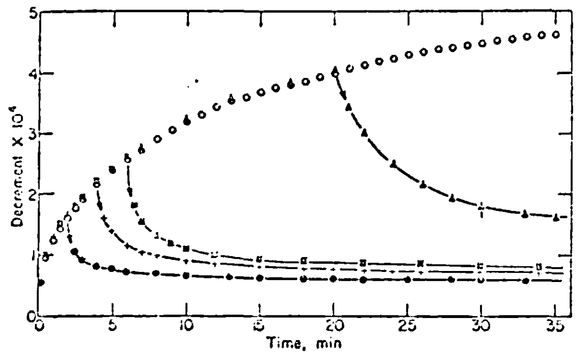

Fig. 7.22. Decay of decrement as a function of time at 60°C [after Chambers & Smoluchowski (60)].

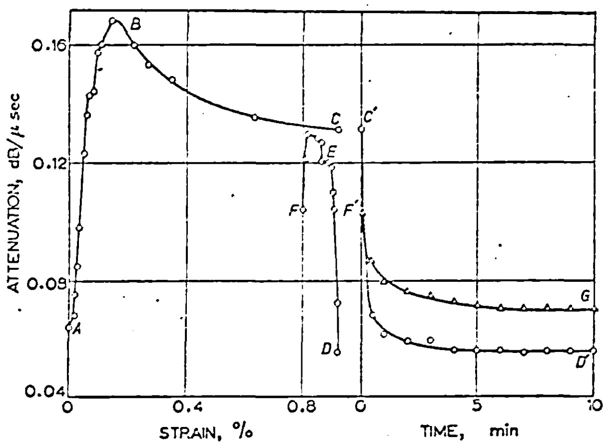

Fig. 7.23. Attenuation as a function of strain [after Granato, Hikata & Lücke (58)].

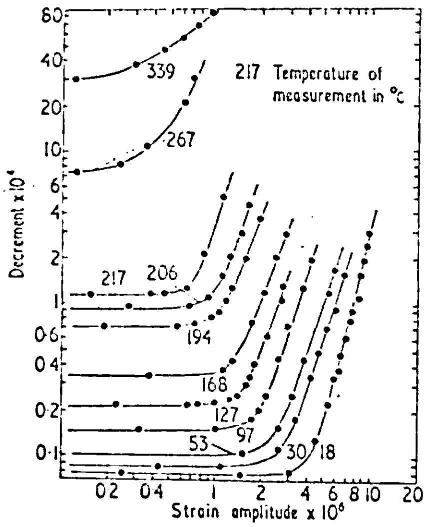

Fig. 7.24. Damping of an Al single crystal at different temperatures and ~15 Kc/s [after Chambers (57)].

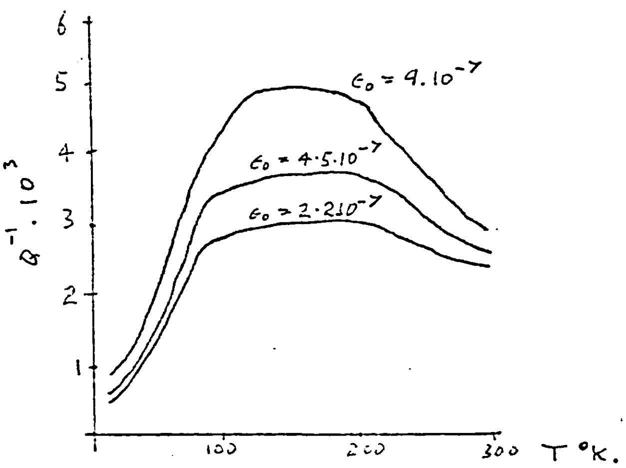

Fig. 7.25. Damping of a Cu specimen extended 5.7% and subsequently annealed for 1 hr. at 475°C [after Niblett & Wilks (59)].

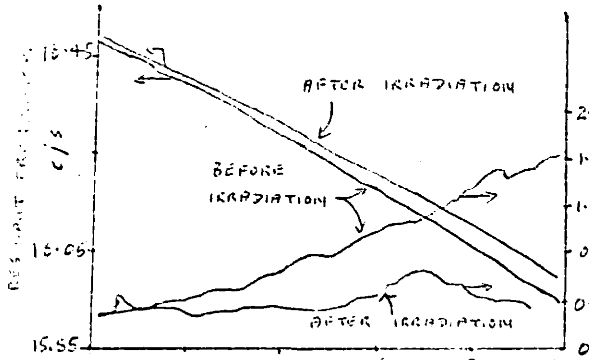

Fig. 7.26. Resonant frequency and Δ of Cu [after Thompson & Holmes (59)].

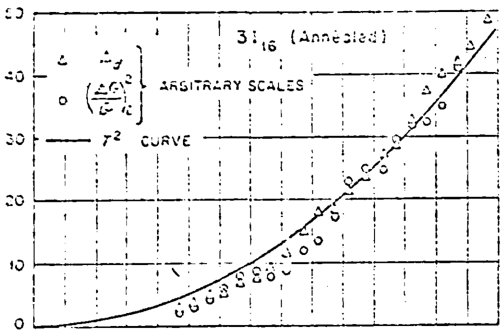

Fig. 7.27. Modulus change and Δ_D vs. T. [after Thompson & Holmes (59)].

dependent complex modulus at 15Kc/s as a function of temperature and time for Mg and Al single crystals.

(a) The experimental results.

The graphs shown in Fig.7.20. give the instantaneous decrement versus strain amplitude as a function of time (4, 100, 2000minutes) after a 20 minute excitation period at a temperature of either 29°C or 60°C. A strain amplitude of 10^{-5} was used during the excitation. Very little change was observed after 2000 minutes in the decay sequence. Each curve was plotted as nearly instantaneously as possible, and a strict control was kept on the temperature in order to obtain reproducible results. It was found that the time dependence and the amplitude dependence were small in freshly strained crystals. The time dependence appears when a crystal begins to show a marked amplitude dependence, and hence a marked break-away stress, as, for example, after a high temperature anneal. It is observed also that if the exciting strain amplitude is less than the break-away strain amplitude, there is no change in the instantaneous curve of either decrement or modulus defect with strain amplitude. The K.G.L. plots of $\ln(\Delta_H \epsilon_0) / \frac{1}{\epsilon_0}$ corresponding to the 60°C curves of Fig.7.20. are shown in Fig.7.21. These are seen to give good straight lines.

The product of ζ, the intercept on the $\ln(\Delta_H \epsilon_0)$ axis, and $\frac{1}{\psi^2}$, where ψ is the slope, remained approximately constant. In Fig.7.22. are shown the results obtained when a crystal was first excited for various lengths of time at a constant strain amplitude and temperature, and then allowed to decay while the decrement was measured at frequent intervals. The reproducibility of the rise in decrement with excitation time, and the tendency to saturate after large excitation times should be noted. In support of the K.G.L. theory it is also noted that the ratio of the decrement to the modulus defect is approximately constant during excitation. When Chambers and Smoluchowski plot $-\ln\left(\frac{\delta-\delta_0}{\delta_1-\delta_0}\right)$ against time, where δ is the decrement at a time t during the decay sequence shown in Fig.7.22, δ_0 is the initial decrement, and δ_1 is the maximum decrement reached at the end of the excitation period, they obtain a straight line. This indicates the decay is described by the relation

$$\delta-\delta_0 = (\delta_1-\delta_0)\ \exp\ -\beta t^n , \qquad (7.26.)$$

where β is a constant. The parameter n is found to be dependent on the excitation period, ranging from about $\frac{1}{3}$ for a 5 minute excitation to $\frac{2}{3}$ for periods extending to saturation. It is also found that, for the decay following short excitation times, the quantity β is inversely proportional to strain amplitude, and proportional to $\left[\frac{D_0}{RT}\ \exp\ \frac{-U}{R}\right]^{1/3}$, where D_0 is the diffusion constant of a defect, and U is an activation energy of the order of 7 to 10K cal./mole.

(b) A theoretical interpretation.

The K.G.L. theory predicts a decrement Δ equal approximately to the modulus defect ΔG, and related to the strain amplitude as

$$\Delta G\,.\,\epsilon_0 = \Delta.\epsilon_0 = P\ \exp\left(\frac{-A'}{\epsilon_0}\right) , \qquad (7.27.)$$

where A' is proportional to $\frac{1}{L}$, that is the concentration of defects, and P is proportional to ΛL_N^3. Neglecting the amplitude dependence outside the exponential, equation (7.27.) may be written as

$$\Delta G(t) = \Delta(t) \doteqdot P\ \exp\left(\frac{-K\,C(t)}{\epsilon_0}\right) . \qquad (7.28.)$$

If $C(0)$ is the concentration of defects on a dislocation immediately after cessation of excitation, then

$$C(t) = C(0) + C'(t) , \qquad (7.29.)$$

where $c'(t)$ is such that $c'(0) = 0$ and $c(\infty)$ is constant.

From equations (7.28.) and (7.29.) we have

$$\delta - \delta_0 = \Delta(t) = P \exp\left[\frac{-K c(t)}{\epsilon_0}\right] = P \exp\left[\frac{-K c(0)}{\epsilon_0}\right] \cdot \exp\left[\frac{-K c'(t)}{\epsilon_0}\right], \qquad (7.30.)$$

or

$$\frac{\delta - \delta_0}{\delta_1 - \delta_0} = \exp\left[\frac{-K c'(t)}{\epsilon_0}\right], \qquad (7.31.)$$

where

$$\delta_1 - \delta_0 = P \exp\left[\frac{-K c(0)}{\epsilon_0}\right]. \qquad (7.32.)$$

Now $c'(t) = \frac{D_0}{RT} \exp\left(\frac{-u}{R}\right) . t^{\frac{2}{3}}$ according to the Cottrell-Bilby (49) strain-aging theory. This relation is valid for the diffusion of impurities onto dislocations from a cylindrically symmetric atmosphere during the early stages of aging. On the other hand, if a planar atmosphere is assumed [Lement & Cohen (56)] the relation becomes

$$c'(t) = \frac{D_0}{RT} \exp\left(\frac{-u}{R}\right) . t^{\frac{1}{3}}. \qquad (7.33.)$$

The experimental results may now be interpreted if it is assumed that the time dependent effect is due to breakaway of dislocations from pinning points, such that the number of long dislocation loop lengths is increased over the number that should exist at a given temperature and impurity concentration. That there is no change in decrement at excitation strain amplitudes below the breakaway strain amplitude then follows, since the number of long loops will not have been increased by breakaway. From the similarity between equation (7.26.) and equation (7.31.), when the latter contains the Cottrell-Bilby expression for $c'(t)$, the excitation time dependence can be considered to be due to the thinning of the Cottrell atmosphere surrounding the longest dislocation network. The decay following excitation results from condensation of the atmosphere by diffusion back to the dislocation according to the Cottrell-Bilby relation. The $t^{\frac{2}{3}}$ dependence suggests the thinning of the atmosphere has cylindrical symmetry, while the $t^{\frac{1}{3}}$ dependence after short excitation suggests a planar distribution of the atmosphere, and a subsequent diffusion of this planar atmosphere back to the dislocation. The value of U in equation (7.33.) can give a guide to the type of impurity responsible.

Granato, Hikata & Lücke (58) have proposed a similar theory, also based on the K.G.L. model, in which they assume the concentration of defects pinning a dislocation varies according to the Cottrell-Bilby $t^{2/3}$ relation. Good agreement with the experimental results is found in the 0·4 to 4·0% deformation range, especially in NaCl. At larger strains the generation of new dislocations must be considered.

The results of Hikata, Truell, Granato, Chick and Lücke (56) who measured the decrement in an Al sample as a function of deformation and time, are shown in Fig.7.23. As the load increases, the attenuation passes through a maximum, and then decreases with further deformation, (A-B-C). If the strain is then held constant, the attenuation recovers to its original value before deformation (C′-D′). If now the load is removed, the attenuation rises to nearly its value before recovery, then decreases, but still has a finite value when the load is completely removed (D-E-F). The remaining attenuation recovers in a way similar to the recovery under load, but less rapidly (F′-G).

Granato, Hikata & Lücke interpret the recovery under load as being due to the pinning of dislocations by point defects. When the load is removed, the dislocations breakaway from these pinning points so that the attenuation increases again. Finally, under no load, the attenuation recovery process repeats itself.

The increase in damping during the unloading after recovery, (D-E) in Fig.7.23. is very difficult to explain if the recovery process is due to either the disappearance of dislocations (the annihilation theory), or to the immobilisation of these dislocations as a result of an interaction between them, (the rearrangement theory). A point defect pinning mechanism is, however, capable of accounting for this effect. Nowick (55) has criticised the pinning theory on the grounds that if recovery is due to point defects, then the recovery should be capable of correlation with the recovery of electrical resistivity; this is not always possible. However, if the damping is proportional to the fourth power of the loop length, it will be influenced at the very beginning of recovery, while the electrical resistivity, which depends on the total number of defects remaining in the lattice, will not be changed appreciably until nearly the end of the migration process. Thus the corresponding resistivity changes should occur at later times or higher temperatures.

7.7. The Effect of Temperature.

(a) The amplitude dependent damping.

The effect of temperature appears in the K.G.L. theory of amplitude dependent damping in three ways. Firstly, the damping constant B is temperature dependent [see ch.8], but in the amplitude dependent region this is a much smaller effect than the other two considered below. [Stern & Granato (62)]. Secondly, it is possible for the break-away of a dislocation to be thermally aided. The stress amplitude at which Δ_H begins to rise should therefore increase with decreasing temperature. This is illustrated in Fig.7.24. by the results of Chambers (57) on Al single crystals at 15Kc/s. From the shift in the break-away point with temperature it is possible to calculate the activiation energy of the break-away process. For the results of Fig.7.24. this is found to be about 0·1 ev. The third effect of temperature will be to change the equilibrium concentration of impurity atoms on a dislocation, according to the equation [Cottrell (48)]

$$c = c_0 \exp\left(\frac{u}{kT}\right), \qquad (7.34.)$$

where c_0 is the mean concentration of impurity atoms in the lattice, and u is the interaction energy between an impurity atom and a dislocation. Since the value of L_c is inversely proportional to c, the slopes of the K.G.L. plots of $\ln(\Delta_H \epsilon_0) / \frac{1}{\epsilon_0}$ are proportional to c. Thus a plot of the logarithm of the slope against $\frac{1}{T}$ should give a straight line of slope $\frac{u}{k}$ according to equation (7.34.). The curves of Fig.7.24. when treated in this way yield a straight line corresponding to an activation energy of 0·12 ev. for temperatures less than 200°C. Similar results have been obtained by Weertman & Salkovitz (55), Wert (49) and Kamentsky (56).

The K.G.L. theory also predicts that the decrement should cease to increase with strain amplitude at very high strain amplitudes and begin to decrease, corresponding to the total unpinning of dislocations. The same effect should be observed at high temperatures. Often it is obscured by other effects, but Niki (58) and Niblett & Wilks (59), whose results are shown in Fig.7.25., have observed a maximum.

(b) The amplitude independent damping.

Because the low amplitude decrement in cold worked metals is strongly influenced by the presence of the Bordoni peak, only annealed metals will be considered here. Care must be taken, also, to ignore the grain boundary relaxation peak observed in polycrystalline metals between 200°C & 500°C. Measurements have been made by Kamentsky (56), Caswell (58), Niblett & Wilks (59) and Thompson & Holmes (59). In general it is found that the temperature dependence of Δ_I is small, a graph of Δ_I against $\frac{1}{T}$ usually being concave upwards, approaching linearity at low temperatures. [Nowick (50) and Kiki (58)] . Kamentsky (56) estimates that if an activation energy exists for this friction it is less than 0·05 ev.

Thompson & Holmes (59) have measured the amplitude independent friction, and the resonant frequency, from which the modulus defect may be calculated, as a function of temperature for annealed copper crystals both before and after neutron irradiation at room temperature. Fig.7.26. shows the results obtained. If it is assumed that the difference between the measurements before and after radiation is due to the suppression of dislocation motion by radiation induced pinning points, then it is reasonable to suppose that the differences between the two curves should be characteristic of the thermal activation of the dislocations themselves. In Fig.7.27. the quantity Δ_i, which is the difference between the pre-irradiation and post-irradiation decrement curves of Fig.7.26. and the quantity $\left(\frac{\Delta G}{G}\right)_i^2$ where ΔG_i is the change in the modulus upon irradiation, are plotted against temperature on an arbitary scale. A curve of T^2 is also shown. It is found that the curves of Δ_i and $\left(\frac{\Delta G}{G}\right)_i^2$ can be brought into coincidence merely by using a scale factor, and that these quantities show a strong tendency to increase as T^2. The relation between the modulus defect and the decrement follows from the K.G.L. theory, since $\left(\frac{\Delta G}{G}\right)_i^2 \propto L^4$ and $\Delta_i \propto L^4$. The temperature dependence almost certainly arises, then, from a thermally activated unpinning of dislocations, giving rise to longer loop lengths. Since the decrement but not the modulus defect involves the damping constant B, the observed

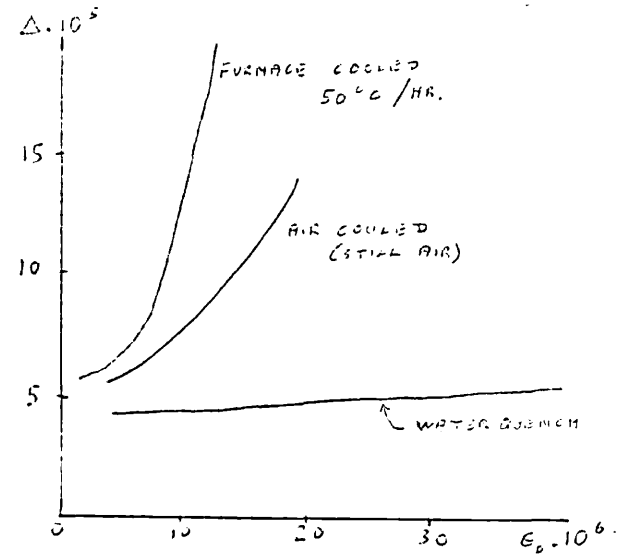

Fig. 7.28. Δ of Al specimen after various rates of cooling following an anneal at 640°C for 24 hrs. [Levy & Metzger (55)].

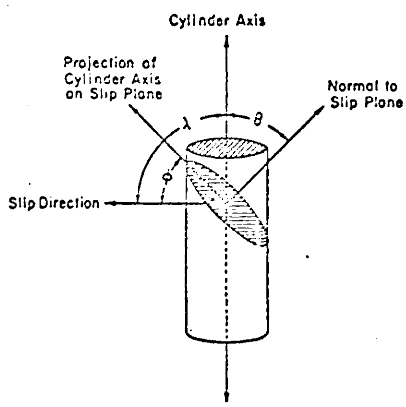

Fig. 7.29. Diagram defining angles between applied stress and slip system. [After Granato & Lücke (56)].

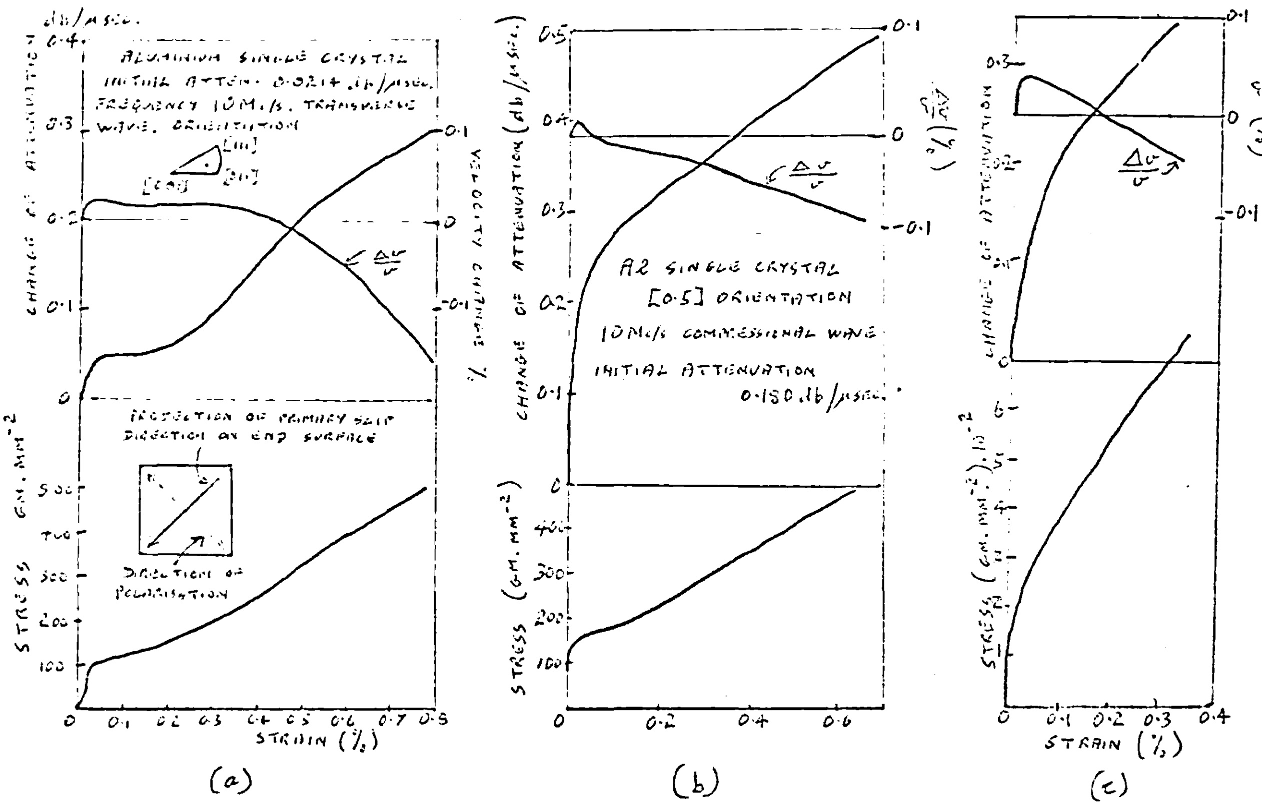

Fig. 7.30. Stress, attenuation and velocity change as a function of strain. [After Hikata, Chick, Elbaum & Truell (62)].

temperature dependence cannot be related to a change of B with T . Thompson & Holmes also deduce a T^2 dependence for the friction which fits quite well the experimental results, although the exact form of the tem-perature dependence will depend on the distribution of pinning points.

At Mc/s frequencies, when normal experimental strain amplitudes are sufficiently low for there to be no break-away of dislocations from point defects, the effect of temperature should appear only in the damping constant B . The theoretical basis of this constant is considered in chapter 8.

7.8. The Effect of Quenching.

Both the amplitude dependent and amplitude independent decrement of metals are reduced by quenching from a high temperature, and usually the faster the quench the greater the reduction. In Fig.7.28. this is illustrated by the results of Levy & Metzger (55) on an Al single crystal which had been annealed at 640°C for one day and then brought down to room temperature at various rates of cooling. For the most rapid quench, i.e. a water quench, the decrement is seen to have become almost independent of strain amplitude. The results shown in Fig.7.28. give curved plots of $\ln(\Delta_H \epsilon_0)/\frac{1}{\epsilon_0}$, but seem to indicate that L_c has been reduced.

Similar results have been obtained by Roswell & Nowick (57), and Barnes et al. (58). The main change produced by quenching is the introduction of vacancies which condense on dislocations [Maddin & Cottrell (55)], the concentration being greater the higher the initial temperature and the rate of quenching.

7.9. The Effect of an Anneal.

The friction is reduced by an anneal at an elevated temperature. [Niblett & Wilks (60)]. In the experiment of Barnes et al. (58), a copper single crystal was irradiated at 78°K but no decrease in damping was observed until the crystal was annealed at room temperature for some hours. An anneal apparently allows point defects to diffuse to dislocations and pin them. At high temperatures dislocations themselves may annihilate and so reduce the damping.

7.10. The Effect of Purity.

(a) The amplitude dependent damping.

The presence of impurities reduces the amplitude dependent damping. [Marx & Koehler (50), Weertman & Salkovitz (55)]. The K.G.L. theory is capable of explaining this if the impurities pin dislocation segments and reduce the average loop length. The effect of impurities on the slope of $\ln(\Delta_H \epsilon_0) / \frac{1}{\epsilon_0}$ plots has already been consideredin chapter 7.5. in connection with the loop length dependence of the damping.

(b) The amplitude independent damping.

In general the addition of small amounts of impurity reduces the low amplitude friction. [Marx & Koehler (50), Paré (58), Beshers (59)]. Takahashi (56) has reported an amplitude independent friction of polycrystalline copper containing small quantities of Al, Zn or P, which decreases as a power function of the concentration of solute atoms as predicted by the K.G.L. theory. On the other hand, Weertman & Salkovitz (55) have found no systematic dependence of the decrement on purity in lead specimens containing Bi. However, this may be due to the previous history of different specimens, e.g. cold working during handling.

7.11. The Effect of Prestrain and Cold Work.

(a) The amplitude dependent damping.

Small amounts of cold work are found to increase the amplitude dependent decrement and decrease the value of the modulus. [Read (41), Nert (49), Nowick (50), Smith (53)]. The K.G.L. plots of $\ln(\Delta_H \epsilon_0) / \frac{1}{\epsilon_0}$ for Read's results have already been considered in chapter 7.3. and have been found to be in at least qualitative agreement with the theory. Prestrain, quenching and irradiation all have very similar effects on the damping, since in each case extra dislocation pinning points are introduced [Barnes et al. (58)].

Measurements by Weertman & Koehler (53) on copper single crystals indicate that after an initial increase with small amounts of cold work, the decrement went through a maximum and then decreased with further deformation. After a deformation of about 3000 p.s.i. the damping was practically independent of strain amplitude for strains up to 10^{-5}. A similar decrease has been observed by Caswell (58). The occurrence of a maximum is predicted by the K.G.L. theory, which leads to a decrement proportional to ΛL_N^3. The initial increase in damping, associated with an increase in dislocation density, is offset at high deformations (i.e. a high dislocation density), by the reduction in the network length, L_N. Finally, when the dislocation density is so great that the network length is shorter than the mean separation between impurity atoms, the unpinning process no longer is possible, and no amplitude dependent damping is observed.

(b) The amplitude independent damping.

Again small amounts of cold work increase the friction. [Nowick (50), Thompson & Holmes (59), Weertman & Koehler (53)]. The measurements of Caswell (58) show that cold working increases the decrement over the entire temperature range from 4°K to 300°K. Niblett (56) has found a maximum value of damping in polycrystalline copper with increasing cold work.

7.12. The Effect of Orientation.

In the expressions derived for the decrement in chapter six the symbols σ and ϵ have the meaning of shear stress and shear strain. In most experiments, however, longitudinal stresses and strains are used which will be denoted by τ and γ respectively. Fig.7.29. defines the angles of the slip system in a solid cylinder. It can be seen that an applied longitudinal stress may be related to a resolved shear stress in the slip plane and direction, as

$$\tau = (\cos\theta \sin\theta \cos\phi).\ \sigma, \tag{7.35.}$$

$$\epsilon_{dis} = (\cos\theta \sin\theta \cos\phi).\ \gamma_{dis}. \tag{7.36.}$$

When considering longitudinal stresses the correct modulus to use will be Young's modulus and not the shear modulus. If there are many different slip systems present, each with a dislocation density Λ_i, then the expressions of chapter 6 may be made applicable to the case of longitudinal stresses simply by multiplying by a factor, [Granato & Lücke (56)]

$$T = \frac{E(\theta,\phi)}{G} \sum_i \frac{\Lambda_i}{\Lambda} \left[\cos^2\theta_i \sin^2\theta_i \cos^2\phi_i\right]. \tag{7.37.}$$

Hikata, Chick, Truell & Elbaum (62) have considered the change in damping with orientation in Al single crystals at around 10⁷c/s. Their results are shown in Fig.7.30. The velocity change, attenuation and stress are plotted against the tensile deformation of a sample. One of the twelve possible $\{111\}\langle 110\rangle$ glide systems of the f.c.c. crystal was inclined at 45° to the long axis of the specimen, so that the resolved shear stress on the one favoured slip plane is 0·5 of the stress along the axis of the sample. The plane of polarisation i.e. the particle displacement, of a 10^7 c/s transverse wave was made perpendicular to the primary glide direction and to its projection on the end face of the crystal, as shown in Fig.7.30(a) (inset). Thus the particle displacement did not have any component in the primary glide direction. Consequently, when dislocation multiplication occurs it is confined to this easy glide direction and will not affect the attenuation. The initial sharp rise in attenuation seen in Fig.7.30(a) is attributed to break-away of dislocations from weak pinning points leading to an increase in loop length before appreciable multiplication occurs. The level portion corresponds to dislocation multiplication in the easy glide system, and the subsequent increase in attenuation corresponds to a third stage in which other glide systems become operative. Fig.7.30.(b) shows the results of a similar experiment using compressional waves instead of transverse. Such compressional waves have shear components along all the glide systems, particularly in the primary one, and the attenuation is seen to increase continuously in this case with no level portion. Fig.7.30 (a) & 7.30.(b) show it is possible to separate the effects of primary and secondary glide systems during the plastic deformation of a f.c.c. metal single crystal. Fig.7.30.(c) shows the results for a compressional wave in the $\langle 100\rangle$ direction.

Hikata, Chick, Truell & Elbaum show that the maximum in $\frac{\Delta v}{v}$ at low strains is predicted by the K.G.L. theory, if it is assumed that the attenuation and velocity changes result from an increase in loop length while A, B, C, Λ and Ω may be considered constant. They show also that the maximum is predicted only when the initial loop length lies between two critical values.

7.13. Discussion.

(i) The dynamic decrement.

At high frequencies, the dynamic loss predicted by the K.G.L. theory accounts well for the observed strain amplitude independent damping. At lower frequencies, however, the agreement is not so good. In particular, the K.G.L. theory predicts a decrement proportional to frequency, while very few experimental results support such a dependence. The alternative theories discussed in chapter 7.1. have only limited success. It is possible that another damping mechanism is operating at low frequencies, or that the fault lies in the string model of dislocation motion itself. In the latter case, the kink model of Brailsford (61) & (65), which was considered in chapter 5.1. with regard to the Bordoni peak, may give a better picture of dislocation motion at these frequencies. This possibility is considered further in chapter 9.

(ii) The hysteretic decrement.

In many cases the hysteretic damping predicted by the K.G.L. theory accounts well for the experimentally observed strain amplitude dependent damping. There are, however, other instances in which the theory appears to bear no relation to experiment. It is possible that in the latter cases the K.G.L. model is not applicable because of its limitations on, for example, loop length ($\frac{L_N}{L_c}>5$) and strain amplitude (the strain amplitude should be smaller than that required to unpin dislocations from all pinning points every cycle). The other theories proposed to account for experimental results not described by the K.G.L. theory have been found to have some success, often because they do not assume all impurities to lie exactly on a dislocation line or that after breakaway a dislocation is repinned by the same pinning point. Indeed, the experiments of Baxter & Wilks (62) on the phenomenon of 'breathing' [chapter 7.3(iii)] indicate that once a pinning point is broken there may be some delay before the dislocation is repinned. Other experiments which cast doubt on the K.G.L. model are those of Roberts & Brown (62) who found symmetric hysteresis loops, and those of Baker (57) who found no significant changes of the amplitude dependent absorption in Cu and Pb with bias stress, although the latter should according to the K.G.L. theory have the same unpinning effect on a dislocation as a stress wave. The theory of Brailsford (61) & (65) may account for some of these anomalies. Alefeld (65) has found that this theory leads to a non-linear stress-strain law at an oscillation or bias stress amplitude of about 10^{-7} (assuming $L = 10^4 b$), whereas for the K.G.L. (string) model the corresponding stress amplitude is about 10^{-5}. Thus Brailsford's kink model predicts strain amplitude dependent effects at very much lower strain amplitudes, lower even than those necessary to cause breakaway in the string model. The kink model is compared further with the string model in chapter 9.

CHAPTER 8

The Damping Constant

The vibrating string model describes many of the properties of the damping but the physical mechanism of the damping is hidden in the damping constant which is defined by the relation

$$\underline{F} = B \cdot \underline{u} , \tag{8.1}$$

where $\underline{F}$ is the force acting per unit length of dislocation and $\underline{u}$ is the velocity of the dislocation. B is assumed to be independent of $\underline{u}$ Experimentally there are two ways of calculating B. The first is from measurements of dislocation velocity as a function of applied stress. The latter method was used by Gilman & Johnston (59), and Mason (60). Johnson & Gilman find a value of 7.10^{-4} dynes sec. cm^{-2} for B in LiF.

Calculations of B from internal friction measurements may be made using the Koehler-Granato-Lücke theory or any theory which relates B to experimental parameters. For frequencies much greater than f_m the former theory predicts (see equation 6.18.)

$$\Delta \rightarrow \Delta_\infty = 4\pi^2 \Omega G b^2 . \frac{\Lambda}{B} . \frac{1}{f} . \tag{8.2.}$$

The value of the dislocation density may be found by an etch-pit technique, and then B may be deduced from the decrement measurements at different frequencies.

8.1. Theories of B.

Eshelby (49) proposed that the drag on a dislocation arose from the thermoelastic damping, cf. chapter 1.2, resulting from a fluctuating temperature distribution around an oscillating dislocation. This mechanism produces no drag on a screw dislocation, which involves only shear stresses, and for an edge

$$B = \mu b^2 \rho \frac{(c_p - c_v)}{2\pi 10 K} \ln \frac{K}{\rho c_p \omega l^2} , \tag{8.3.}$$

where ℓ is a 'cutoff' length, about 10^{-7} cm. However, this effect has been found to contribute only a small amount to the total damping [Mason (60)].

All other theories consider the origin of the frictional force to be the interaction between a moving dislocation and lattice vibrations. Stern & Granato (62) have shown that the phonon-dislocation interaction is sufficient to account for the observed order of magnitude of the damping. Two different approaches to this problem have been given, due to Leibfried (50), and Mason (60).

(a) Leibfried's theory.

Leibfried (50) explained the drag force on a moving dislocation in terms of the scattering of lattice phonons by the strain field associated with a dislocation. The theory of Leibfried predicts

$$B = \frac{a E_o}{10 V_s} , \qquad (8.4.)$$

where a is the lattice parameter, E_o the thermal energy density and V_s the shear wave velocity. At high temperatures, E_o may be written

$$E_o = \frac{3kTZ}{a^3} , \qquad (8.5.)$$

where Z is the number of atoms per c.c. This should hold in fact until temperatures are reached where either E_o, or the specific heat, start to fall rapidly. This theory has been criticised by Nabarro (51) and Cottrell (53), on the grounds that there is a confusion between the scattering of phonons by the strain field around a stationary dislocation, and by that around a moving dislocation. When both these mechanisms are considered, the value of B is found to be much too small. However, Lothe (60) considered the phonon radiation from a vibrating dislocation and found the value of B was restored to approximately Leibfried's value.

Leibfried used a phonon scattering cross-section independent of the phonon wave-length, and of magnitude between a and $a \ln\left(\frac{R}{r}\right)$, where R and r are respectively the outer and inner cut-off radii of the dislocation stress field. This cross-section is difficult to calculate accurately. Klemens (58) has shown, using elasticity theory, that the cross-section at low temperatures is proportional to phonon frequency. For short phonon wave-lengths (high temperatures) a cross-section independent of wave-length seems reasonable.

(b) Mason's theory.

Phonons interact with each other through the non-linear properties of a medium, and equalise the energy between shear and longitudinal modes in a time given by the thermal relaxation time, τ. Since they can transfer energy and momentum, they have an effective viscosity.

Mason (60) points out that phonon viscosity may act directly on a stress wave, and convert acoustic energy into thermal phonon energy [Mason & Bateman (64)] and indirectly through a moving dislocation stress field. For the latter loss Mason calculates, using classical viscous fluid flow theory, a damping constant, for screw and edge dislocations of the form

$$B = \frac{b^2 \eta}{8 \pi r_0^2}, \quad (\text{SCREW}) \tag{8.6.}$$

$$B = \frac{3 b^2 \eta}{32 \pi (1-\nu)^2 r_0^2} + \text{SMALLER TERM}, \quad (\text{EDGE}) \tag{8.7.}$$

with

$$\eta = \frac{E_0 K_p}{C_{vp} \bar{V}^2}, \tag{8.8.}$$

where ν is Poisson's ratio, r_0 is an effective dislocation core radius, η is the viscosity of the phonon gas (from kinetic theory), E_0 is the thermal energy density, K_p is the lattice thermal conductivity, C_{vp} is the lattice specific heat and $\bar{V}$ is the weighted average velocity of transverse and longitudinal waves.

An approximation necessary for Mason's calculation is that the mean free path of the phonons is small compared with the space variations of the stress field, so that the phonons may be regarded as a gas in a uniform stress field. However, the dominant Fourier components of the stress field must have wave-lengths of the order of the dislocation core dimensions, so the approximation may not be good, even at quite high temperatures where the phonon wave-length is small.

8.2. A Comparison of theory and experiment.

Both Mason's theory and Leibfried's theory predict similar magnitudes of B at room temperature. In Table III some experimental values of B found by various experimenters are given, together with the theoretical values calculated according to Eshelby's thermoelastic damping model, Leibfried's phonon scattering model, and Mason's phonon viscosity model. The theoretical values appear, on the whole, to be slightly less than the experimental values.

B DYNES . SEC. CM^{-2}	LiF	NaCl	Cu	KCl	QUARTZ	Cu + 0.13% Mn
THERMOELASTIC	$1.7.10^{-4}$ (b)	$7.1.10^{-5}$ (b)	10^{-6} (b)		$2.5.10^{-5}$ (b)	
PHONON SCATTERING	$5.6.10^{-5}$ (b)	$7.7.10^{-5}$ (b)	$1.1.10^{-4}$ (b)	$5.9.10^{-5}$ (a)	$4.0.10^{-5}$ (b)	10^{-4} (a)
PHONON VISCOSITY	$4.5.10^{-5}$ (a)	$1.1.10^{-4}$ (a)	$7.0.10^{-5}$ (a)	$1.9.10^{-4}$ (a)		$9.0.10^{-5}$ (a)
EXPERIMENTAL	$1.3.10^{-3}$ (a)	$2.0.10^{-3}$ (d)	$7.9.10^{-5}$ (a)	$3.5.10^{-4}$ (a)	$6.0.10^{-4}$ (b)	$4.5.10^{-4}$ (a)
EXPERIMENTAL	$7.0.10^{-4}$ (c)		$5.0.10^{-4}$ (e)			
EXPERIMENTAL			$6.5.10^{-4}$ (f)			

(a) SUZUKI, IKUSHIMA & AOKI (64) (b) MASON (60) (c) JOHNSTON & GILMAN (59)
(d) GRANATO, HIKATA & LÜCKE (58) (e) ALERS & THOMPSON (61) (f) STERN & GRANATO (62)

TABLE III. VALUES OF B AT ROOM TEMPERATURE.

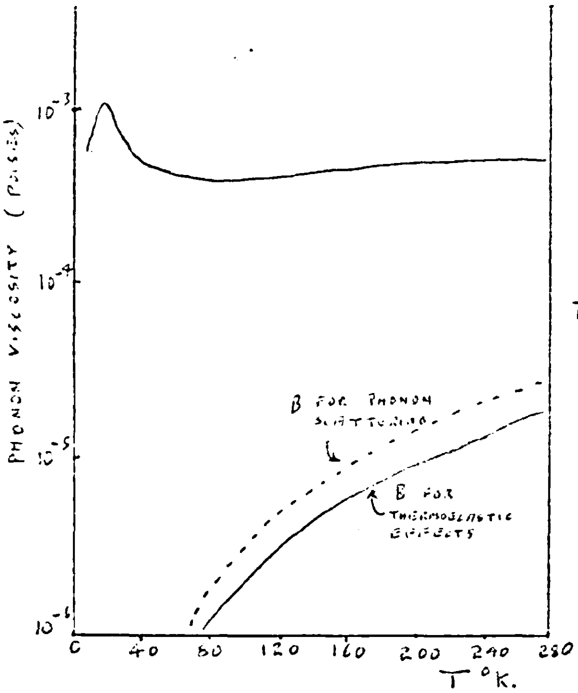

Fig. 8.1. CALCULATIONS OF SHEAR PHONON VISCOSITIES FOR A.T. CUT QUARTZ CRYSTAL AT 5 Mc/s [AFTER MASON (60)].

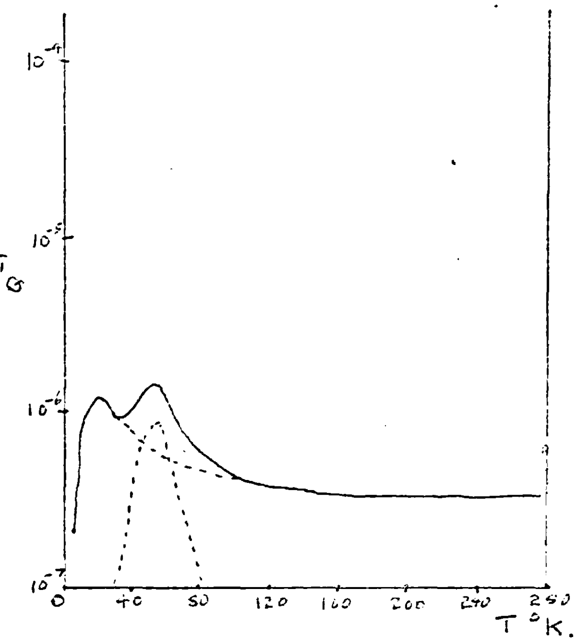

Fig. 8.2. DAMPING OF AN A.T. CUT QUARTZ CRYSTAL AT 5 Mc/s. IMPURITY RELAXATION HAS BEEN SUBTRACTED OUT [AFTER MASON (60)].

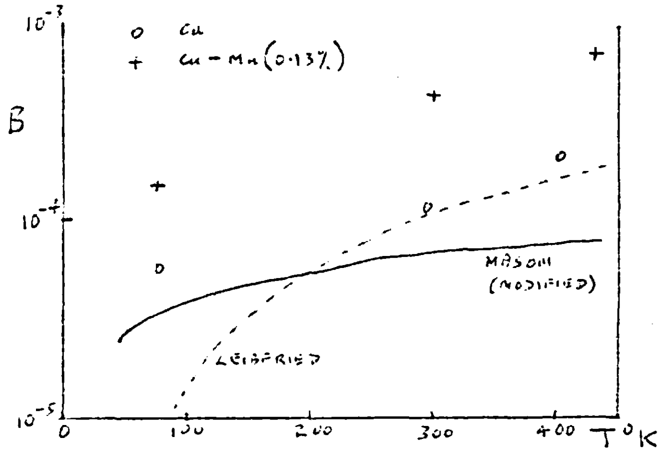

Fig. 8.3. TEMPERATURE DEPENDENCE OF B WITH THEORETICAL CURVES FOR PURE COPPER [AFTER SUZUKI, INUSHIMA & AOKI (64)].

The values given for phonon viscosity have been calculated from Mason's theory, with two changes [Suzuki et al.(64)]. Firstly, a cut-off length of 0·75b [Mason (64)] has been used instead of $\frac{b}{6}$, since the former is more generally accepted. Secondly experimental values of the lattice thermal conductivity were used for both metals and insulators. Mason used the electrical conductivity for metals in his original treatment.

There is seen to be a slight tendency for B to be greater in insulators than in metals. This difference is expected on the phonon viscosity model, but not on the phonon scattering model. The agreement between experiment and theory might be improved if not all the dislocations counted in a particular experiment contribute to the damping; Λ would then be smaller and hence B larger. Stern and Granato (62) have found that B is approximately the same for both edge and screw dislocations in Cu, as might be expected from equations (8.6) and (8.7.)

The scattering of thermal phonons by dislocations will also affect the thermal resistivity at low temperatures. Lomer & Rosenberg (59) found that the theoretical values of resistivity were four to six times smaller than the experimental values. The phonon scattering may be underestimated by a similar amount in the calculations of Leibfried.

8.3. The temperature dependence of B.

Another method of comparing experiment and theory is to consider the temperature variation of the internal friction in relation to the predicted temperature variation of B. In Fig. 8.1. is shown the variation with temperature of the damping constant calculated from phonon viscosity, and phonon scattering, for quartz. [Mason (60)]. In Fig. 8.2. is shown the corresponding damping of quartz, as a function of temperature.

The damping is seen to correspond more to Mason's calculation of B. Fig. 8.3. shows the temperature dependence of B measured for Cu (o) and a copper-manganese alloy (+) after Suzuki et al. (64), together with the theoretical curves according to Leibfried and Mason, the latter modified as in Table III. It appears that neither of the theoretical curves agrees with the experimental values, which are roughly proportional to temperature. This temperature dependence is also observed by Alers and Thompson (61). Lothe (62) has concluded that phonon scattering at a kink in a dislocation would produce a frictional force linearly dependent on temperature down to $\frac{\theta a}{D}$, where θ is the Debye temperature, a the lattice parameter, D the kink width. Eshelby (62) has also considered this scattering.

Measurements of B have been made for lead down to 4.2°K by Lenz and Lücke (63). If, as Lothe (63) and Eshelby (62) calculate, B is proportional to the thermal energy, then B should approach zero quite rapidly for low temperatures. In this case the usually overdamped dislocations should show resonances at low temperatures, but such resonances have not yet been reported. In fact, at 4.2 K the damping constant of lead remains so high that no resonance-like behaviour could be detected. A possible explanation may be found in the kink model of Brailsford (61) [See chapter 5.1(iv)] If H is the activation energy for sideways motion of kinks over small Peierls potentials, one expects $B \sim kT\exp\left(\frac{H}{kT}\right)$. Thus B is proportional to kT for $kT \gg H$, yet does not go to zero at low temperatures but increases again. The exact temperature dependence of B according to this model has not yet been worked out.

8.4. The Damping in an Alloy.

In Table III it is seen that the presence of Mn in Cu alters the value of β should not be affected by impurities, only by the Debye temperature. However, Mason's value may be affected through k_P, but k_P should decrease and not increase with alloying. Hence neither theory accounts for this effect. Fiore & Bauer (64) have shown that the value of β in a very dilute Cu-Fe alloy is in reasonable agreement with Mason's value of β for pure Cu, if the experimental value is calculated using Rogers' (62) modification of the F. G. L. theory. It is possible, however, that alternative mechanisms are responsible for the damping.

The first possibility arises from the interaction between a moving dislocation and the stress field round an impurity. Cokawa & Yaza (63) have considered the radiation from a dislocation in an impurity stress field, and Takamura & Morimoto (63) have considered an energy loss from a dislocation by the excitation of impurity atom vibrations. Both of these mechanisms, however, predict a damping constant proportional to the velocity of the dislocation, differing in this respect from the theories of Mason & Leibfried. Such a velocity dependence has little experimental support, and the effect is probably negligible, at least in the results of Fig. 8.3.

Other possible mechanisms may be a change in E_o, brought about by the presence of the alloying atoms, or a thermoelastic damping mechanism similar to that outlined by Eshelby for pure metals.

CHAPTER 9

Discussion and Concluding Comments.

In this chapter the current position with regard to the five characteristic types of damping considered in this dissertation is summarised, and some suggestions for further work made.

The three Hasiguti peaks P_1, P_2 and P_3 have been related with some certainty to a relaxation mechanism involving an interaction between dislocations and point defects. Possible mechanisms have been proposed by Okuda & Hasiguti (63), Bruner (60), Schiller (64), Hasiguti (63) and Koiwa & Hasiguti (65). It is not yet possible to say definitely whether any of these mechanisms can account completely for the Hasiguti peaks, although the thermal unpinning theory of Koiwa and Hasiguti appears to give an excellent agreement with the experimental results of P_1 in copper. Koiwa and Hasiguti suggest the difficulties encountered in this theory may be due to the dislocation model assumed, rather than to the mathematical analysis they apply. The kink model of dislocation motion is suggested as an alternative model. The presence of internal stresses may also be important.

The friction observed at high temperatures (chapter 5.3.) is not very well understood, but is probably associated with the formation of defects by a moving dislocation. More measurements of the frequency dependence and the activation energy of both the friction and the associated modulus defect would be useful.

The Bordoni peaks are accounted for quite well by two distinct theories. That of Seeger & Donth (57), modified by Paré (61) and Seeger & Schiller (62), attributes the peaks to a relaxation mechanism involving the thermal activation of kink pairs, an allowance being made for the presence of internal stresses. The other theory, due to Brailsford (65), assumes dislocations are already present in a dislocation and that the relaxation is determined by the recombination, under the influence of the applied oscillating stress, of any kink concentration in excess of the thermal equilibrium value. This excess is assumed to arise from the presence of large internal stresses. It is difficult to devise a clear-cut test to distinguish between these two theories. However, if an accurate determination of the attempt frequency associated with the Bordoni peak yields a value in excess of $10^{-3}\omega_D$ c/s, where ω_D is the Debye frequency, then Brailsford concludes his mechanism cannot be operating. Brailsford also predicts a relaxation time which is a function of loop length, in contrast to Seeger et al. The two theories are also based on different models of dislocation motion, namely the string model of Koehler and the kink chain model of Brailsford. Attard & Southgate (63) Alefeld (65) have attempted to show that the Seeger-Schiller model and the Brailsford model are conceptually related to each other. However, Alefeld finds some significant differences in the dislocation behaviour predicted by the two models. These differences are considered below.

The dynamic loss theory of K.G.L. is found to account well for the strain amplitude independent damping observed at megacycle frequencies, but not at all well at lower frequencies. This failure may be due to the presence of some other damping process which, in particular, is independent of frequency, or to the inapplicability of the K.G.L. model.

The hysteresis loss arising from dislocation unpinning predicted by K.G.L. is found to be in very good agreement with experiment in many cases. There are several assumptions made in the K.G.L. theory, however, which may mean it is unable to describe the dislocation behaviour in a particular specimen. For example, the pinning points may be distributed in an atmosphere round a dislocation rather than exactly on it. Alternatively, the string model of dislocation motion may itself be inapplicable. This might account for many of the difficulties mentioned above. The kink chain model of Brailsford (65) may better describe dislocation motion in certain circumstances. Alefeld (65) has investigated the points of difference between these two models. In the region where both models predict a linear stress-dislocation strain relation (low stress), the essential difference between the two models is expected in the size and temperature dependence of the damping constant, B. The kink chain model predicts for B a larger value at very low temperatures with possibly a minimum value below the Debye temperature. There are not many measurements of B at low temperatures, but those of Lenz & Lücke (63), for example, favour the kink model. In the non-linear region of the stress-dislocation strain relation significant differences between the two models are found. Firstly, the presence of a finite Peierls stress leads the kink chain model to predict a non-linear stress-strain relation for static bias or oscillating stress amplitudes of 10^{-7}, assuming $L = 10^4 b$, while the corresponding stress amplitude according to the string model is 10^{-5}. Thus the kink model is able to predict a strain amplitude dependent decrement at stresses below those necessary to produce mechanical unpinning according to the string model. Secondly, the anelastic strain as measured by low amplitude oscillations increases with bias stress for the string model, whereas it decreases for the kink model. The physical reason for this may be seen for, ignoring double kink generation, once all kinks are forced into a close-packed direction by a bias stress kink motion is exhausted. On the other hand, the more a dislocation string bows out, the smaller is the restoring force (neglecting changes in the line tension with bias stress), so the anelastic strain is easily increased. At high stress amplitudes, or high temperatures, double kink generation is possible and the anelastic strain increases with bias stress according to the kink chain model.

A convenient way of distinguishing between these two models will be to investigate the role which internal stresses play in determining the internal friction of a specimen. Measurements on cold worked specimens with static bias stresses applied are, therefore, required. The nature of dislocation breakaway at high frequencies where oscillating stress amplitudes are small may also be investigated by applying a static bias stress, since both a bias stress and a high amplitude stress wave are expected to produce similar dislocation unpinning effects.

A different approach to the problem which is likely to prove profitable is the study of the generation of harmonics of a stress wave in a cold worked crystal. The generation of these harmonics is related to the second and higher order terms in the stress-dislocation strain relation, and so gives information on the dynamics of dislocation motion. The presence of static stresses is again found to be an important factor.

REFERENCES

Alefeld,G. (65)	J. Appl. Phys. 36.2633 & 2642
Alers,G. & Thompson,D.O. (61)	J. Appl. Phys. 32.283
Attard,A.E. & Southgate,P.D. (63)	J. Appl. Phys. 34.855
Baker,G. (57)	J. Appl. Phys. 28.734
Baker,G. & Carpenter,S. (65)	Rev. Sci. Instrum. 36.29
Balmouth,L. (34)	Phys. Rev. 45.715
Barnes,R.S. Hancock,N.H. & Silk,E. (58)	Phil. Mag. 3.519 & 527
Barone,A. (62)	Handb. Phys. (Akustik II) p.74
Baxter,W.J. & Wilks,J. (62)	Phil. Mag. 7.427
Baxter,W.J. & Wilks,J. (63)	Acta Met. 11.979
Berry,B.S. (62)	Acta Met. 10.271
Berry,B.S. & Nowick,A.S. (60)	Bull. Am. Phys. Soc. 5.153
Beshers,D.N. (55)	Thesis, Univ. of Illinois
Beshers,D.N. (59)	J. Appl. Phys. 30.252
Birnbaum,H.K. (55)	Acta Met. 3.297
Birnbaum,H.K. & Levy,M. (56)	Acta Met. 4.84
Blewitt,T.H. (60)	J. Nuc. Mater. 2.277
Blistanov,A.A. & Shaskol'skaya,M. (64)	Sov. Phys. (Solid State) 6.573
Bömmel,H.E. & Dransfeld,K. (60)	Phys. Rev. 117.1245
Bordoni,P.G. (47)	Nuovo Cim. 4.177
Bordoni,P.G. (54)	J. Acoust. Soc. Am. 26.495
Bordoni,P.G. Nuovo,M. & Verdini,L. (59)	Nuovo Cim. 14.273
Bozorth,R.M. (51)	J. Phys. Radium 12.308
Bozorth,R.M. Mason,W.P. & McSkimin,H.(51)	Bell Syst. Tech. J. 30.970
Bradley,D. (65)	J. Acoust. Soc. Am. 37.700

Brailsford, A.D. (61)	Phys. Rev. 122.778
Brailsford, A.D. (65)	Phys. Rev. 137.A1562
Briggs, N.W. (55)	Thesis, Cornell Univ.
Broom, T. & Ham, R.K. (59)	Proc. Roy. Soc. A 251.186
Brown, N. & Lukens, K.F. (61)	Acta Met. 9.106
Bruner, L.J. (60)	Phys. Rev. 118.339
Bruner, L.J. & Mecs, B.M. (63)	Phys. Rev. 129.1525
Caswell, H.L. (58)	J. Appl. Phys. 29.1210
Chambers, R.H. (57)	Carnegie Inst. Tech. Rep. No. AT(30-1)-1193
Chambers, R.H. & Schultz, J. (62)	Acta Met. 10.467
Chambers, R.H. & Smoluchowski, R. (60)	Phys. Rev. 117.725
Chick, B. Anderson, C. & Truell, R. (60)	J. Acoust. Soc. Am. 32.186
Cottrell, A.H. (43)	Rep. on Conf. on Strength of Solids (London, Phys. Soc.)
Cottrell, A.H. (53)	Dislocs. and Plastic Flow in Crystals (Oxford)
Cottrell, A.H. & Bilby, B.A. (49)	Proc. phys. Soc. A 62.49
David, R. (64)	Philips Res. Rep. 19.6.526
Dey, B.N. & Quader, M.A. (65)	Canad. J. Phys. 43.1347
Diehl, J. (62)	Radn. Dam. in Solids I (Int. Atom. Energy Agency, Venice) p.129
Dienes, G.J. (52)	Phys. Rev. 86.228
Donth, H. (57)	Z. Phys. 149.111
Druyvesteyn, W.F. & Blaisse, S. (62)	Physica 28.695
Einspruch, N. Wittenholt, E. & Truell, R. (60)	J. Appl. Phys. 31.806

Eshelby,J.D. (49) Proc. Roy. Soc. A 197.396

Eshelby,J.D. (62) Proc. Roy. Soc. A 226.222

Federighi,T. (59) Phil. Mag. 4.502

Filloux,J. Harper,H. & Chambers,R.H.(64) Bull. Am. Phys. Soc. 9.230

Fiore,N.F. & Bauer,C.L. (64) J. Appl. Phys. 35.2242

Fischer,J. (62) Z. Naturforsch 17(a).603

Flinn,P.A. (62) Strengthening Mechs. in Solids,p.17 (Am. Soc. for Metals, Cleveland)

Frank,F.C. & Read,W.T. (50) Phys. Rev. 79.722

Friedel,J. (55) Phil. Mag. 46.1169

Friedel,J. (63) The Relat. between Struct. and Mech. Props. Metals I, p.409 (HMSO)

Friedel,J. Boulanger,C. & Crussard,C.(55) Acta Met. 3.380

Gelli,D. (62) J. Appl. Phys. 33.1547

Gelli,D. Panseri,C. & Federighi,T. (62) Nuovo Cim. Suppl. I.36

Gilman,J.J. & Johnston,W.G. (59) J. Appl. Phys. 30.129

Gobrecht,H. & Bartschat,A.B. (59) Z. Physik 153.529

Granato,A.V. & Lücke,K. (56) J. Appl. Phys. 27.583 and 789

Granato,A.V. & Lücke,K. (57) Dislocs. and Mech. Props. of Crystals (Wiley)

Granato,A.V. Hikata,A. & Lücke,K. (58) Acta Met. 6.470

Hasiguti,R.R. (63) J. Phys. Soc. Japan,Suppl.I,18.114

Hasiguti,R.R. (65) Phys. Stat. Sol. 9.157

Hasiguti,R.R. Igata,N. & Kamoshita,G.(62) Acta Met. 10.442

Hikata,A. Chick,B. & Elbaum,C. (63) Appl. Phys. Lett. 3.195

Hikata,A. Chick,B. & Elbaum,C. (65) J. Appl. Phys. 36.229

Hikata,A. Chick,B. Elbaum,C.
& Truell,R. (62) Acta Met. 10.423

Hikata,A. Chick,B. Granato,A.V.
Lücke,K. & Truell,R. (56) J. Appl. Phys. 27.396

Hiki,Y. (58) J. Phys. Soc. Japan 13.1138

Huntington,H.B. (47) Phys. Rev. 72.321

Hutchison,T.S. & Hutton,C.J. (58) Canad. J. Phys. 36.82

Hutson,A.R. & White,D.I. (62) J. Appl. Phys. 33.40

Jacobs,R.B. & Bancroft,D. (38) Rev. Sci. Instrum. 9.279

Kamel,R. (61) Acta Met. 9.65

Kamentsky,L.A. (56) Thesis, Cornell Univ.

Kê,T.S. (47) Phys. Rev. 72.41

Kê,T.S. (49) J. Appl. Phys. 20.1226

Kê,T.S. & Ma,Y.I. (57) Scientia Sinica 6.81

Kessler,J.O. (57) Phys. Rev. 106.646 and 654

Kharitonov,A.V. (61) Sov. Phys. (Acoustics) 7.83

Kharitonov,A.V.(63) Sov. Phys. (Acoustics) 9.62

Kittel,C. (58) Phys. Rev. 110.836

Klemens,P.G. (58) Proc. Phys. Soc. 71.843

Koehler,J.S. (52) Imperfections in nearly Perfect Crystals (Wiley) p.197

Koehler,J.S. & de Wit,G. (59) Phys. Rev. 116.1113

Koga,I. Aruga,M. & Yoshinaka,Y. (58) Phys. Rev. 109.1467

Koiwa,M. & Hasiguti,RR. (63) Acta Met. 11.1215

Koiwa,M. & Hasiguti,R.R. (65) Acta Met. 13.1219

Köster,W. (40) Z. Metallk. 32.282

Kyame, J.J. (49) J. Acoust. Soc. Am. 21.159

Leak, G.M. (61) Proc. Phys. Soc. 78.1520

Leibfried, G. (50) Z. Phys. 127.344

Leibfried, G. (57) Disloc. and Mech. Props. of Crystals (Wiley)

Lement, B.S. & Cohen, M. (56) Acta Met. 4.469

Lenz, D. & Lucke, K. (63) Phys. Verhandlungen 2/3, 56

Levy, M. & Metzger, M. (55) Phil. Mag. 46.1021

Lomer, J.N. & Niblett, D.H. (62) Phil. Mag. 7.1211

Lomer, J.N. & Rosenberg, H.M. (59) Phil. Mag. 4.467

Lothe, J. (60) Phys. Rev. 117.704

Lothe, J. Jøssang, T. & Skylstad, K. (63) Relat. between Struct. & Mech. Props. Metals II, p.527 (HMSO)

Lothe, J. & Hirth, J.P. (59) Phys. Rev. 115.543

Lücke, K. (56) J.Appl. Phys. 27.1433

Ludloff, H.F. (40) J. Acoust. Soc. Am. 12.193

Maddin, R. & Cottrell, A.H. (55) Phil. Mag. 46.735

Marx, J. (51) Rev. Sci. Instrum. 22.503

Marx, J. & Koehler, J.S. (50) Symp. on Plast. Def. of Cryst. Solids (Carnegie Inst. of Tech.)

Mason, W.P. (55) J. Acoust. Soc. Am. 27.643

Mason, W.P. (56) J. Acoust. Soc. Am. 28.1207

Mason, W.P. (58) Physical Acoustics and Properties of Solids (van Nostrand)

Mason, W.P. (60) J. Acoust. Soc. Am. 32.458

Mason, W.P. (64) J. Appl. Phys. 35.2779

Mason,W.P. & Bateman,T.B. (64) J. Acoust. Soc. Am. 36.644

Mason,W.P. & McSkimin,H.J. (48) J. Appl. Phys. 19.940

Mecs,B.M. & Nowick,A.S. (65) Acta Met. 13.771

Morse,R.W. Cavenda,J.D. & Olsen,T. (59) Phys. Rev. Lett. 3.15

de Morton,M. Lott,S. & Stainsby,D. (63) J. Sci. Instrum. 40.441

Mott,N.F. (52) Imperfections in Nearly Perfect Crystals (Wiley) p.173

Mott,N.F. & Nabarro,F. (48) Rep. on Conf. on Strength of Solids (London, Phys. Soc.) p.1

Mott,N.F. & Nabarro,F. (52) Imperfections in Nearly Perfect Crystals (Wiley)

Muss,D.R. & Townsend,J.R. (62) J. Appl. Phys. 33.1804

Nabarro,F.R.N. (51) Proc. Roy. Soc. A 209.278

Niblett,D.H. (56) Thesis, Oxford Univ.

Niblett,D.H. (61) J. Appl. Phys. 32.895

Niblett,D.H. & Wilks,J. (55) Conf. Phys. Bass. Temp.(Paris)p.484

Niblett,D.H. & Wilks,J. (56) Phil. Mag. 1.415

Niblett,D.H. & Wilks,J. (57) Phil. Mag. 2.1427

Niblett,D.H. & Wilks,J. (59) Proc. Int. Conf. Refrig.Copenhagen

Niblett,D.H. & Wilks,J. (60) Advances in Phys. 9.1

Nowick,A.S. (50) Phys. Rev. 80.249

Nowick,A.S. (53) Prog. Met. Phys. 4.1

Nowick,A.S. (55) Acta Met. 3.312

Okuda,S. (63) J. Appl. Phys. 34.3107

Okuda,S. & Hasiguti,R.R. (63) Acta Met. 11.257

Ookawa,A. & Yaza,K. (63) J. Phys. Soc. Japan 18, Suppl.I,36

Panseri,C. Federighi,T. & Celli,D. (62) Nuovo Cim. Suppl. 26.1.23

Papadakis,E.P. (65) J. Acoust. Soc. Am. 37.711

Paré,V.K. (58) Thesis, Cornell Univ.

Paré,V.K. (61) J. Appl. Phys. 32.332

Pearson,S. & Rotherham,L. (56) J. Metals (New York) 8.894

Quimby,S.L. (25) Phys. Rev. 25.558

Read,T.A. (40) Phys. Rev. 58.371

Read,T.A. (41) Trans. AIME 143.30

Redwood,M. (65) Ultrasonics 2.174

Roberts,J.M. & Brown,N. (60) Trans. AIM(M)E 218.454

Roberts,J.M. & Brown,N. (62) Acta Met. 10.430

Roderick,R.L. & Truell,R. (52) J. Appl. Phys. 23.267

Rogers,D.H. (62) J. Appl. Phys. 33.781

Roswell A.E. & Nowick,A.S. (57) Acta Met. 5.228

Sack,H.S. (62) Acta Met. 10.455

Schiller,P. (64) Phys. Stat. Sol. 5.391

Schoeck,G. Bisogni,E. & Shyne,J. (64) Acta Met. 12.1466

Seeger,A. (55) Handb. Phys. 7/1.383

Seeger,A. (56) Phil. Mag. 1.651

Seeger,A. Donth,H. & Pfaff,F. (57) Disc. Farad. Soc. 23.19

Seeger,A. & Schiller,P. (62) Acta Met. 10.348

Shibata,A. (59) Thesis, Cornell Univ.

Shoeck,G. & Seeger,A.(59) Acta Met. 7.469

Smith,A.D.N. (53) Phil. Mag. 44.453

Snoek,J.L. (41) Physica 8.711

Steinberg,M.S. (58) Phys. Rev. 111.425

Stern,R.M. & Granato,A.V. (62) Acta Met. 10.358

Stevens,R.R. (57) Thesis, Cornell Univ.

Suzuki,T. Ikushima,A. & Aoki,M. (64) Acta Met. 12.1231

Swartz,J.C. (61) Rev. Sci. Instrum. 32.335

Swartz,J.C. (62) Acta Met. 10.406

Swartz,J.C. & Weertman,J. (61) J. Appl. Phys. 32.1860

Takamura,J. & Morimoto,T. (63) J. Phys. Soc. Japan 18, Supp.I,28

Takahashi,S. (56) J. Phys. Soc. Japan 11.1253

Teutonico,L. Granato,A. & Lücke,K. (64) J. Appl. Phys. 35.220

Teutonico,L. Granato,A. Lücke,K. & Schlipf,J. (64) J. Appl. Phys. 35.2732

Thompson,D.O. & Glass,F.M. (58) Rev. Sci. Instrum. 29.1034

Thompson,D.O. & Holmes,D.K. (56) J. Appl. Phys. 27.191 and 713

Thompson,D.O. & Holmes,D.K. (59) J. Appl. Phys. 30.525

Thompson,D.O. & Paré,V.K. (60) J. Appl. Phys. 31.528

Thompson,D.O. & Paré,V.K. (65) J. Appl. Phys. 36.243

Truell,R. & Elbaum,C. (62) Handb. Phys. (Akustik II) p.153

Tsui,R. (61) Thesis, Cornell Univ.

Van Bueren,H.G. (61) Imperfections in Crystals (North Holland)

Wadsworth,N. (57) Dislocs. and Mech. Properties of Crystals (Wiley) p.479

Weertman,J. (55) J. Appl. Phys. 26.202

Weertman,J. (57) J. Appl. Phys. 28.193 and 636

Weertman,J. & Koehler,J.S. (53) J. Appl. Phys. 24.624

Weertman,J. & Salkovitz,E.I. (55) Acta Met. 3.1

Weinig,S. (55)	Rev. Sci. Instrum. 26.91
Weinig,S. & Machlin,E.S. (56)	J. Appl. Phys. 27.734
Wert,C.A. (49)	J. Appl. Phys. 20.29
Whitworth,R.W. (60)	Phil. Mag. 5.425
Wilks,J. (59)	Phil. Mag. 4.1379
Woodruff,T.O. & Ehrenreich,H. (61)	Phys. Rev. 123.1553
Ying,C.F. & Truell,R. (56)	J. Appl. Phys. 27.1086
Young,F.W. (62)	J. Appl. Phys. 33.3553
Zener,C. (40)	Proc. Phys. Soc. 52.152
Zener,C. (48)	Elastic. and Anelastic. of Metals (Chicago)
Zener,C. (52)	Imperfections in Nearly Perfect Crystals (Wiley)
Zener,C. Otis,W. & Nuckolls,R. (38)	Phys. Rev. 53.100
Zener,C. Rose,F.C. & Randall,R.H. (39)	Phys. Rev. 56.343